STUDIES ON DIFFUSION IN METALS

Thesis

Submitted by

THOMAS J. RENOUF, M.M., B.Sc.,

for the degree of

Doctor of Philosophy

University of Edinburgh

May, 1970.

PREFACE

The research described in this thesis was carried out in the Department of Natural Philosophy of the University of Edinburgh under the supervision of Professor N. Feather, F.R.S. and Professor A.F. Brown. A paper based on the work dealing with volume diffusion presented herein, was published in the Philosophical Magazine[(a)], and a paper based on the grain boundary diffusion work has been accepted and is at present awaiting publication in the same journal.

(a) Details of the published work are given in Appendix 4.

LIST OF TABLES, PLATES AND FIGURES

CONTENTS

C O N T E N T S (Contd.)

Page No.

CHAPTER V RESULTS AND DISCUSSION

CHAPTER 1

INTRODUCTION AND REVIEW

1.1 Historical Background

Although the history of metallurgy illustrates the continuous practice of diffusion controlled processes, it was not until fairly recent times that an interest was to be shown in the study of diffusion on its own account.

The first contribution was by Fick[1] in 1855. This gave a theoretical treatment of diffusion which followed closely the work on thermal conductivity by Fourier in 1854. The treatment gave mathematical expression to an observation that for diffusional flow to occur between two points a concentration gradient must exist, and it also gave the means of interpreting experimental measurements in terms of a diffusion coefficient. With certain modifications the laws of Fick remain as the basic differential equations for the solution of diffusion problems.

The first diffusion measurements reported were those of Spring[2] in 1878, but it is the classic experiments of Roberts-Austin[3,4] in the period 1891 to 1899 that are considered to be the first quantitative studies. The noteworthy features of his work have proved to be topics of major consequence in the field. His concern with the effects of small amounts of impurities on the properties of metals and his association of the temperature variation of diffusion with the concept of activation energy,

announced in 1889 by Arrhenius[5], illustrate his remarkable insight into the subject. The accuracy and the result he obtained for the diffusion of gold into lead compares surprisingly well with current values.

In the earlier diffusion experiments the measurements were made by chemical methods and consequently the diffusant was used in relatively large concentrations. At the same time the solutions of the Fick equations that were used to interpret the data assumed a diffusion coefficient that was constant. Most of this early work is summarised in the review articles of Mehl[6,7] and in other works[8-11]. In 1933 Matano[12] applied the Boltzman[13] solution to the data given by Grube and Jedel[14] for a nickel-copper diffusion couple and found that the diffusion coefficient varied by a factor of ten. In this solution the diffusion coefficient is assumed to vary with concentration, its value depending only on the point within the diffusion zone at which the analysis is applied. This interdiffusion coefficient is some average value that depends upon the diffusion rates of the elements of the couple and for it to be meaningful should be related to the diffusion coefficients of the two species. This was first done by Darken[15] in 1948 in an interpretation that related specifically to the Kirkendall effect. The work of Kirkendall[16,17] in 1942 was to prove instrumental in realising a deeper understanding of chemical diffusion in particular and of the related atomic processes in general. The Kirkendall effect shows that inert markers placed at the interface of a binary diffusion couple move relative to the fixed ends of the couple as diffusion proceeds. In some cases this is accompanied by the formation of pores or voids, and also by lateral distortion.

Darken[15], examining the effect phenomenologically, pointed out that if the markers were used as a reference point, two chemical diffusion coefficients should be used, one for each diffusing species, and showed that if these were not equal then there would be a mass flow proportional to their difference. He gave the interdiffusion coefficient in terms of these two coefficients specified to the relevant concentration levels and also in terms of the corresponding tracer diffusion coefficients and the nonideality of the alloy.

In an atomistic description of the effect Bardeen[18] and Seitz[19] showed that if the total number of lattice sites was to be conserved then a difference between the net rates of flow of the two species should be balanced by a flow of imperfections. If the thermal equilibrium of the imperfections was to be maintained everywhere, then this would result in removing planes of atoms from one side of the boundary and adding planes of atoms on the other so as to produce the marker motion relative to the ends of the specimen. If a vacancy mechanism was assumed, then the varying amount of porosity could be explained by condensation of the vacancies in excess of the thermodynamic equilibrium value at centres other than vacancy sinks.

The subsequent volume of experimental data was to show that the assumptions of the Darken analysis were not always justified and Le Claire[20] points out that there may be other factors resulting from the large chemical gradients which affect the interpretation and so make it difficult to know what theoretical significance may be attached to the results, complications which might

be avoided in tracer self and impurity diffusion studies in pure metals and in homogeneous alloys. Recently Manning[21] developed from an atomistic treatment, expressions similar to those of Darken, but which contain additional terms allowing for the effect of the net flow of vacancies. The experimental data of Meyer and Slifkin[22] and of Manning[23] show much better agreement with the modified expressions.

The first tracer experiments were performed with the naturally occurring radioactive elements thorium B and thorium C in the self diffusion studies of lead by von Hevesay[24] in 1932 and of bismuth by Seitz[25] in 1933. The subsequent availability of artificial radioactive isotopes was to allow a continuous improvement in the scope and in the accuracy of experiments.

Much of the work in recent years has been related to theoretical considerations. The study of the atomic mechanism of the diffusion process and the development of the theoretical consequences of proposed models has required the search for agreement in experimental data. This has required not only data of the highest quality but also measurements bordering so closely on the limits of resolution that the demand for the development and improvement of experimental techniques has been continuous. The various theoretical predictions have led to diffusion experiments investigating the effects of short circuiting paths high pressure, non-equilibrium defect concentration, isotopic mass difference, magnetic ordering, chemical, electric and temperature gradients, and further to related experiments measuring numerous other properties. Most of these topics have been treated in the reviews by Le Claire[20,26], Lazarus[27], Shewmon[28] and Peterson[29].

1.2 Mechanisms for Diffusion

Diffusion is the process by which atoms and molecules intermix as a result of their random thermal motion. The motion is taken to resemble a random walk pattern and in solids it depends upon the thermally induced movement of the atoms from one stable position in the lattice to another. Any inhomogeneous system tends to a state of equilibrium as a consequence of the process and this is usually a state of homogeneity.

The various types of solids tend to have a characteristic lattice defect structure and each structure tends to show a preferred atom transport mechanism, however it is assumed that many factors determine which mechanism operates and that in a given solid there may be more than one mechanism.

The models most acceptable to diffusion in metals are as follows.

a) In the vacancy mechanism the diffusing atom moves by jumping into a vacant neighbouring lattice site. There is a substantial body of evidence, based on experimental observation and on theoretical calculation, to indicate that this mechanism operates in most pure metals and substitutional alloys.

b) In the interchange mechanism the diffusing atom moves by exchanging lattice sites with a neighbouring atom or by the ring rotation of a number of atoms. This mechanism predicts that the flow of atoms in opposite directions is equal, something that has not been observed.

c) In the interstitial mechanism the diffusing atom moves by jumping from one interstitial position to another. In the interstitialcy mechanism the diffusing atom pushes a neighbouring atom

from a lattice site into an interstitial position. In the crowdion mechanism a number of atoms move by a line series of interstitialcy jumps. The diffusion of small atoms such as H, C, O and N in metals, and of the noble metals in Pb, Sn, In and Tℓ is assumed to occur by the interstitial mechanism and interstitialcy is assumed for the diffusion of Ag in AgCl and AgBr.

d) In the relaxation mechanism[30] the diffusing atoms move freely within locally melted regions which are taken to move through the lattice.

e) Voidal diffusion[230] is taken to occur in some open structures, the atoms diffusing along the continuous voidal channels.

Any study of the atomic mechanism of diffusion must be made indirectly, since the process is to be observed only on the macroscopic scale. This is achieved by deriving suitable parameters which can be used to describe the atomic mechanisms and relating these to the experimentally measured diffusion parameters.

Investigations can then be carried out by making theoretical calculations of the atomic parameters and comparing the results with the experimental values. In this way it may be possible to determine which mechanism operates in a given case and reveal other features of the atomic processes. The required interrelation can be obtained by deriving the concentration distribution for given diffusion conditions by probability methods and comparing this with the solution obtained from Fick's laws.

1.3 The Interrelation of Atomic Parameters and Diffusion Parameters

The problem of random flights in its present form was first considered by Pearson[31] but later it was identified with a problem formulated at an earlier date by Lord Rayleigh[32].

If a particle starts at an origin and undergoes a series of n jumps, the final position is given by a vector $\underline{R}$ where

$$R = \sum_{i=1}^{n} \underline{r}_i$$

and $\underline{r}_i$ is the vector representing the i^{th} jump. The magnitude and direction of each jump is taken to be independent of all previous jumps, but is governed by a probability distribution p. The solution to the problem defines the probability $P(R)dR$ that after n jumps a particle lies in the interval between R and $R + dR$. Smoluchowski[33] gave a solution for the one dimensional case and Chandrasekhar[34] following Markov[35] gave solutions for the general case. When n is large the solution, for most forms of p that were considered, is given as

$$P(r) = \frac{1}{(2\pi n\, \bar{r}^2/3)} \exp - \left(\frac{R}{(2n\, \bar{r}^2/3}\right) \qquad (1.1)$$

where $\bar{r}^2 = \frac{1}{n} \sum r_i^2$.

The solution is the same for a large number of particles starting under the same initial conditions and undergoing the jumps without any mutual interference, giving in this case, the fraction of the particles found in a given element.

If the problem is treated as the diffusion from a point source of mass M, the solution by Fick's laws (see Crank[36]) for a concentration independent diffusion coefficient D, gives the concentration C as

$$C = \frac{M}{(4\pi Dt)^{3/2}} \exp - \left(\frac{R^2}{4Dt}\right) \qquad (1.2)$$

In order to identify the two solutions as being the same, it is necessary that D in this case satisfies the relation

$$D = \frac{1}{6} \bar{r}^2 \tau \quad , \qquad (1.3)$$

where $\tau = n/t$ is the jump frequency. With this substitution Chandrasekhar shows that equation 1.1 corresponds to a solution of a partial differential equation, which can be identified in general as the diffusion equation. On this basis it is possible to describe the motion of a large number of particles describing random flights without mutual interference as a process of diffusion with the diffusion coefficient D given by equation 1.3. If the magnitude and direction of each jump is not independent of previous jumps then equation (1.3) becomes

$$D = \frac{1}{6} \bar{r}^2 \tau f \qquad (1.3A)$$

where f is called the correlation factor.

1.4 Theory of Diffusion

1.4.1 Derivation of D

Each diffusing system is distinguished by the value of the quantities D_o and Q that are contained in the Arrhenius equation

$$D = D_o \exp - \left(\frac{Q}{RT}\right) \qquad (1.4)$$

and which are taken to be the best temperature-independent constants which fit the experimental data in the temperature range considered.

If equation 1.3 can be expressed in a suitable form for each of the atomic mechanisms then a comparison of D_o and Q with the corresponding values calculated from the atomic parameters will in principle determine the mechanism. This requires a derivation of γ the average number of jumps per second for each tracer atom, and to do this γ is written as

$$\gamma = wz$$

where w is the jump rate of the tracer atom into one of the available neighbouring sites and z is the number of neighbouring sites. If it is further required that the neighbouring site be vacant then

$$\gamma = wzn_v$$

where n_v is the fractional concentration of vacancies, zn_v now being the probability that a tracer atom has a neighbouring vacancy. Equation 1.3 can now be written in the form

$$D = \alpha a_o^2 fzwn_v \qquad (1.5)$$

where a_o is the lattice parameter and α a geometric constant.

Two different approaches have been used to derive w, (a) the equilibrium method based on reaction rate theory and, (b) the dynamical method given by Rice[37] and by Manley[38]. In the latter w is developed by evaluating the probability that the migrating and the surrounding atoms attain special amplitude displacements from their rest positions which allow the migrating atom to jump. The approach avoids the direct use of equilibrium statistics by using random variable arguments, but the resulting expression is difficult to simplify and provides little help for

the fundamental calculation of w. The calculations that can be made by using suitable approximations require a normal mode analysis of the crystal.

In the earlier treatments by Barrer[39] and by Wert and Zener[40] the jump from one lattice site to another was considered as a jump from one level of configurational energy to another of the same level. In the transition a potential energy barrier defining a state of higher energy had to be surmounted. Under certain assumptions it was possible to apply equilibrium statistical mechanics to the problem. It was assumed that the configuration passed through a sequence of states during the transition, that the energy level of each state was narrow compared to the gap between levels, that all states were in thermal equilibrium with the lattice and that all changes in configurational coordinates occurred in times long compared to the thermal relaxation times of the lattice. On this basis the theory of absolute reaction rates[41] could be used to calculate the jump rate, which was given as

$$w = \bar{\nu} \exp - \left(\frac{\Delta E}{kT}\right) .$$

Zener[42] has given the conditions under which ΔE can be interpreted as the isothermal work necessary to move the system slowly to the saddle point configuration and $\bar{\nu}$ interpreted as an effective vibration frequency in the initial site.

Vineyard[43] has given a more rigorous many-body treatment which largely eliminates the shortcomings of this approach. It does not require that the jump occur slowly and it clearly defines the saddle point as a special configuration. The result is expressed in terms of the normal frequencies of the system in the

ground and the excited states, the latter are instantaneous and clearly not observable. It is to be noted that quantum mechanical corrections should be applied to both of these forms on account of the finite width of the energy levels. Pound et al.(44) have effected some simplification in this treatment by use of the Einstein formulation of the lattice dynamics.

Recently Glyde(45) further developed the idea that a jump arises as a result of a particular fluctuation of a lattice in equilibrium, that fluctuation in which one atom has a large amplitude displacement and the surrounding atoms open up a hole so that this atom can pass to the adjacent vacant site without a tremendous potential energy increase in the lattice. The jump rate has been derived following the Rice and Manley and the Vineyard treatment, and give near identical results differing only in the treatment of the minimum potential configurations of the lattice atoms during the jump. The minimum potential hole (saddle-point) configuration has been reconsidered without introducing a new set of lattice frequencies, providing an explicit expression of $\bar{\nu}$ for calculation and determining its mass dependence as $m^{-\frac{1}{2}}$. The pre-exponential factor and the activation energy was calculated for solid argon, using the expression derived by statistical mechanics and this shows excellent agreement with experiment. Munday et al.(46) however offer accurate evidence that w is not proportional to $m^{-\frac{1}{2}}$, and suggests that the reduction in the power of m is related to how far the surrounding atoms must move in order to reach the saddle point. An intuitive expression for this reduction has been developed by Le Claire(47).

The following simplified treatment illustrates the basic approach of the equilibrium thermodynamic method first applied by Zenner[42]. The jump rate w is given by

$$w = n_m \bar{v}/\delta$$

where n_m is the fractional concentration of "activated complexes" or saddle point configurations, $\bar{v}$ the velocity of the atoms at the saddle point and δ the width of the saddle point barrier. $\bar{v}/\delta$ is a frequency found to be of the order of $\bar{\nu}$. To calculate the number of atoms at the saddle point at any instant it is necessary to know ΔE_m the increase in the Gibbs free energy of a region when an atom in it moves from a normal site to the saddle point position, this is equal to the work done if the process is isothermal, isobaric and reversible, then

$$\Delta E_m = \Delta H_m - T\Delta S_m$$

where ΔH_m and ΔS_m are the enthalpy and entropy changes for the movement. By considering the ideal entropy of mixing, basic thermodynamic requirements show that the equilibrium value of activated complexes is given by

$$n_m = \exp - \left(\frac{\Delta E_m}{kT}\right)$$
$$= \exp\left(\frac{\Delta S_m}{k}\right) \exp - \left(\frac{\Delta H_m}{kT}\right)$$

where k is Boltzman's constant.

Similar considerations show that the fractional concentration of vacancies in thermal equilibrium is given by

$$n_f = \exp - \left(\frac{\Delta E_f}{kT}\right)$$

$$= \exp \left(\frac{\Delta S_f}{k}\right) \exp - \left(\frac{\Delta H_f}{kT}\right)$$

where ΔE_f is the free energy change per vacancy added and ΔH_f and ΔS_f the corresponding changes in enthalpy and entropy for vacancy formation. Substituting for w and n_v in equation 1.5 gives

$$D = \alpha a^2 f z \bar{\nu} \exp \left(\frac{\Delta S_m + \Delta S_f}{k}\right) \exp -\left(\frac{\Delta H_m + \Delta H_f}{kT}\right)$$

Assuming a temperature dependence for f the following relations are obtained

$$Q = \Delta H_m + \Delta H_f - C \qquad (1.6a)$$

$$D_o = \alpha a^2 z \bar{\nu} \exp \left(\frac{\Delta S_m + \Delta S_f}{k}\right) \qquad (1.6b)$$

where $$C = R \frac{\partial \ell n f}{\partial (1/T)} \qquad (1.6c)$$

Zenner gave a semi-empirical method for determining ΔS_m in terms of elastic constants and ΔH_m, so allowing a comparison with D_o for the case of interstitial diffusion. The calculated values give order of magnitude agreement with good quality experimental data. Zenner applied a rationalised approximation of the method to vacancy diffusion and obtained a similar agreement except for some bcc metals. Several authors have[20,48] attempted to extend and refine Zenner's theory.

The formulation of the entropy and enthalpy changes are based

on solid state models which are generally too complex to allow any but an approximate calculation, and although these are less accurate than experimental values determined from thermal expansion and quenching experiments, they are sufficient to indicate in simple cases the operative mechanism and the validity of the formulation. Huntington and Seitz[231] calculated the activation energy for the interchange, interstitial and vacancy mechanisms in the case of copper and found by comparison with the experimental value that the vacancy mechanism was clearly indicated. The calculations have been extended to other metals, and refinements and corrections have been added by Brooks[49], Amar[50] and other authors. A summary of these calculations has been given by Lomer[51].

1.4.2 Correlation Effects

Bardeen and Herring[52] first pointed out that many mechanisms would impose certain restrictions on the successive jumps of a diffusing atom so that they are not truly random, and that if an atom requires a defect at a neighbouring site correlation effects arise. After a tracer atom has made one exchange with a vacancy, the vacancy is immediately available to effect a second jump of the atom in the reverse direction, hence the probability is greater than random that the next jump of the tracer will be a reversal of the first.

The problem of calculating f the correlation coefficient can be reduced to evaluating the average cosine of the angle between

successive atom jumps. This has been done by a matrix method by Le Claire and Lidiard[53] and applied to self and impurity diffusion in cubic crystals and by Mullen[84] to non-cubic crystals. Howard[55] has discussed the effect for diffusion by a divacancy mechanism. A method introduced by Compaan and Haven[56] makes use of an analogy between the flow of vacancies in the lattice and the flow of electric charge in a network of resistors. In many cases the network equations were solved exactly, and for others a network was built and the important parameters were determined experimentally. Some of the values given by Compaan and Haven for self-diffusion by the vacancy mechanism are 0.781 for face-centered cubic, 0.727 for body-centered cubic and 0.781 for hexagonal close-packed cubic lattices. For tracer impurity diffusion the correlation factor will in general be temperature dependent since the effect depends upon the various jump rates of the impurity and the solvent atoms[53,57]. For self-diffusion in a cubic lattice f is a geometrical factor that depends only on the crystal structure and the atomic mechanism, a determination of f therefore can indicate the mechanism in simple cases[58,59].

1.4.3 The Isotope Effect

If a tracer element has a suitable pair of radioactive isotopes then the correlation factors can be obtained from tracer diffusion studies by using the isotope effect.

Wert[60] has shown that the jump frequencies of two different isotopes α and β of the same element diffusing in a lattice can be related to the atomic masses in the following way,

$$\frac{w_\alpha}{w_\beta} = \left(\frac{m_\beta}{m_\alpha}\right)^{\frac{1}{2}}$$

if it is assumed that they have the same activation energy. From equation (1.5) it follows that the diffusion coefficients D_α and D_β will differ because of the difference in the jump rates w_α and w_β, and further if the correlation factors are dependent upon w_α and w_β and other jump rates, as in impurity diffusion, then f_α and f_β will also differ.

If the difference is expressed as follows:

$$\frac{D_\alpha - D_\beta}{D_\beta} = \frac{w_\alpha f_\alpha - w_\beta f_\beta}{w_\beta f_\beta} = \left(\frac{w_\alpha - w_\beta}{w_\beta}\right)\left(1 + \frac{w_\alpha (f_\alpha - f_\beta)}{f_\beta (w_\alpha - w_\beta)}\right)$$

then it can be shown that

$$\left(\frac{D_\alpha}{D_\beta} - 1\right) = \left(\left(\frac{m_\beta}{m_\alpha}\right)^{\frac{1}{2}} - 1\right) f_\alpha \ .$$

This equation was first derived by Schoen[61] and rederivedmore rigorously byTharmalingam and Lidiard[62]. Mullen[63] and Le Claire[58] re-examined the problem by different methods and gave a more general form

$$\left(\frac{D_\alpha}{D_\beta} - 1\right) = \Delta K\left(\left(\frac{m_\beta}{m_\alpha}\right)^{\frac{1}{2}} - 1\right) f_\alpha$$

where ΔK is associated with the translational energy of the diffusing atom at the saddle-point.

Experimental results yield the product $f\Delta K$. For self-diffusion where f is known for each diffusion mechanism, the results are usually consistent with only one mechanism and give a ΔK value. From impurity diffusion results f cannot be

obtained without knowing ΔK. Barr and Munday[64] proposed the empirical relation that ΔK is approximately equal to the activation volume for self-diffusion ΔV divided by the molar volume V, a relation that holds for all cases investigated to date. Le Claire[47] gives a relation for ΔK which depends on ΔV_f, the activation volume for vacancy formation. The activation volume measurements of Bonanno and Tomizuka[65] show that ΔK for impurity diffusion approximately equals ΔK for self-diffusion for In and Sb diffusing into Ag.

Although the experimental technique is demanding, the results obtained from isotope effect measurements are most powerful in deducing the details of the diffusion process. For close packed metals the results are consistent only with the vacancy mechanism. The study of this effect has also contributed to the complex problem of determining the defect structure and diffusion mechanism in bcc metals.

The correlation coefficient can be determined from measurements of the tracer diffusion coefficient and of the ionic conductivity in a pure ionic conductor[66,67], and also from the effect of solute additions on self diffusion[68,69].

1.4.4 The Temperature Dependence of D.

It is now convincingly established that diffusion in normal metals obeys the Arrhenius relation closely. Normal diffusion currently implies that the following empirical rules are approximately obeyed.

$\frac{Q}{T_m} \sim 36 \frac{cal}{^oK}$ $\qquad$ $\frac{Q}{L_m} \sim 16$

$10^{-1} < D_o < 10$ cm^2 per sec. $\qquad 30 < Q < 50$ k.cals per mole.

where T_m is the melting point and L_m the latent heat of fusion.

In the Arrhenius relation D_o and Q are taken to be independent of temperature and this is generally true for the range over which diffusion measurements are practical. If the correlation coefficient is temperature dependent then equation (1.6a) gives

$$Q = \Delta H_f + \Delta H_m - C \quad .$$

Le Claire[70] has shown that a small but definite variation in the correlation term C is to be expected in tracer impurity diffusion and that Q should increase slowly with decreasing temperature. This kind of variation would lead to slightly depressed values of D at low temperatures, however the variations that have been reported are comparatively large and generally show an enhanced D value. This has been taken to indicate the dominance of some other effect.

Nowick and Dienes[71] have examined the possibility of curvature of the Arrhenius plot. Using the thermodynamic theory of activated processes and assuming a monovacancy mechanism, they show that if the activation enthalpy is temperature dependent then the plot will have a small curvature and they derive an expression which gives an absolute value for this.

The corresponding values calculated from the experimental data of several investigations were found to be higher by at least one order of magnitude and from this it was concluded that the observed curvature was not due to an inherent effect but to the existence of more than one mechanism of diffusion. Diffusion down dislocations is generally taken to be the additional mechanism and at lower temperatures the contribution from this becomes increasingly significant. The contribution of a divacancy and possibly a trivacancy mechanism has also been suggested.

For gold the curvature is relatively small but a lively controversy has developed, mainly on account of the interpretation of the quenching and annealing experiments[72,73]. Stoebe and Dawson[74] attempt to fit the self-diffusion data with a relation that allows for a temperature dependent energy of migration and Wang et al.[73] give an equation based on a monovacancy - divacancy model. These interpretations are criticised by Seeger[75] who examines all the experimental data and concludes that the Arrhenius equation given earlier by Mackin et al.[76] is the best fit over the range of temperatures covered, and suggests that the deviation of experimental points from this equation can be accounted for either by a small divacancy contribution at high temperatures or by a weak temperature dependence of the activation energy due to monovacancies or by both. In order to determine the relative contributions of these effects Seeger analyses the curvature using a model similar to that previously developed[72] for the case of nickel. This gives an equation for the temperature dependence of the diffusion coefficients which contains five

parameters, and by using the self-diffusion data and the vacancy concentration data[77] a set of parameters are obtained which are shown to be the best self-consistent values.

During the last few years much attention has been given to diffusion in bcc metals. A number of these β-Ti, β-Zr, β-Hf γ-U, V and Cr show diffusion properties that are not normally found. (See the review by Le Claire[78].) They do not obey the Arrhenius equation, and they have D_o and Q values that are anomalously high or low. The favoured explanation is based on the hypothesis that there are two or more mechanisms operating. An analysis on this basis shows one of the mechanisms, the one dominant at high temperatures, to have the normal D_o and Q values, leaving the second as the anomaly to be identified. Although convincing suggestions have been given, accounting for this by dislocation and impurity effects, it is unlikely that the matter can be resolved before the mechanisms of diffusion in bcc metals have been verified. Lundy[79] has recently emphasised that the observed pressure effects[80] cannot be reconciled by the present models.

1.4.5 Non-equilibrium Concentration of Defects

Many striking changes in the properties of solids result from an excess concentration of point defects. The embrittlement produced by irradiation and the pinning of dislocations[81] are examples of the effect. By the study of these changes it is possible in principle to investigate the properties of defects and the way in which they influence various processes, however

the effects arise from complex interactions making interpretation possible only in the simpler cases.

Quenching from high temperatures can freeze in a high concentration of vacancies[82,83], then by a subsequent experiment the change in some property can be measured as the vacancies are annealed out. Electrical resistivity measurements of thin wires have been used to obtain activation energies of vacancy formation and of vacancy migration[84,85]. Suitable irradiation can produce excess vacancy and interstitial pairs sufficiently removed from one another to allow the study of the migration, the resistivity and the concentration of these defects[86,87,88]. Plastic deformation is particularly suitable for the study of a steady state excess of vacancies and can be used to give an approximate value of the vacancy lifetime[89,90].

Since the diffusion coefficient is proportional to the vacancy concentration, and at low diffusion temperatures the vacancy excess can be much greater than the equilibrium value[91], it follows that D can be appreciably enhanced. Of the many experiments that have been made to measure the effect, a significant number have reported large enhancements of diffusion but the balance of evidence at this time appears to favour no enhancement (for a critical review see Barry[92]). Lomer[93] and Dienes and Damask[94] have calculated the enhancement in the diffusion penetration that would result under the most favourable experimental conditions from largely enhanced D values and they have shown that this is too small to be detected. Microdiffusion experiments[94,95] have reported enhancements in agreement with theoretical predictions, and further indirect evidence has been

obtained from other experiments. These indicate enhancements in the form of ordering during irradiation[96], overaging, enhanced precipitation[97] and high growth rates in segregation[98].

1.5 Impurity Diffusion in Pure Metals

The rate of diffusion of impurity atoms added to a pure metal in tracer amounts is found to be different from that of self-diffusion of the solvent atoms. At concentrations less than 1 per cent, a tracer atom moves in a solvent lattice completely isolated from other impurities, its motion however is quite different from a solvent atom. The following have been suggested as the cause - a size effect, a valence effect and a correlation effect.

Overhauser[99] considering the atoms as hard spheres calculated both the elastic strain in the region surrounding the impurity and the change in barrier height for motion of the impurity resulting from this strain and found the energy of motion decreased by an amount proportional to the dilatational strain. According to this result, impurities that expand the lattice diffuse faster than those that contract the lattice and both somewhat more rapidly than the solvent atoms. Swalin[100] has employed a similar model considering also the compressibility of the impurity. The predictions of the model are only in fair agreement with experiment, and not consistent with slow-diffusing impurities.

In considering electrostatic interactions, the impurity is assumed to fit exactly into the lattice and to interact with the Fermi electrons in such a way as partially to screen the excess

charge of the solute. Lazarus[101], following Mott[102], assumes that the field around the impurity can be described by an approximate solution of the Thomas-Fermi equation of the form

$$\Delta V(r) = \frac{Ze}{r} \exp(-qr)$$

in which the screening parameter q is given in terms of the Fermi energy E_m by $q^2 = kE_m^{\frac{1}{2}}$ and Ze is the excess charge. The interaction energy between an impurity and a neighbouring solvent ion at a distance r_o is $\Delta E_c(r_o) = e\Delta V(r_o)$. Considering ΔE_c to be a perturbation to the normal interionic energy, changes in energy around the impurity can be calculated relative to the solvent value. If it is assumed that the electron distribution remains unchanged when a solvent ion is removed, the change in the energy of formation of a vacancy adjacent to the impurity would be $-\Delta E_c$, and the change in the energy of motion ΔH_2 treated as a result of the corresponding change in the appropriate elastic constants. Using this simplified model Lazarus derived expressions for the activation energy and the frequency factor of the impurity as changes relative to the values for the pure solvent. Activation energies for the diffusion of a number of impurities in copper and silver were calculated and compared with experimental values. The fairly good agreement found in the case of silver was considered somewhat fortuitous because of the approximations that were made. Alfred and March[103] and Fujiwara[104] applied exact solutions of the Thomas-Fermi equation to the calculation of ΔE_c but obtained only marginal improvement.

Le Claire[70] re-examined the electrostatic theory of Lazarus and proposed a model which allows a more direct estimation of the

difference in the activation energy of motion of an impurity and a solvent atom. This is taken to be the difference in electrostatic energy between the configuration corresponding to the impurity at the saddle point and the impurity at the equilibrium position. The sum of the energy differences $\Delta E_c + \Delta H_2$ is then found to depend only on the choice of the saddle-point configuration. Le Claire also emphasises the effect of the correlation factors. As already stated, in pure metals this is a geometrical factor whereas for impurity diffusion the correlation factor f_2 depends on the relative rates of the various kinds of jumps, each of which will vary differently with temperature and so cause f_2 to vary with temperature. This effect contributes significantly to the change in the activation energy ΔQ in the form shown in the equation

$$\Delta Q = \Delta H_2 + \Delta E_c - R \frac{\partial \ell n f_2}{\partial (1/T)} \quad .$$

The calculation of this term requires the experimental values of the frequency factors. The agreement between the theoretical and the experimental values was found to be good for the electropositive impurities but poor for electronegative impurities in noble metal solvents. Le Claire states that the reason for the discrepancy of the electronegative impurities is that the Z values corresponding to the valency are not appropriate and gives the values required to obtain agreement. He also suggests that the Thomas-Fermi potential is a less adequate description of the charge distribution around an electronegative ion than around an electropositive ion.

Rothman and Peterson[105] have measured the temperature

dependence of the correlation factor for impurity diffusion of Zn in Ag by the isotope-effect technique and also the temperature dependence of the various jump frequency ratios by the effect produced by increasing Zn impurity content and obtain results in general agreement with the Le Claire theory.

Theories following Le Claire's treatment have been derived for the hexagonal close packed structure by Ghate[106] and for the body-centred cubic structure by Peterson and Rothman[107] and extended by Le Claire[108], each showing areas of agreement with experiment.

Although the electrostatic theory of impurity diffusion has achieved considerable success in the case of monovalent metal solvents, two assumptions require to be noted. The Thomas-Fermi potential only gives a poor description of the distribution about an impurity, and for metals with a high density of states at the Fermi surface, it shows appreciable deviations from the more accurate oscillating potentials of March and Murray[109], also the saddle-point model of Le Claire is an arbitrary one although it does give good agreement with experiment.

The presence of an impurity may appreciably alter the jump frequencies of neighbouring solvent atoms; at tracer concentrations this would produce no measurable effect, but as the concentration is increased, the changes in the solvent diffusion rate would become measurable. Lidiard[68] has shown how this effect can be used together with impurity diffusion results to obtain the impurity correlation factor. Howard and Manning[69] have reanalysed the problem and removed the assumption that all solvent atom jumps occur with a common correlation factor. Gibbs[110]

and Peterson and Rothman[107] have applied the Lidiard analysis to the bcc structure. The results from analyses of this sort, combined with isotope effect measurements, provide a powerful tool for obtaining detailed information on the various jump frequencies near an impurity-vacancy pair.

1.6 Paths of High Diffusivity and the Near Surface Effect

The defect structure of any crystalline material contains line and plane defects in addition to point defects. These are observable as dislocations, grain boundaries and free surfaces. In and around these defects the lattice structure is known to be destroyed or disturbed so that in this region the atomic process of diffusion is expected to be different. The diffusivity in the defect is found to be high and also characteristic of the defect, and so diffusion measurements with short-circuiting paths present will not only reveal the effect that is produced on the diffusion results but may also be used to study the diffusion mechanism in the defect and the nature of the defect.

1.6.1 Dislocation Diffusion

In a well annealed single crystal the dislocation density is found to be 10^6 to 10^7 dislocations per square centimeter, and these are distributed randomly. At high temperatures the diffusion that takes place through the lattice is much greater than from other paths, but at lower temperatures, diffusion by short-circuiting paths becomes predominant, and the effect is seen as an enhanced diffusion coefficient in the Arrhenius plot.

Dislocation diffusion has been observed in several investigations[111,112,113] and has often been identified in the tail of the Gaussian penetration plot as an enhancement. Hart[114] using a random walk analysis derived an expression for D, the diffusion coefficient determined from the penetration measurements, which leads to the equation

$$\frac{D - D_\ell}{D_\ell} = \frac{1}{3} da^2 \frac{D_d}{D_\ell} \exp\left(\frac{V}{RT}\right) ,$$

where D_ℓ is the true lattice diffusion coefficient, D_d is a defined dislocation diffusion coefficient, d is the dislocation density, a is the lattice parameter and V is the binding energy of a tracer atom to a dislocation. If it is assumed that dislocation diffusion follows the Arrhenius relation, then the above equation can be used to determine the parameters of the process. The conditions for the observation of Hart enhancement has been discussed by Lidiard and Tharmalingam[115] and by Harrison[116].

Harrison has described three types of diffusion behaviour. His types A and C are limiting cases where lattice diffusion occurs with only slight effects from dislocations and where dislocation network diffusion occurs with only slight effects from lattice diffusion. For a semi-infinite geometry and unidirectional diffusion from a plane source he points out that Gaussian penetration should be observed for both types. Harrison's type B is that for which non-negligible contributions exist for transport by both mechanisms and the concentration distribution does not approximate to any simple form. For some of these cases, if the concentration profile could be observed as a function of time, the behaviour would

initially be type C and would develop into type B and ultimately type A. Lundy and Pawel[79] have observed a marked type B diffusion, using a microsectioning technique, at low temperatures and short time anneals in tungsten. This shows a penetration with complete departure from a Guassian distribution and the authors emphasise the possibility of misinterpretation if the experimental measurements are insufficiently sensitive.

Lothe[118] has indicated that there must be at least two paths of high diffusivity in a dislocation core in order that diffusion should not be inhibited by correlation effects. Li[119] suggests that diffusion does not take place in the core but over the inner surface of a dislocation pipe by a surface diffusion-like mechanism. Interchange of atoms in the core can also take place in the model suggested by Love[120]. He considers the core of an edge dislocation to contain the last line of filled sites in the inserted plane of the dislocation and the line of vacant sites into which that plane would grow by negative climb. The proposed mechanism depends upon atoms being displaced from the last line of filled sites into the line of vacant sites forming an interstitial defect in the latter and a vacancy in the former. Love shows how the migration of these defects leads to correlated diffusion and illustrates the application of the model to dislocation arrays and grain boundaries.

1.6.2 Surface Diffusion

Surface diffusion is characterised by very high diffusion coefficients and low activation energies. There are few quantitative results and these show little evidence of good agreement. There are several reasons for this. The presence of minute traces of

impurities produce large changes in surface properties and processes. Surface diffusion varies with orientation and direction and is very much dependent on surface condition. For most experimental conditions there are effects of volume diffusion and of surface evaporation that are difficult to take into account. Surface diffusion theory has been developed in the same way as the theory of diffusion within the crystal. Free energy considertions lead to formation and migration energies of the diffusing atom, and an Arrhenius relation has been assumed. There are several difficulties in developing the model. Few details are known of the structure of real surfaces, such as the nature of the atomic sites, atomic bonding and depth of the surface layer and little is known about surface processes, especially atomic adsorption and atomic migration. Mathematical treatments of surface diffusion have been given by several authors[121-123], the solutions correspond to the various source conditions that can be used. Although the similarity of surface and grain boundary diffusion has been emphasised[124], it is a grain boundary grooving technique[125] that is most commonly used in experiment.

Several developments have taken place in recent years that can be expected to assist in surface studies. There are, for example, improved ultra high vacuum facilities, new methods of surface examination (see review by Reviève[126]) and methods of analysis which take account of volume diffusion[124].

1.6.3 The Near Surface Effect

Several investigations have reported that in a region very near ($\sim$ 1 micron) to the surface the concentration distribution varies in a way that is anomalous when compared with the volume diffusion that occurs at deeper penetrations. This shows as a region of steeper slope in a Guassian penetration plot and is generally described as having a lower diffusion coefficient. The effect may be very marked in some diffusing systems and undetectable in others. Lundy and Pagett[127] have investigated the effect for the diffusion of cobalt-58 and cobalt-60 in mono-crystalline silver at 927°C. They found that in the near surface region the concentration distribution is not Gaussian and that the effect can be removed by longer anneals. The investigation was able to eliminate all but one of the suggested causes of the effect, the remaining suggestion, described as "the propensity for solute segregation to the surface", could not be tested. Similar effects have been found to be due to other causes[128]. The formation of a chemical compound at the surface which inhibits the diffusion of the tracer has been found by several workers[129].

1.6.4 Grain Boundary Diffusion

Although it has always been known that the properties of metals are affected by the presence of grain boundaries, it is only in recent years that the effect produced on diffusion has been investigated. The difficulty of such an investigation is indicated by some of the methods that were used in the early experiments. Most of these observed the effect by varying the

grain size of specimens which were otherwise similar. Dushman and Kohler[130] and Clausing[131] demonstrated that the rate of diffusion of thorium to the surface of a thoriated tungsten wire increased with decreasing grain size by measuring the electron emission from the surface. Langmuir later interpreted the results using the Langmuir-Dushman[232] relation and obtained activation energies for grain boundary and volume diffusion of 90 and 120 kilocalories per mole respectively.

Rhines and Wells[132] observed that when zinc specimens thinly coated with copper were heated at 215°C the copper colour vanished "presumably by diffusion", and further that the copper colour took six times longer to vanish from the surface of a single crystal than it did from the surface of a polycrystal. Other observations of the high diffusivity of grain boundaries were made by microscopy[133] and by chemical analysis[134].

The work of Smoluchowski and of Turnbull in 1949 signifies the start of an active period of grain boundary diffusion studies. Achter and Smoluchowski[135-138] measured the diffusion of silver in [100] tilt boundaries of copper. The experimental method was based on etching and metallographic examination and the analysis was carried out using the Gaussian and the Arrhenius relations. The results given were 38 and 24 kilocalories per mole for the activation energies of volume and grain boundary diffusion respectively. They found that the rate of grain boundary penetration increased as the difference in relative orientation of the adjacent grains increased and also that coherent boundaries were indicated by a drop in the penetration value. Using radioactive silver Turnbull[139] measured self

diffusion in single crystal and in polycrystalline specimens by a surface counting technique and calculated diffusion coefficients from the normal Gaussian penetration plots. At lower temperatures the grain boundary coefficients were 2 to 6 times larger than the volume diffusion coefficients. Similar results were obtained by Fensham[140] for tin. Barnes[141] developed an etching technique which revealed concentration contours of copper diffusing in nickel grain boundaries.

In 1951 a much needed mathematical analysis of simultaneous grain boundary and lattice diffusion was given by Fisher[142]. The solution contains several approximations but it is easily applied and effective in assessing the contributions from the two processes.

Hoffman and Turnbull[143] redetermined the self diffusion of silver by sectioning thin layers and using the Fisher analysis. The solution was found to show reasonable agreement with the data and gave coefficients which were independent of grain size and larger by several orders of magnitude. Flanagan and Smoluchowski[144] measured the diffusion of zinc into copper using the same etching technique but basing the interpretation on a form of the Fisher equation. The results showed an orientation dependence similar to that found with silver diffusion in copper. This was taken to indicate a variation of the activation energy with the orientation, a feature that was to form a basic part of the Smoluchowski model[145] of grain boundary structure. This work was continued by Couling, Haynes and Smoluchowski varying the basic method slightly with the use of radioactive isotopes, autoradiography and bicrystals. They

observed a variation in the diffusion of silver in the boundary plane of copper bicrystals for low and intermediate tilt angles; diffusion was rapid in the direction of the dislocations parallel to the common cubic direction and less rapid in the direction perpendicular to this[146]. The penetration of iron in the [011] tilt boundary of 3 per cent silicon iron bicrystals was found to show a similar dependence on orientation[147]. Huntington and co-workers measured the grain boundary self diffusion in zinc[148] and in cadmium[149] using polycrystals, the sectioning technique and the Fisher solution. In this work the ratio of grain boundary to volume diffusion activation energies was considered to be unduly high and this has been taken to indicate shortcomings in the Fisher solution[228], and in the method of data analysis[160]. Yukawa and Sinnot[150] measured the grain boundary diffusion of nickel into copper bicrystals by autoradiography and also determined the orientation dependence. Preferential penetration was observed at low boundary angles and the activation energy was taken to vary with orientation.

In 1954 Whipple[151] gave an exact solution of simultaneous grain boundary and lattice diffusion. The model was the same as that assumed by Fisher but the solution is in integral form.

A third investigation of silver self diffusion was made by Turnbull and Hoffman[152] using bicrystals with a common [100] direction, the sectioning technique and the Fisher analysis. Diffusion parallel to the common direction of symmetric tilt boundaries misoriented at 9°, 13°, 16° and 28° was measured at temperatures from 400°C to 525°C. The grain boundary diffusion

coefficients were found to increase by a factor of 500 as the misorientation increased from 9 to 28 degrees and gave activation energies that were independent of misorientation and approximately the same in value as that determined from polycrystalline specimens. The authors interpreted the results in the following way. They assumed that the preferential diffusion into low angle boundaries took place by diffusion along dislocation pipes of diameter ℓ, the axis of which were the dislocation lines, and that the boundary width δ changed with boundary angle θ as

$$\delta(\theta) = \frac{\ell^2}{a} 2 \sin\left(\frac{\theta}{2}\right)$$

where a is the lattice spacing. The observed grain boundary diffusion coefficient D' is effectively D_p the coefficient for diffusion along the dislocation pipes, so that

$$D'\delta = D_p \frac{\ell^2}{a} 2 \sin\left(\frac{\theta}{2}\right) .$$

Values of D_p were determined from the data and found to be independent of θ over the range considered, giving agreement with the Burgers model for small angle boundaries and with dislocation pipe theory. Further confirmation of this interpretation was obtained by Hoffman(153) who measured the ratio of the diffusion penetration, parallel and perpendicular to the dislocation lines and found that it decreased as the boundary angle increased. Self diffusion measurements on lead bicrystals(154) were essentially in agreement with the results for silver. Dislocation enhanced diffusion was convincingly demonstrated in polygonised silver single crystals by Hendrickson and Machlin(155) and subsequently by others(112,113).

At this point in time a difference in the interpretation of

the experimental results was to emerge. Smoluchowski and co-workers had not observed preferential grain boundary diffusion into copper for boundary tilt angles less than 18 degrees in the case of silver and 10 degrees in the case of zinc. On this basis they concluded that preferential diffusion did not occur in isolated dislocations but only in highly distorted crystalline regions. As the boundary angle increases the dislocations start to bunch together, as described in the Smoluchowski model and only then does preferential diffusion occur. Further the variation of penetration with orientation was taken to indicate a change in the activation energy. Turnbull and Hoffman showed that according to the Whipple model the failure to detect any preferential grain boundary penetration could still imply grain boundary coefficients several orders of magnitude larger than volume diffusion coefficients, and that this could arise as a result of the resolution of the technique.

The solution of Suzuoka[159,160], although derived in the same way, is based on boundary conditions that are different from those of Whipple. The models proposed by Whipple and Fisher assume the source at the free surface to be of constant concentration, whereas the source assumed by Suzuoka is one with a finite amount of material which suffers depletion during the experiment. The conditions of tracer diffusion are described only by the Suzuoka solution although the others also assume diffusion coefficients that are independent of concentration. Suzuoka adapts the solution to the experimental technique of sectioning polycrystals, taking into account the total length of grain boundaries on the free surface and using a self consistent

analysis of the experimental data to separate lattice and grain boundary diffusion. The method was used to measure the tracer diffusion of cobalt in γ-iron[161].

A quantitative examination of the detail of the grain boundary region was made by Austin and Richard[162] by diffusing nickel into copper bicrystals and measuring the concentration distribution by the microprobe analyser. Symmetrical bicrystals with tilt angles of 8°, 22°, 30° and 45° were annealed at 750°C for various periods of time. The nickel electrodeposited on the surface was 125μ thick and was diffused both parallel and perpendicular to the common cubic direction. The following were the main conclusions:- the grain boundary coefficients showed concentration dependence above 3 per cent nickel for 45° boundaries and above 0.5 per cent nickel for 30° boundaries; grain boundary diffusion decreased rapidly above 5 per cent nickel concentration; there was a negligible increase in penetration with time above 10 per cent nickel concentration; for concentrations less than 0.5 per cent nickel the orientation dependence varied according to the dislocation model. Poor agreement with the Fisher and the Whipple solutions was concluded, mainly on the basis of the concentration dependence of the results, and partly on account of unpredicted minima observed at the grain boundary. The need for a solution in which the grain boundary coefficients are concentration dependent was emphasised. Austin and Richard[163] measured the diffusion of gold into 45° copper bicrystals by the same method. The electroplated gold was 125μ and 0.5μ thick so that analysis could be made both by the Whipple and the Suzuoka solutions, and

anneals were made at 760°C and 706°C. A decrease in the grain boundary diffusion coefficient with increasing solute concentration was again observed, but the decrease was less for gold than it was for nickel. This was contrasted with the change in chemical lattice diffusion which increases for increasing colute concentrations in the case of gold but decreases in the case of nickel relative to the solvent. For the thick source the conclusions were similar to those in the case of nickel. For the thin source it was concluded that the Suzuoka solution was to be preferred although it did not take into account diffusion along the surface towards the grain boundary, a factor which was observed to be significant. The lattice diffusion coefficients at low concentrations determined by this method are about twice as large as the tracer diffusion results.

A study of the effect of solute impurity and of orientation on the self-diffusion of lead was made by Stark and Upthe grove[164]. Bicrystals with symmetrical tilt and with twist boundaries were grown from zone refined lead and from lead containing varying amounts up to 1.5 per cent of tin, thallium, indium and bismuth. A layer of radioactive lead 40 microns thick was used, the penetration was measured by autoradiography and the Fisher and Whipple solutions were applied in the same way as was used by Yukawa and Sinnott[150]. The grain boundary diffusion parameter $D'\delta$ was found to decrease up to 50 per cent with increasing impurity content. The decrease in the activation energy with increasing impurity content was stated to be quite definite in the case of thallium, less pronounced in the case of tin and indefinite in the case of indium. The authors suggest that the observed decreases

are partially attributable to a decrease in the effective width of the grain boundary. An increase in the diffusion parameter and a decrease in the activation energy were observed with increasing angle of tilt for pure lead self-diffusion. The volume activation energy was given as 25 kilocalories, in good agreement with Okkerse[165] and the limiting value of the boundary activation energy as 5.5 kilocalories per mole. Gertsriken and Revo[166] investigated the grain boundary diffusion of tin and antimony in copper and in 0.1 per cent alloys of tin and of antimony in copper. They report that 0.1 per cent tin in solution in copper lowers D_o', the apparent pre-exponential factor for tin diffusion in the grain boundary, by 50 per cent but introduces no change in Q', the activation energy, and that 0.1 per cent antimony lowers D_o' by 13 per cent with no change in Q'.

The mathematical treatments represent the grain boundary as a uniform and isotropic slab of material of width δ within which diffusion obeys Fick's laws with a diffusion coefficient D' and the solutions permit D' to be determined from other measurable quantities only in terms of the grain boundary diffusion parameter $D'\delta$. The variation of δ with temperature and other parameters cannot be approportioned. For high angle boundaries the width has generally been taken as 5.10^{-8} cm.[142,161,163], although other values of two or three lattice spacing have also been used[164,167].

Some attempts have been made to determine δ from diffusion experiments in other ways. An absolute method suggested by Gertsriken[168] is based on the assumption that the amount of diffusant passing from the boundary into the grain is not significant

when $D' >> D$. By using the normal volume diffusion formula and substituting D' for D an absolute value of D' can be found, δ can then be determined from this and the grain geometry. In this way Gertsriken and co-workers obtained an average value of 10 Å for δ. Some confirmation of this value was given by Arkarov[169] and by Klotsman[170] and their co-workers from indirect measurements of the width δ in a study of internal boundary absorption in alloys. Bokshteyn and co-workers[171] in a study of the surface diffusion of tin in nickel powders have determined D' and δ independently; the value obtained for δ was several hundred angstroms.

Panteleyev and Metrikin,[172] using the Whipple form, calculate the total diffusant in a section well removed from the volume diffusion zone as the sum of two terms, M_1 the usual grain boundary term giving the amount of diffusant outwith the boundary slap and an additional term, M_2, giving the amount of diffusant within the boundary slab. $M_2 >> M_1$ is taken as an experimental condition for the absolute methods and the authors show that this and other conditions were not satisfied in the above cases. The authors show that if M_2 is appreciable then the penetration plot for the layerwise sectioning analysis (logarithm of concentration against penetration distance to the power 6/5) is no longer linear. They also suggest an analysis of this departure from linearity that can be used to indicate the value of δ and to specify the experimental conditions for determining δ by the absolute methods.

Klotsman and co-workers[173], in an analysis of the results of diffusion in polycrystals, used the Fisher solution to derive criteria for the conditions under which grain boundary diffusion

would predominate. The criteria were applied to nearly all of the published results and this showed that because of the distorting effect of volume diffusion more than half of these were unreliable. The reliable results allowed certain conclusions to be made about the diffusion parameters. In solvents with a face centered cubic structure the ratio of the activation energies Q'/Q were found to lie in the range 0.35 to 0.45, and the ratio $\delta D_o'/D_o$ in the range 10^{-11} to 10^{-5} cm. On this and on other evidence Klotsman and co-workers criticised the suggestion that diffusion in dislocations and in grain boundaries takes place by a simple vacancy mechanism[152,168,175] and extended the dislocation diffusion model proposed by Love[120]. Following this the elementary act of boundary diffusion was taken to be the migration and annihilation of the defects formed in the core of the dislocations by vacancies and interstitials. In metals with a low stacking fault energy, similar extended defects were taken to exist in the region between partial dislocations, and the elementary act of diffusion was taken to occur by an analogous process in which a number of participants co-operate.

Using a result of Pound et al.[44] which gives a measure of the reduction that would occur in the pre-exponential factor should diffusion take place by a cooperative instead of a non-co-operative single atomic process, Klotsman calculated values of D_o' and the ratio D_o'/D_o for metals of low staking fault energy. The qualtitative agreement that was achieved between the experimental and the theoretical values of D_o'/D_o and the difference in the experimental values between metals of low and metals of high stacking fault energy, were taken as confirmation of the proposed model.

At the suggestion of Klotsman a series of experiments is currently being carried out by Kaygorodov and co-workers to investigate the grain boundary diffusion of impurity elements in silver[176,177]. By diffusing impurities belonging to the same series of the periodic system as the solvent, it may be possible, following considerations similar to those in the case of volume diffusion, to obtain some indication of the mechanism of grain boundary diffusion. An active layer 1000 Å thick was evaporated on polycrystalline silver of unspecified grain size. After annealing the specimens were chemically sectioned and the concentration distribution determined from the activity of the removed layers and from the integral activity of the residue for the volume diffusion measurements, but only by the residual method for the grain boundary measurements. The temperature ranges, chosen so as to satisfy the Klotsman criteria[173] were 770°C to 950°C for volume diffusion and 200°C to 500°C for grain boundary diffusion, and the Klotsman[174] value (5.10^{-7} cm.) used for the grain boundary width.

The analysis was carried out in terms of a parameter α which is proportional to $D^{\frac{1}{2}}/\partial D'$, using the Fisher equation and making due allowance for grain geometry[157]. An Arrhenius-type plot (parameter α against 1/T) furnishes a quantity Q_α which is used in the following relation to give the grain boundary activation energy.

$$Q' = \frac{Q}{2} - Q_\alpha \quad .$$

The method, it is noted, assumes that the high temperature volume

diffusion data can be extrapolated to the grain boundary diffusion temperature range, but no experimental verification of this assumption is reported. For the diffusion of indium[176] and of antimony[177] into silver the results give $Q'/Q \sim 0.35$ and the ratio $D_o'/D_o \quad 10^{-3}$. This is taken to support the model of co-operative elementary acts of diffusion in grain boundaries, proposed by Klotsman[174], for a metal of low stacking fault energy. The values of Q and D_o were stated to be consistent with the electrostatic theory of impurity diffusion[101] and the values Q' and D_o' were also stated to follow the predictions of the theory.

The most significant feature of the results is the break in the temperature dependence of the parameter α. The Arrhenius-type plot shows a reversal of the slope at 250°C, but the significance of this is obscured because of the approximations and the inadequacy of the method.

1.7.1 The Measurement of Grain Boundary Diffusion

After diffusion from a free surface into a grain boundary, the concentration distribution of the diffusant is similar to that shown in Fig. 1. If the free surface and the grain boundary are normal to the plane of the figure and to one another, then the distribution can be analysed in terms of a grain boundary diffusion equation and this will furnish the volume and the grain boundary diffusion coefficients.

The two main types of analysis are as follows:

(1) the experimental distribution corresponding to that of Fig. 1

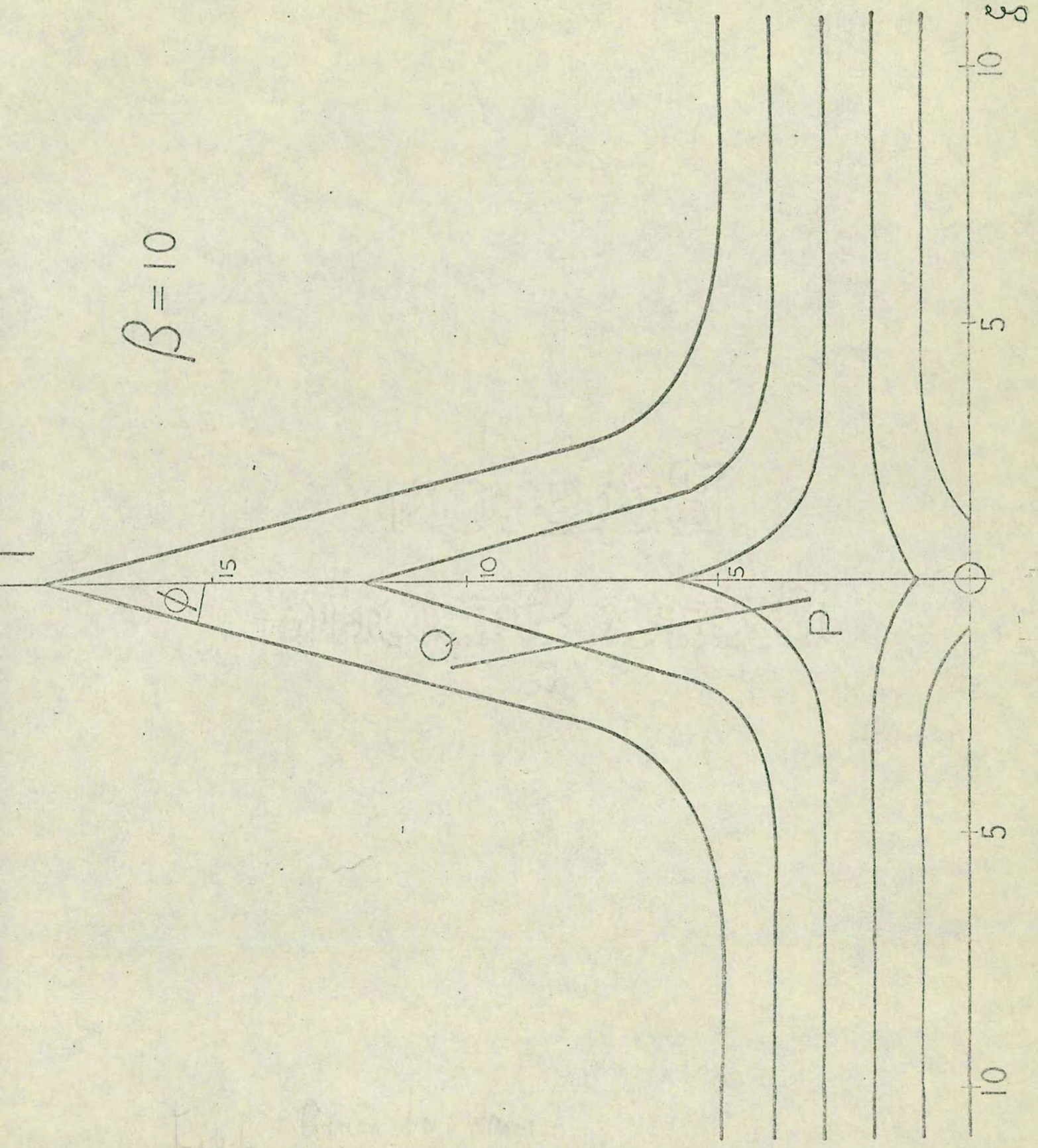

Fig. 1. Grain boundary concentration contours.

is compared with the theoretical distribution of the grain boundary equation, the comparison being made over the complete area or over some selected part of it;

(2) the specimen is sectioned parallel to the free surface and the amount of diffusant in each layer is measured, the penetration plot is then compared with the appropriate form of the diffusion equation.

A variety of other methods have been used, such as measuring the decrease of diffusant from the plated surface[178], measuring the increase of diffusant on the surface opposite to the plated surface[155], and measurements of the changes produced by sintering[179].

The sectioning method is to be viewed favourably mainly because it has proved to be the most accurate and reliable in measuring volume diffusion. In this case volume diffusion penetrations tend to be very small, some tens of microns in extent, while grain boundary penetrations may range up to twenty times larger, and so the method is required to measure with accuracy both the small and the large scale penetrations. The lathe sectioning form is frequently unsuitable because the minimum thickness of a cut, 20 microns, is comparable with the total penetration of the volume diffusion. Precision grinding is suitable for small penetration depths but the uniformity of sectioning is difficult to preserve over large penetrations[147] and this can be a critical factor. Both of these forms can be applied only to flat surfaces and are much less satisfactory with ductile or brittle material. Chemical sectioning is only suitable for very small penetrations and there are relatively few cases where a chemical polish or etch is known

to give uniform attack. It is obvious that the forms of sectioning that are suitable in the case of very small volume diffusion penetrations are not suitable for large grain boundary penetrations, and these conditions do occur in practice.

To examine the grain boundary region in detail demands a technique that will resolve high concentration gradients at low concentration levels on a macroscopic scale. The microprobe analyser was used by Austin and Richard[162,163] to examine the complete experimental distribution. Other abbreviated versions have been used. These include the measurement of the concentration distribution down the grain boundary[167], the measurement of the angle of contact ϕ between the boundary and a contour of known concentration[181], and the measurement of the penetrations to some given concentration level[150,164].

The mathematical analysis that is to be applied depends upon the experimental conditions. If the source is thick then the Whipple or the Fisher solution should be used. Now these solutions assume both a thick source of constant concentration and diffusion coefficients that are independent of concentration, but experimental investigations indicate that these two conditions cannot be satisfied simultaneously[152]. If the source thickness is chosen so as to avoid concentration effects, then source depletion is certain to occur and these solutions are no longer appropriate. On this basis the choice would appear to favour the use of tracer amounts of diffusant and the application of the Suzuoka solution. There are, however, other factors to be considered. After diffusion the amount of diffusant in the grain boundary is relatively small and in many cases it has been necessary to increase this by using

thick sources and by using polycrystalline specimens in preference to bicrystals, so as to make the amount measurable. In nearly all such cases, sources one to several hundred microns have been used and in most of these concentration effects are likely to have occurred.

The effects that are introduced by the use of polycrystalline specimens require discussion. The angles at which the grain boundaries meet the surface vary within a range; for an arbitrary plane in the specimen this range may cover all possible values, although for well annealed specimens the boundaries tend to stand normal in the near vicinity of the surface in order to lower the free energy. The misorientations of the grains and the boundary angles may assume all possible values and so the diffusivities of the boundaries vary from the volume diffusion value to the maximum grain boundary value and this may range over several orders of magnitude. The grain size is important. It must be sufficiently large for diffusion to occur only within the first monolayer of grains and for the diffusion in each boundary to be independent of that in the others, it must also be sufficiently small for the amount of diffusant to be measurable. Some of these factors have been considered elsewhere[159,217], but there are others which have not been discussed and which are likely to introduce some effect, for example the complex features of the grain pattern and the relative variation of the effects with temperature.

The diffusivity that is being measured is therefore an average value which corresponds to multivariate grain boundary conditions and it is unlikely that this can be related to any specific grain boundary condition. The result of each diffusion measurement must be quoted relative to specified grain boundary

conditions. For the intercomparison of results to be valid or for a theoretical interpretation of a series of experiments to be possible, the grain boundary conditions must be the same. This condition can best be satisfied by using specimens from the same bicrystal, although Smoluchowski achieved this by using the individual boundaries of a polycrystalline specimen. Bicrystals and a mechanical sectioning technique have been used in a few investigations but in nearly all of these cases it was found that a relatively thick source was necessary to measure adequately the diffusant.

1.7.1 Outline of the Present Work

The purpose of the work was to develop a more exact and general treatment of the method of autoradiography as applied to diffusion studies. The method was known to be effective both in detecting radioactive tracers in all sorts of applications - such as segregation[182] and surface diffusion[123] studies - and in revealing an amount of detail that is not observable by other methods, but its use in quantitative measurements has been strictly limited. The first problem was to develop a method of interpretation which could be applied quite generally to volume diffusion. Preliminary trials were to indicate a range of application and an accuracy sufficient to justify the extension of the method to the grain boundary case. This was particularly appropriate, for the method offered the opportunity of measuring grain boundary diffusion under a set of conditions thst were consistent and meaningful by using accurately oriented

bicrystals, a diffusant in tracer amounts and an analysis based on the Suzuoka solution.

Autoradiography has been used in a number of grain boundary diffusion studies[150,164,167,216,218], but most of these have used thick source conditions, and all of them have used an incorrect method of interpretation.

If the method proved sufficient to reveal the grain boundary zone in adequate detail then it could be used to further advantage. A number of authors have emphasised the need to make a detailed comparison of the several mathematical solutions with the experimental distribution. This was the main purpose of the investigations carried out by Austin and Richard, but it achieved limited success because of the concentration effects. It is clear that similar investigations using tracer diffusion conditions are necessary, and that a method suitable for this purpose requires to be developed.

In order to assess the value of the method and determine its limitations, the radioactive isotopes were chosen so as to be representative of very high, medium and very low energy emitters. The isotopes chosen on this basis were nickel-63, silver-110 and antimony-124, but these are also suitable from other considerations such as half-life, high specific activity and ease of deposition. The solvent chosen was copper partly because the facility for growing copper specimens was available, but a main consideration was that accurately known results should be available for comparison, and copper is one of the most widely studied metals.

Although the mathematical solutions predict that the concentrations within the grain boundary zone are comparable with the concentrations within the volume diffusion zone, for measurement by autoradiography, it is necessary that the film densities of these two zones should be comparable; with very high energy isotopes, however, an image spread occurs and this tends to cause the grain boundary image to lose its feature and merge into the image of the volume diffusion zone. For very low energy isotopes and for diffusion zones of small dimensions, it may not be possible to observe the image in adequate detail, simply on account of the resolution of the measuring technique. It is therefore to be expected that the range of application of the method will be limited by these and other factors.

1.8 The Nature of Grain Boundaries

Our immediate interest in the study of grain boundary diffusion is in the contribution it can make to our understanding of the diffusion process and to the development of the theory of diffusion, such studies however are no less important as a means of investigating the nature of the grain boundary defect. With the aid of the field ion microscope it has become possible to make observations that indicate the atomic arrangement of static grain boundaries in some refractory metals, and it is to be assumed that within the next few years the general structure of high angle boundaries will be established, however much is yet to be learned about grain boundary processes before the observed properties can be reconciled with the physical structure. Grain boundary diffusion is likely to prove a factor of particular

relevance in the development of a model that will account for all the experimental facts, and therefore it is not inappropriate at this point to review some of the features of our present knowledge of grain boundaries.

1.8.1 Earlier Models

For many years attempts to understand the properties of grain boundaries were dominated by the amorphous cement theory. Championed by Rosenhain[183] and built on the ideas Beilby[184] had developed as a result of studies of surface polishing and plastic deformation, the theory proposed that the crystals of the metal were surrounded and held together by a thin layer of the metal in an amorphous form whose properties corresponded to the supercooled liquid metal. Although the model gave reasonable agreement with many of the experimental observations of that time, it required the boundary layer to be appreciably thicker than was permitted theoretically and it could not account for the rapid diffusion in the boundary at relatively low temperatures. The rival concept that developed was the transition lattice. Hargreaves and Hill[185] argued that the forces which determined the atomic positions in the lattice also operated at the boundary, and that atoms occupied their correct lattice positions, except for one or two layers at the boundary; the atoms in these layers occupied compromise positions. They concluded that the boundary had definite structure in that a given boundary orientation always produced a definite pattern of arrangement of atoms, that pattern representing the lowest possible potential energy in the circumstances.

Chalmers[186] pointed out that according to the transition lattice theory, the grain boundary properties were dependent upon the orientation difference of the separated grains but that according to the amorphous cement theory they were not. By showing that slip in the grain was dependent upon this orientation, he provided strong evidence to support the transition lattice theory. The theory however could not explain some of the observed mechanical properties that were explained by the amorphous cement theory, notably grain boundary sliding and fracture, although it was a more satisfactory explanation of the physical structure.

Most of the subsequent theories that have been proposed retain the concept of the transition lattice. Each one proposes a different matching criterion in the transition layer to account for a particular property, and while giving quantitative agreement in this fails to explain other properties. To be acceptable a model is required not only to show agreement between the predicted and the observed properties but at the same time offer a boundary structure that is physically and theoretically realistic. The main difficulty in achieving this is reconciling the mechanical properties, some of which are best explained by a thick and viscous boundary.

1.8.2 The Dislocation Model

Burger[187] in discussing the boundaries between mosaic blocks in an imperfect crystal described how the transition of orientation from one mosaic block to another might be brought about by a system of

dislocation lines. This was clearly applicable to grain boundary misorientation and, following this, Burgers[188] and then Bragg[189] suggested that it was possible to consider the transition layer as a suitable array of dislocations. By this model a simple tilt boundary was considered to be a row of edge dislocations, a simple rotation boundary considered to be a square grid of screw dislocations and an arbitrary boundary considered to consist of a combination of sets of dislocations of both kinds (see van der Merwe[190], Frank[191]). The dislocation model gives an acceptable physical structure in the case of small angle boundaries and further, the theoretical calculations by Read and Shockley[192] of the variation of the grain boundary energy with orientation show good agreement with all the experimental results up to a misorientation of 20° and higher in some cases. Although the model gives only qualitative agreement with the observed mechanical properties, the dislocation structure is confirmed by the direct evidence of dislocation decoration and etching[193]. The Burger dislocation model is considered to break down at a misorientation of approximately 16°. Above this the dislocations overlap, lose their separate identity and produce a change in the physical structure of the model. Much of the evidence however suggests that there is no abrupt transition, the notable exceptions being grain boundary melting and segregation (see the review article by Weinberg[194]).

Most of the early models were concerned with proposing a structure that would account for the mechanical properties and in the attempt were essentially speculative, however in recent years direct structural studies have become possible and so the emphasis of the approach has been shifted.

Before describing the various models it is well to note the features of the mechanical properties that require to be reconciled. Zener[195] pointed out that the results of investigations involving small relative movement at the boundary were consistent with the hypothesis that boundaries behave in a viscous manner. Ke[196] carried out comprehensive investigations of dynamic rigidity, creep, internal friction and stress relaxation in aluminium and showed that the results satisfy the derived relationships given by Zener. There are other properties like microhardness, embrittlement and migration which suggest a liquid-like region of considerable width, and most important, the fracture behaviour, as Rosenhain[183] pointed out, is typical of a viscous amorphous fluid. Above a certain temperature characteristic of the metal there is deformation at the boundaries and fracture tends to be intercrystalline and, below this fracture, tends to be transcrystalline. Many of these topics are discussed in the review article by Aust and Chalmers[197].

1.8.3 Mott's Model[198]

The island model was Mott's attempt to reconcile the features of the mechanical properties with a transition lattice one or two atoms thick, and was the result of an idea inspired by Kê's experiments[196], namely that the act of sliding was due to local melting. Mott pictured the boundary plane to consist of islands where the atomic matching was good, surrounded by regions where it was poor, and assumed that the resistance to slip was negligible in the islands. The elementary act of sliding was suggested to occur by the disordering or melting of

the atoms around an island so that resistance to shear vanished locally as a result of thermal agitation. Regions of good and bad fit could then be imagined to be constantly shifting their position under stress and possibly even when there was no relative motion. This mechanism would be expected to produce a region of stress concentration skirting the islands.

Mott derived an expression for sliding, assuming that the activation energy of the process was the sum of a stress energy and an energy of melting, the former resulting from the work done in an elementary act of slip, and the latter, the free energy of melting, being a temperature interpolation of the latent heat of melting per atom. The same ideas were applied to the migration of a grain boundary during recrystallisation. The assumed elementary action was that a group of atoms at the edge of a strained grain disorders or melts and crystallises on to the adjoining unstrained grain, with work being done against the stress. An expression was derived for the rate of boundary migration in a similar way. Both equations however tend to give results that are high by comparison with experiment.

1.8.4 Kê's Model[199]

From his experiments on torsion in aluminium Kê had observed that grain boundaries behaved in a viscous manner at higher temperatures, however he pointed out that this could be attributed both to a layer of disturbed crystallinity and to an amorphous layer so that the viscous behaviour in itself was not conclusive of the boundary structure. In considering the internal friction experiments Kê assumed that the stress relaxation occurred by the

squeezing of individual atoms past neighbouring atoms following the mechanism proposed by Orowan[200] for creep. He then compared the activation energy for the stress relaxation with that determined for volume diffusion and that for steady state creep in several materials and found that in each material they were approximately equal. From this he concluded that the operative mechanism was the same in the three cases and that this would require the structure of the grain and the grain boundaries to be essentially similar.

In deriving an expression for the rate of sliding, Kê assumed that slip took place by the thermally activated movement of the vacancies or disordered groups in the disturbed crystalline structure of the boundary, and that the activation energy for this was the same as that for volume diffusion. Mott rejected this expression in favour of his own for several reasons and it is a fact that it gives poorer agreement with experiment. Further, one of the important assumptions made by Kê was shown to be wrong when it was found that the activation energy for stress relaxation is in general markedly different from that for volume diffusion. Both of the models assume that boundary shear is the mechanism of stress relaxation but Weinberg[194] states that this has not been clearly demonstrated.

Recently Walter and Cline[201], deforming polycrystals and bicrystals of pure aluminium in tension, have shown the sliding rate to be in agreement with the internal friction measurements of Kê and state that the observations are consistent with a viscous sliding mechanism.

1.8.5 Smoluchowski's Model[145]

Smoluchowski had observed that diffusion along grain boundaries varied with the misorientation of the grains[138] and in an attempt to explain this and the variation of activation energy he proposed that the structure of the boundary also changed with the misorientation. The sequence of changes for the case of a tilt boundary was described as follows. At small angles of misorientation he proposed that the dislocation model was applicable, and as the tilt angle increases so does the dislocation density. He suggested that enhanced diffusion takes place along the dislocations and that it is proportional to the dislocation density, but this occurred only for interacting dislocations and not for isolated dislocations. When the tilt exceeds about 15° the dislocations condense into groups forming misfit regions parallel to the tilt axis, separated by relatively undistorted regions. With increasing tilt each condensed group increases, more and more of the boundary consisting of misfit regions until for tilt angles greater than about 35° the misfit regions join up to cover the whole boundary plane. Introducing a tilt about an axis lying in the boundary and at right angles to the dislocation direction will be seen to produce a structure similar to the Mott island model for intermediate angles of tilt. The variation of the activation energy which is observed to decrease from a maximum at maximum misorientation to lower values at intermediate misorientations is shown to be the result of the structural changes. Theoretical expressions for the activation energy based on the model show good agreement with the experimental

values. The model is also taken to agree with the observed variation of boundary energy[197] and anisotropy of diffusion[146].

Several other models have been proposed since Smoluchowski's work, most notable have been those by Friedel et al.[202], Frank[203] and Li[204], Brandon et al.[205], Fletcher and Adamson[206] and Bollman[207, 208]. Some of these are the result of structural studies, based on the direct observation of grain boundaries at the atomic level. The Brandon model is an important contribution.

1.8.6 Brandon's Model[205]

For certain specific axes and angles of misorientation two grains separated by a boundary will hold a number of lattice sites in common and these sites will comprise a single three dimensional lattice called the coincidence lattice. The main parameter of the coincidence lattice is the reciprocal density of common lattice points Σ, which takes all odd values in the face-centered and the body-centered cubic systems. Boundaries to grains having these special misorientation relationships are called coincidence boundaries and these are specified relative to the coincidence lattice by σ the reciprocal density of coincidence sites in the boundary plane. The value of σ lies between 1 for a densely packed plane and infinity for a boundary passing between the planes of the coincidence lattice. The model does not define the degree of fit at the boundary, although the disturbance is shown to be dependent on the coincidence density and is one to two atomic diameter in extent.

Boundaries lying in coincidence planes of high density are expected to have low energy, so Brandon[205] suggests that

boundaries running at a small angle to these planes would take up a stepped structure with a maximum area in the high density coincidence plane, the steps being disordered regions. For an arbitrary boundary the steps form a terraced structure at the boundary. Deviations from the angular misorientations required for exact coincidence can be described by a sub-boundary network of dislocations superimposed upon the coincidence boundary. It was noted that the density of dislocations that could be introduced into the coincidence boundary without destroying coincidence was limited by the density of coincidence lattice at the boundary. Brandon gave a criterion for this which leads to an estimate of 0.42 for the proportional coverage of all possible orientations by the model in the cubic system, but emphasises that the model is not a general description of a high angle boundary.

Brandon points out that the model is an extension and combination of the work of Kronberg and Wilson[209] and Read and Shockley[192]. The former introduced the concept of the coincidence lattice and the coincidence boundary, later developed by Frank[203] and by Dunn[210]. The model of Read and Shockley for a twin boundary was described in terms of two arrays of dislocations, one a dense dislocation array which corresponds to the coincidence boundary in this case and a low density array equivalent to the coincidence lattice sub-boundary. The regions of good and bad fit are identified as a feature which is common to this and to the island model; Mott however regards all high angle boundaries as structurally equivalent whereas here the variation in structure is a characteristic of the model, and is

expected to show up in those properties which are strongly structure sensitive.

The model was developed as a result of the features observed in field ion microscope studies of tungsten and tungsten-rhenium alloys by Brandon and co-workers[211, 212]. Similar observations have been reported on other materials by a number of other groups[213] and further evidence to support the coincidence boundary model has been reported from studies using the high voltage electron microscope[214]. In contrast with this, a recent study of the electrical resistivity of grain boundaries[215] can be reconciled only with a boundary region some twenty times greater than the width indicated by transition lattice models.

1.8.7 The 'O' Lattice Concept

Bollman[207,208] has given a more general method for studying grain misorientation and grain boundaries which resembles the coincidence lattice approach. The lattice of the grains are considered as interpenetrating. The transformation which defines lattice 2 from lattice 1 is used in a way that produces another, the O lattice. This is the same lattice which is formed by all possible origins or 'O' points of the original transformation. The cells of this lattice are centered by these O points, which are also the locations where the two lattices fit optimally. The points of lattice 1 and 2 are associated with the nearest O point and the relationship between these points are referred to this O point. The pattern of lattice points for the various grain misorientations and the possible boundaries are studied

relative to the O cells. Planes containing a high density of O points indicate the best fit between grains and are therefore preferred as boundary planes. If the orientation of the boundary deviates slightly from a preferred plane then the boundary will become stepped. If a coincidence lattice exists then it is a superlattice of the O lattice. A crude measure of the boundary energy can be obtained from O lattice considerations, and the dislocation structure can be determined from the intersection of the boundary with the cell walls. Bollman suggests many applications of this concept.

CHAPTER II

SOLUTIONS OF THE DIFFUSION EQUATIONS AND THE ANALYSIS OF GRAIN BOUNDARY MEASUREMENTS

2.1 Fick's Equations

Fick's[1] mathematical treatment showed that the quantity of diffusing material passing per unit time through unit area normal to the diffusion direction is proportional to the concentration gradient, and defined D the diffusion coefficient as the constant of proportionality. For diffusion in the y direction only Fick's first law is written as

$$J = -D\frac{\partial C}{\partial y} \tag{2.1}$$

where diffusion takes place down the gradient and where the dimensions of D are L^2T^{-1}. This equation applies only to stationary flow, a more general form, Fick's second law, is obtained from it for concentrations that vary with time by using the conservation of matter

$$\frac{\partial C}{\partial t} = \frac{\partial}{\partial y}(D\frac{\partial C}{\partial y}) \tag{2.2a}$$

and if D is constant this becomes

$$\frac{\partial C}{\partial t} = D\frac{\partial^2 C}{\partial y^2} \tag{2.2b}$$

These equations can be made quite general so as to account for diffusion in three dimensions, anisotropic diffusion and diffusion in the presence of additional driving forces[27,28,29].

Fick's laws imply that C is a continuous function of y, which is true for macroscopic diffusion where distances are large by comparison with interatomic spacing, and also that diffusion occurs only in the presence of a concentration gradient, but this cannot account for many observations such as self-diffusion. A number of authors[219,220] have emphasised the statistical features of the process and derived laws assuming that a continuous process of random motion occurs as a result of the thermal agitation of the atoms. Le Claire[219] shows that if complete random motion can be assumed, as for self diffusion in a very low gradient, then equation (2.1) is valid but for diffusion in other cases the chemical gradient superimposes a driving force upon the random motion resulting in a nett drift of atoms, and the relation between the flux J and the gradient is not simple. This can be expressed in the form of equation (2.1) only by showing D as the appropriate function of concentration. The diffusion equations have been rederived on a phenomenological basis by several authors[15,221,222], and when expressed in the form of equation (2.1), D is found to be the product of two concentration dependent factors, one a mobility term effective even in the absence of a concentration gradient and the other a measure of the departure of the solid solution from ideality, the diffusion force being the chemical potential gradient.

Although the Fick equations are only approximate and can be applied only by making simplifying assumptions about D, it is the solution of these equations that is normally used to solve diffusion problems.

2.2 Volume Diffusion from a Plane Source

Fick's laws are more closely obeyed for diffusion under conditions of extremely dilute concentrations, and so studies using radioactive isotopes in tracer amounts have a greater theoretical significance, and are also preferred on experimental grounds. The simplest and possibly the best way of determining accurate diffusion coefficients is to obtain the concentration of the tracer as a function of distance after diffusion has taken place from a thin plane source of active isotope deposited on a free surface. In these conditions the problem reduces to solving Fick's second law for a constant diffusion coefficient and one dimensional flow. An exact solution for this is given by Crank[223] as

$$C(y,t) = \frac{C_o}{\sqrt{\pi Dt}} \exp - \left(\frac{y^2}{4Dt}\right) \qquad (2.3)$$

where diffusion takes place for a time t and C_o is the mass per unit area initially deposited on the free surface.

Equation (2.3) is of the same form as the normal Gaussian distribution, with the precision index corresponding to $\sqrt{2Dt}$. This quantity, the mean diffusion penetration, measures the average distance that the atoms diffuse after time t, the average being taken over a very large number. This relation is analogous to the Einstein[224] relation derived in random walk studies of the Brownian motion. At a penetration distance of $4.3\sqrt{Dt}$ the concentration falls to one per cent of its peak value.

The thin source conditions for which the above solution is considered to be valid has been defined more precisely by

Johnson[229] as $h^2/6Dt \ll 1$ where h is the thickness of the source.

2.3 Grain Boundary Diffusion Equations

2.3.1 The Smoluchowski Analysis

In this work the orientation dependence of grain boundary diffusion was determined by examining the boundaries of adjoining grains in a columnar copper specimen having preferred [100] orientation in the columnar direction, along which diffusion occurred from a thick source. The maximum depth of penetration of the diffusant was determined by etching and used to specify the orientation dependence. This was interpreted as a variation of the boundary diffusion coefficient with orientation, but it should be noted that the grain boundary diffusion coefficient is proportional to the square of the penetration depth only for low temperature annealing conditions.

In determining both activation energies the following formulae were used initially[137]

$$y^2 \sim Dt$$

$$D \sim \exp - \left(\frac{Q}{RT}\right)$$

where y, the maximum depth of penetration, was taken to occur at a constant concentration level of the diffusant and so, if anneals at two different temperatures are made, then

$$Q = R \frac{T_1 T_2}{T_1 - T_2} \ln \frac{t_2 y_1^2}{t_1 y_2^2} .$$

This formula is valid for the volume diffusion conditions that were employed, but using it for the grain boundary diffusion makes the assumptions that diffusion takes place within the boundary slab, but not laterally outwards from it, and that this is volume type diffusion. These assumptions are only approximately valid at very low temperatures, and when the Fisher solution became available, the formula was revised[144] and extended[145] to allow for the structural changes described in the Smoluchowski boundary model.

2.3.2 The Fisher Solution[142]

The grain boundary region is represented by a uniform and isotropic slab of material of width δ within which diffusion occurs, according to Fick's laws, with a coefficient D' much greater than D the coefficient for diffusion in the grains on either side. The problem is then to solve Fick's equation for the two regions inside and outside the slab, subject to the normal continuity conditions that C' the concentration on the inside of the slab boundary equals C the concentration on the outside of the boundary and that $D' \frac{\partial C'}{\partial x} = D \frac{\partial C}{\partial x}$. These were combined so as to give

$$\frac{\partial C}{\partial t} = D' \frac{\partial^2 C}{\partial y^2} + \frac{2D}{\delta} \frac{\partial C}{\partial x} \qquad (2.4)$$

as the condition to be satisfied at the boundary in solving the following equation for the concentration outside the slab.

$$\frac{\partial C}{\partial t} = D\left(\frac{\partial^2 C}{\partial y^2} + \frac{\partial^2 C}{\partial x^2}\right) \qquad (2.5)$$

Fisher made further assumptions to simplify the analysis — D' and D were taken to be independent of concentration, the concentration C_o at the free surface $y = 0$ was taken to remain constant during the anneal, the diffusion outwards from the boundary was taken to occur only in the direction normal to it so that $\frac{\partial^2 C}{\partial y^2} = 0$ and the concentration across the width of the boundary was taken to be constant.

Using numerical integration of the appropriate differential equations, Fisher found that the concentration in the boundary rose quickly at first but continued rising at a rapidly decreasing rate. By assuming the boundary distribution $M(y)$ to have the distribution characteristic of time $t = t$ from time $t = 0$, the lateral diffusion from it can be described as volume diffusion from a constant source, and gives the equation

$$C(x,y,t) = \phi(y)\ \mathrm{erfc}\left(\frac{x}{2(Dt)^{\frac{1}{2}}}\right) .$$

Other features of the numerical distributions are sufficient to suggest that the true function $\phi(y)$ is not significantly different from that for which $\frac{\partial C}{\partial t} = 0$ in the slab and therefore

$$\frac{\partial^2 \phi}{\partial y^2} \frac{\delta D'}{2D} (\pi D t)^{\frac{1}{2}} - \phi = 0 .$$

Using the conditions that $C = 1$ at $y = 0$ gives the solution for ϕ as

$$\phi = \exp - \left(y \left(\frac{2D}{\delta D' (\pi D t)^{\frac{1}{2}}}\right)^{\frac{1}{2}}\right)$$

and the final approximate expression for the concentration as

$$C(x,y,t) = C_o \exp - \left(y\left(\frac{2D}{\delta D'(\pi Dt)^{\frac{1}{2}}}\right)^{\frac{1}{2}}\right)\operatorname{erfc}\left(\frac{x}{2(Dt)^{\frac{1}{2}}}\right) \quad (2.6)$$

If a sectioning technique is used then the amount of activity in the slice between the depth y and $y + \Delta y$ is

$$Q = \int_{y}^{y+\Delta y} \int_{-\infty}^{\infty} C \, dx \, dy$$

i.e. $$Q \sim \frac{C_o (Dt)^{\frac{1}{2}}}{\delta} \exp - \left(y \left(\frac{2D}{\delta D'(\pi Dt)^{\frac{1}{2}}}\right)^{\frac{1}{2}} \Delta y \right) .$$

The mean concentration $\bar{C}$ in a section is proportional to $Q/\Delta y$ and a plot of $\ell n \, \bar{C}$ against y gives

$$\frac{d \ell n \, \bar{C}}{dy} = - \left(\frac{2D}{\delta D'(\pi Dt)^{\frac{1}{2}}}\right)^{\frac{1}{2}}$$

from which the boundary coefficient D' can be obtained.

This treatment of the problem ignores the effect of volume diffusion and so it can be applied only when grain boundary diffusion can be adequately separated from volume diffusion.

It has been emphasised[20] that the solution is obtained only by making very considerable simplifications in the mathematics and may lead to serious errors in the interpretation of experimental results, although its merit as a simple and practical method of analysis is recognised.

2.3.3 The Whipple Solution

The conditions used by Whipple[151] were much the same as those chosen by Fisher. The concentration C' within the slab was taken to be an even function of x and approximated by a power series in x^2 and there was no similar restriction on the lateral diffusion outward from the boundary. The differential equations (2.4) and (2.5) were used to give the following homogeneous boundary condition to be satisfied by C at $x = \pm \frac{1}{2}\delta$.

$$D' \frac{\partial^2 C}{\partial x^2} - \frac{D}{\frac{1}{2}\delta} \frac{\partial C}{\partial x} = \left(\frac{D'}{D} - 1\right) \frac{\partial C}{\partial t} \qquad (2.7)$$

In order to solve the diffusion equation (2.4) the function $C(x,y,t)$ is transformed by both a Fourier and a Laplace transform, and the solution of the function so defined found to be of the form

$$\psi = \psi_1 + \psi_2 .$$

The inversion of these functions is achieved by introducing the dimensionless parameters

$$\xi = \frac{x - \frac{1}{2}\delta}{(Dt)^{\frac{1}{2}}} \qquad \eta = \frac{y}{(Dt)^{\frac{1}{2}}}$$

$$\beta = \frac{(D'/D-1)^{\frac{1}{2}}\delta}{(Dt)^{\frac{1}{2}}} \qquad \Delta = \frac{D'}{D}$$

giving the final solution as

$$C = C_1 + C_2$$

$$= C_o \operatorname{erfc} \tfrac{1}{2}\eta + \frac{\eta}{2\pi^{\frac{1}{2}}} \int_1^{\Delta} \frac{d\sigma}{\sigma^{3/2}} \exp - \left(\frac{\eta^2}{4\sigma}\right) \operatorname{erfc} \tfrac{1}{2}\left(\left(\frac{\Delta - 1}{\Delta - \sigma}\right)^{\frac{1}{2}} \left(\frac{\sigma - 1}{\beta} + \xi\right)\right) \qquad (2.8)$$

if $\Delta >> \eta$ then $\frac{\Delta - 1}{\Delta - \sigma}$ can be taken as unity and the integration extended to infinity. The term C_1 gives the contribution to C from direct volume diffusion and C_2 that from diffusion via the grain boundary. Whipple also gives an asymptotic form of C_2 derived from a steepest descent approximation and indicates where the Fisher formula

$$C \sim \exp(-\pi^{-1/4}\,\eta\,\beta^{-\frac{1}{2}})\ \operatorname{erfc}\left(\frac{\xi}{2}\right)$$

is incorrect.

2.3.4 The Suzuoka Solution

Suzuoka[159] considers the same model as Whipple but assumes that a thin uniform layer of diffusant is deposited on the surface at $t = 0$ and that this now finite amount diffuses into the specimen, but without any diffusion in the layer parallel to the surface. Following exactly the same mathematical treatment as Whipple but with the appropriate surface conditions Suzuoka obtains

$$C(x,y,t) = C_1(\eta) + C_2(\xi, \eta, \beta)$$

$$= \frac{K}{(\pi D t)^{\frac{1}{2}}}\left[\exp - \left(\frac{\eta^2}{4}\right) + \frac{1}{4}\int_1^{\Delta}\left(\frac{\eta^2}{\sigma} - 2\right)\exp\left(-\frac{\eta^2}{4\sigma}\right)\right.$$

$$\left.\operatorname{erfc}\left(\left(\frac{\Delta - 1}{\Delta - \sigma}\right)^{\frac{1}{2}}\left(\frac{\xi}{2} + \frac{\sigma - 1}{2\beta}\right)\right)\frac{d\sigma}{\sigma^{3/2}}\right] \quad (2.9)$$

where C_1 represents the lattice diffusion that would take place

from the thin source of surface density K and C_2 indicates the redistribution of this material due to the presence of the grain boundary, having negative values in the volume diffusion region and positive values at greater penetrations, while its net contribution is zero. Suzuoka also gives an expression for the average concentration, due to the boundary diffusion term C_2, found within a section parallel to the free surface as a function of depth as

$$\bar{C}_1(y,t) \sim \int_1^\infty \left(\frac{\eta^2}{\sigma} - 2\right)\exp -\left(\frac{\eta^2}{4\sigma}\right)\left[\frac{1}{\pi^{\frac{1}{2}}}\exp\left(-\left(\frac{\sigma-1}{2\beta}\right)^2\right) - \left(\frac{\sigma-1}{2\beta}\right)\operatorname{erfc}\left(\frac{\sigma-1}{2\beta}\right)\right]\frac{d\sigma}{\sigma^{3/2}} \qquad (2.10)$$

and compares this with the corresponding expression for the Whipple and the Fisher solutions

$$\bar{C}_1(y,t) \sim \frac{2\eta}{\pi^{\frac{1}{2}}}\int_1^\infty \exp -\left(\frac{\eta^2}{4\sigma}\right)\left[\frac{1}{\pi^{\frac{1}{2}}}\exp\left(-\left(\frac{\sigma-1}{2\beta}\right)^2\right) - \left(\frac{\sigma-1}{2\beta}\right)\operatorname{erfc}\left(\frac{\sigma-1}{2\beta}\right)\right]\frac{d\sigma}{\sigma^{3/2}} \qquad (2.11)$$

$$\bar{C}_F \sim \exp -\left(\pi^{-1/4}\eta\beta^{-\frac{1}{2}}\right) \qquad (2.12)$$

When the specimens are polycrystalline a grain size parameter n is defined by (grain size)/2 $(Dt)^{\frac{1}{2}}$ and the total average concentration written as

$$\bar{C}_s(y,t) \sim \frac{K}{(\pi Dt)^{\frac{1}{2}}}\left[\exp -\left(\frac{\eta^2}{4}\right) + \frac{\bar{C}_{11}}{n}\right] .$$

Suzuoka discusses the inaccuracies that are introduced by the

the use of polycrystals and outlines a self-consistent method that can be used to distinguish the grain boundary from the lattice diffusion and so determine D and D' from the observed concentration penetration curve.

2.3.5 Other Solutions

Borisov and co-workers[225] use the same boundary model with thin source conditions, and follow the treatment of Whipple, but the inversion of the transformation is not the same and gives the solution in a different integral form. From this they claim compatibility between the Whipple and a modified Fisher solution and give other approximate solutions but these are shown by Wood and co-workers[226] to be of limited utility. Two applications are given, one for making continuous measurements at the free surface during annealling and the other for use with autoradiography.

Levine and MacCallum[157] give an alternative method of solving the grain boundary equation directly for $\bar{C}$ for use with polycrystals and the sectioning technique but the indications are that the approximations restrict the results to large β values. The authors also suggest that $\ell n\, \bar{C} \sim y^{6/5}$ and indicate how this would assist in interpretation.

2.4 Comparison of the Models and the Analysis of Grain Boundary Diffusion Measurements

The features of the various models have been examined carefully by several authors. Maneri and Milford[227] in a mathematical re-appraisal conclude that the Whipple solution is exact and that the solution obtained by Borisov and co-workers is equivalent to that of Whipple. No conclusion could be reached about the validity of the Fisher solution solely on account of not being able to check that the distribution represented by the function $\phi(y)$ varies little with annealing time.

Wood and co-workers[226] evaluate Whipple's exact solution for a range of parameters appropriate to experimental conditions, present the results graphically and in tabular form, and examine some of the characteristic features of the distributions. The validity of the approximate solutions is discussed on the basis of the numerical results and the useful range of the Fisher solution found to be very small. The approximate formulae given by Whipple show large errors, excepting that for the gradient of the concentration contours $(\frac{d\eta}{d\xi})_{\xi=0}$ which shows values 10 to 20 per cent low. The approximations of Borisov and co-workers are also shown to be of limited utility.

A similar but more comprehensive comparison of the Fisher and the Whipple solutions is made by Le Claire[228], who achieves considerable simplification in the interpretation by introducing the parameter $\eta\beta^{-\frac{1}{2}}$. In the Fisher formula and in the asymptotic formula at large β values, the boundary concentration is given as a function only of this parameter, and for $\beta > 100$

numerical calculation shows this dependence to hold for the exact Whipple solution. The latter is an indication that as β increases $\frac{\partial^2 C}{\partial y^2}$ becomes less relevant, and this is confirmed by the improved agreement between the calculated values of the asymptotic and the exact solutions. No such improvement is noted with the Fisher solution which is shown to hold only for large β and small $\eta\beta^{-\frac{1}{2}}$ values, and this is taken to indicate that the time independent features of the function $\phi(y)$ is not justified.

Le Claire states that Q' values determined experimentally from boundary penetration measurements and the Fisher solution can be high by as much as 50 per cent and discusses this effect on the results reported by Sinnott and co-workers[150]. The analysis which uses the average concentration $\bar{C}$ obtained from sectioning measurements is also studied. Numerical calculation shows that for the exact Whipple solution the dependence of $\ell n\, \bar{C}$ on $\eta\beta^{-\frac{1}{2}}$ varies continuously from 1 to 1.5 although the variation of $\left(\frac{\partial\, \ell n\, \bar{C}}{\partial(\eta\beta^{-\frac{1}{2}})}\right)$ with β is small at large β values, that the asymptotic solution does not show agreement with this, and that the Fisher solution shows a constant value of 0.75. An analysis by the Fisher solution would therefore give small D' values and large Q' values. The dependence of $\ell n\, \bar{C}$ on $(\eta\beta^{-\frac{1}{2}})^{6/5}$ suggested by Levine and MacCallum[157] is found to be nearly constant at 0.78 for the exact solution and on the basis of this dependence, it is stated that the analysis should be carried out by plotting $\ell n\, \bar{C}$ against the penetration depth to the power 1.2.

For the contact angle measurements numerical calculation shows that the results obtained by the two solutions could differ by a factor greater than two.

A comparison of the two exact solutions with particular reference to the sectioning technique is made by Suzuoka[160]. The fact that the dependence of $\ell n\, \bar{C}$ on the parameter $\eta\beta^{-\frac{1}{2}}$ shows so little difference for the two solutions prompts the author to suggest that the characteristic contour of grain boundary diffusion is nearly independent of the source condition and also that this will be true even when the source conditions show the departure from ideality that has been found to occur[162,163]. The author defines the ranges of penetration within which grain boundary diffusion is observable and for these examines the linearity of $\ell n\, \bar{C}_{11}$ with $(\eta\beta^{-\frac{1}{2}})^{6/5}$. At large β values $\frac{\partial\, \ell n\, \bar{C}}{\partial(\eta\beta^{-\frac{1}{2}})^{6/5}}$ equals 0.78 and so using this value β can be determined from the relation

$$\frac{\partial(\ell n\, \bar{C})}{\partial\, y^{6/5}} = \frac{\partial(\ell n\, \bar{C})}{\partial(\eta\beta^{-\frac{1}{2}})^{6/5}} \left(\frac{\beta^{-1}}{Dt}\right)^{0.6} \qquad (2.13)$$

derivable from the defined dimensionless parameters, where $\frac{\partial\, \ell n\, \bar{C}}{\partial\, y^{6/5}}$ is obtained from a penetration plot of the experimental data. For other values of β the author finds that the relation

$$\frac{\partial(\ell n\, \bar{C})}{\partial(\eta\beta^{-\frac{1}{2}})^{6/5}} = A\,\beta^{m} \qquad (2.14)$$

describes the small variation, and gives values of A and m for the two ranges $\beta < 100$ and $\beta > 100$. In examining the validity of the Fisher solution Suzuoka gives the relation

$$\frac{D'_{exact}}{D'_{Fisher}} = \frac{\beta_{exact}}{\beta_{Fisher}} \sim 2.5 \qquad (2.15)$$

noting that this ratio increases with decreasing β, a contradiction of Le Claire's conclusion which the author states is due

to the difference in the observable ranges, and indicates that the activation energies are approximately the same. The author concludes that the application of the instantaneous source conditions and the sectioning technique are the most suitable combination for grain boundary diffusion studies.

CHAPTER III

THE EXPERIMENTAL METHOD

3.1 The Crystal Furnace

The specimens were grown by the Bridgman technique in the vacuum furnace shown in Plate 1. The features of the furnace design are the graphite heating element, the time-switch control, the molybdenum radiation shield assembly and the water cooled metal bell jar. Temperatures higher than 1700°C can be reached with the 7kVA output of the motor driven Variac transformer. At the operating temperature an Ether Transitrol anticipatory controller responding to a Pt/Pt 13% Rh thermocouple located within the hot zone maintains a constant temperature by regulating the power supply.

After correctly positioning the loaded crucible and pumping down to a pressure less than 10^{-5} mm. Hg, the furnace temperature was raised to approximately 1300°C. This was done over a period of two hours so as to prevent excessive outgassing. After allowing a further period of 15 minutes to establish thermal stabilisation, the dropping mechanism was started and the crucible withdrawn from the hot zone with a velocity of 2 mm per minute. The temperature gradient in the region of the melting point isotherm was approximately 25°C per cm. On completion of the withdrawal the power was switched off and after a cooling period of at least 3 hours the crucible was removed from the furnace

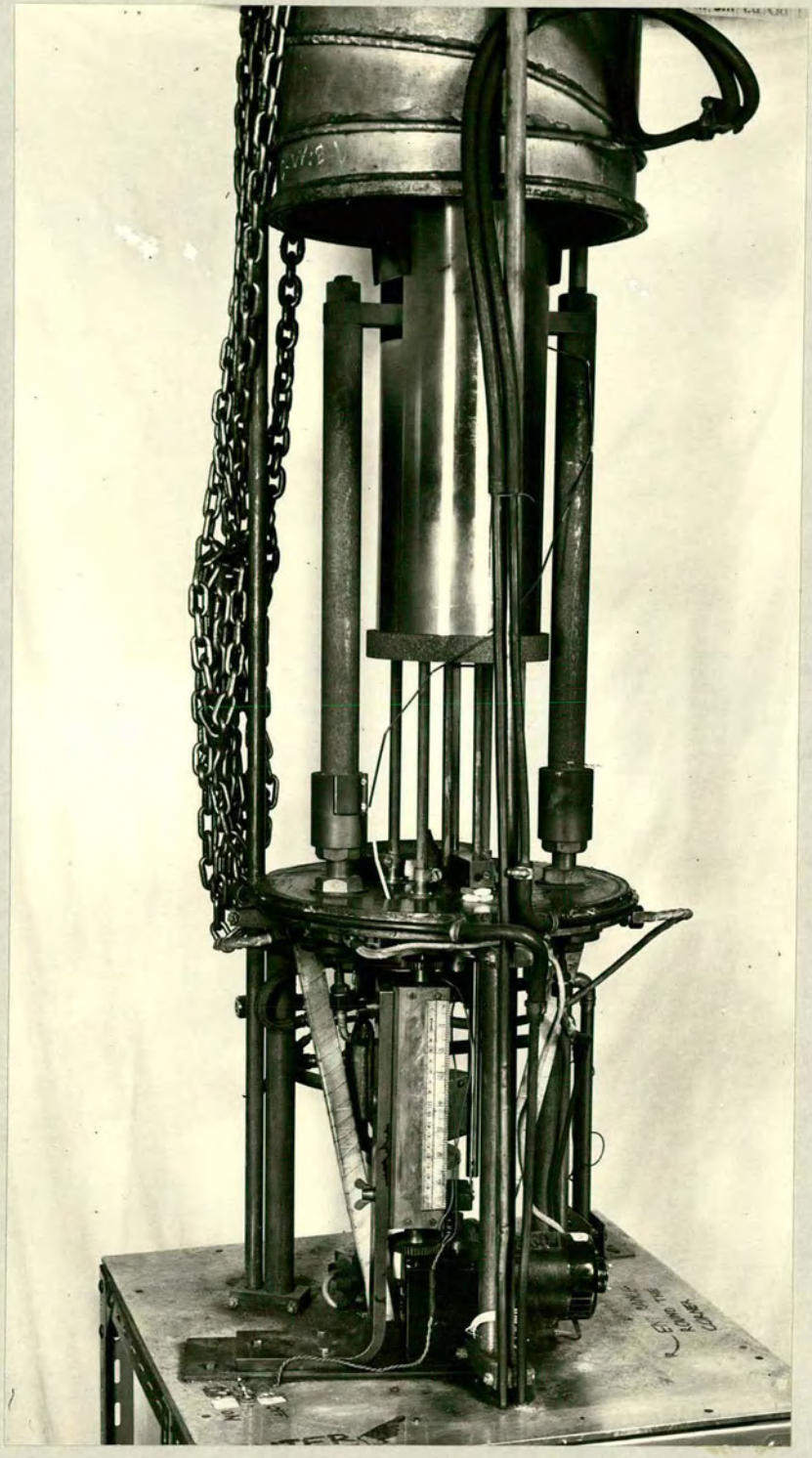

Plate 1. The crystal-growing furnace.

3.2 Crystal Growth

There are a number of excellent reviews[236,237] which detail the methods and the procedures for growing metal crystals. All crystals were grown in split crucibles made from high purity graphite of the type shown in Plate 2. To assist regular growth, the specimen recess was machined and finished so that the faces were especially smooth and the edges sharply defined and to avoid barrelling of the crucible and consequent leakage the loaded copper was a loose fit in the specimen recess and the end rings were made a tight fit.

The four growing operations that were necessary to produce bicrystals of the required orientation are illustrated in Plate 2. Single crystals of random orientation 10 cm. long and 2 mm. in diameter were grown in the three channel crucible from Specpure copper wire. The orientations were determined, then each crystal was bent so that a length of about 6 cm. lay along a [100] direction. Pairs of these crystals were packed with alumina powder into the wide channel crucible and were regrown to form [100] axial crystals using the shorter parts as seeds. A length of the [100] axial crystal was used as a seed in the five channel crucible to produce crystals of 2 mm. square cross section, with the required angle between the [010] axis and the face normals. Two of the square section crystals were used to seed the crystal, the required misorientation being achieved by placing them antiparallel in the seed channels as indicated by Fig. 2, and Specpure copper strip 15 mm. x 3 mm. in section and 12 cm. long used to load the crucible. After growth the bicrystal

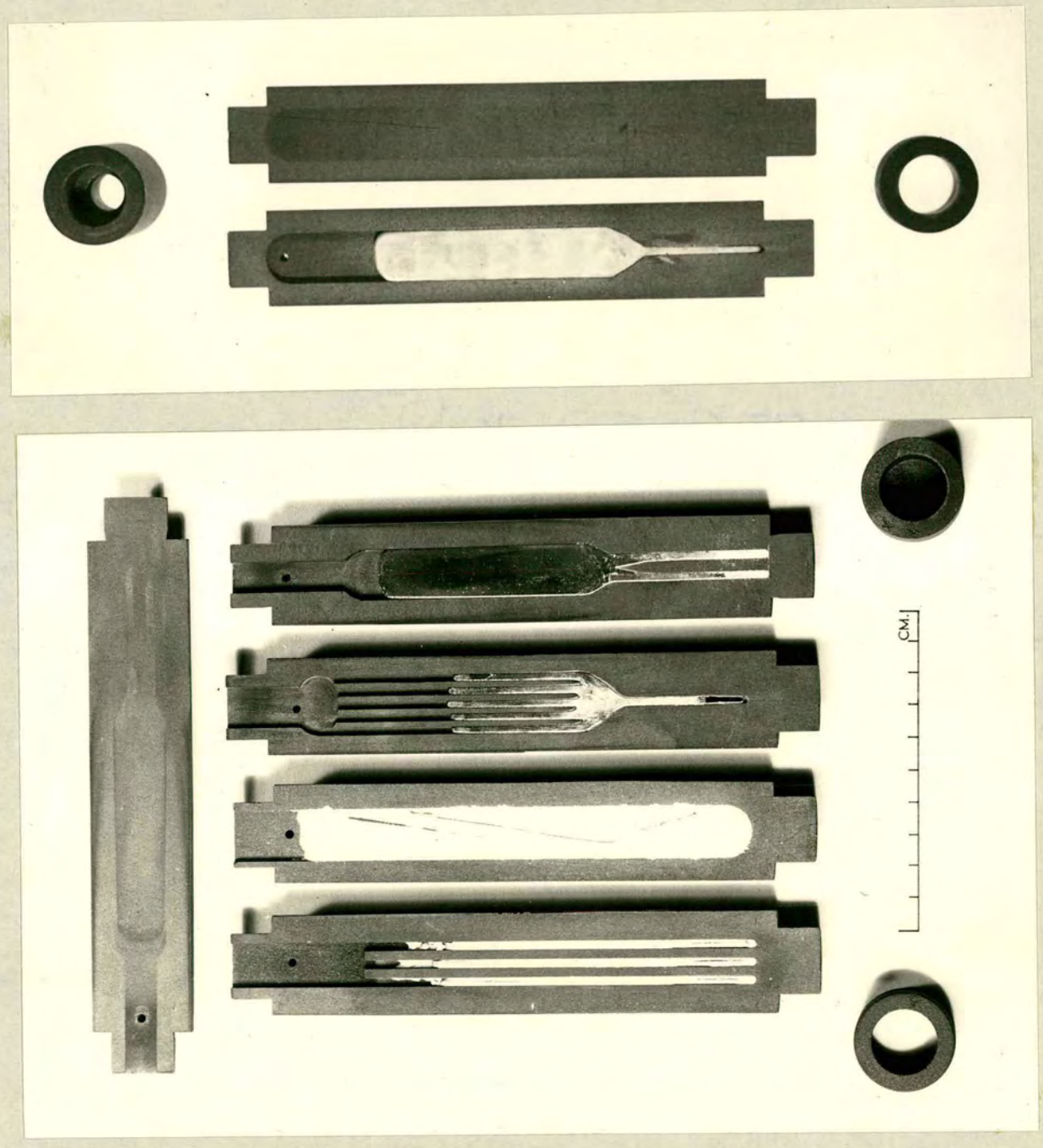

Plate 2. Split graphite crucibles a) for bicrystals
b) for single crystals

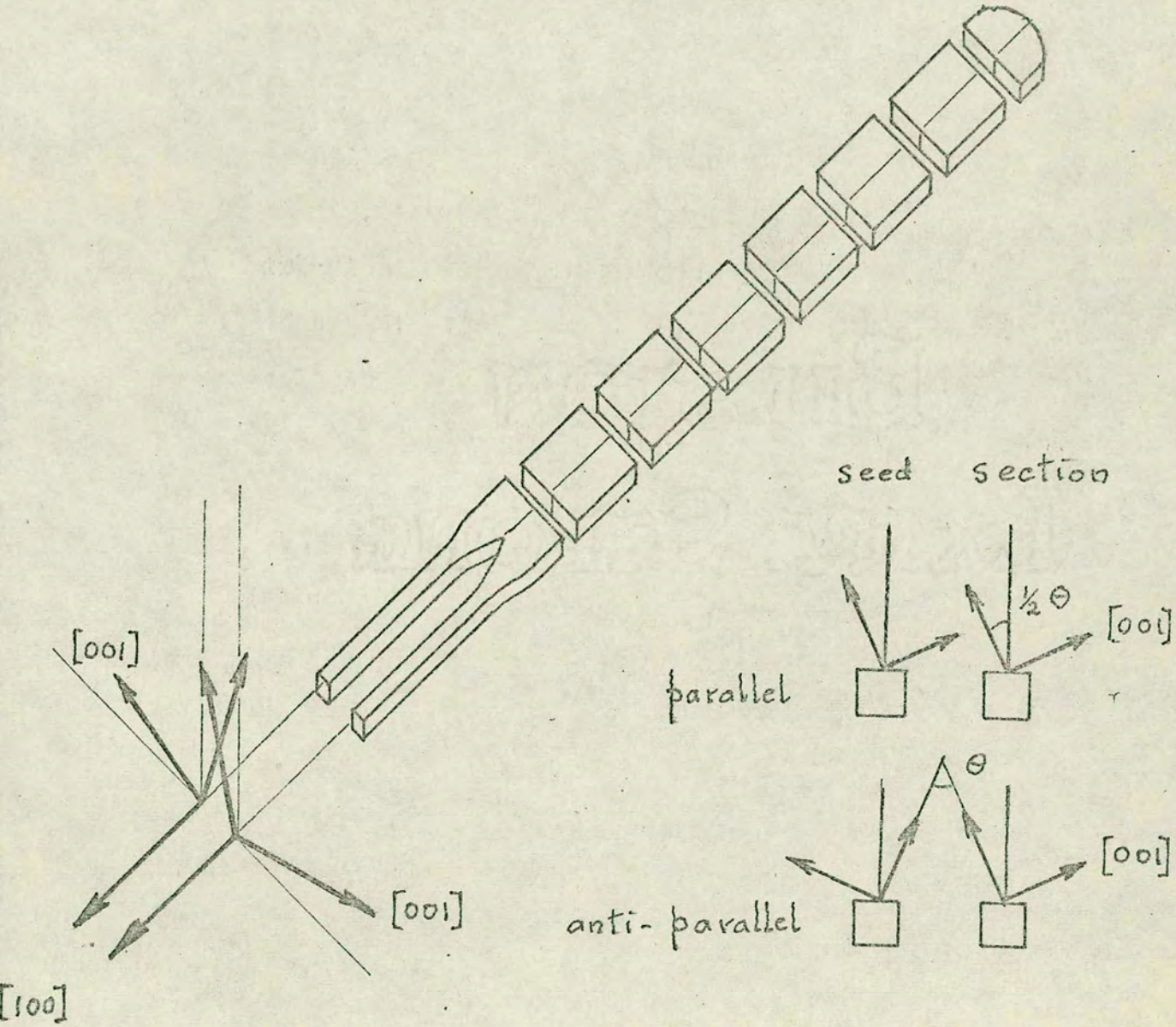

Fig. 2. Bicrystal orientation.

was cut 1 cm. from the seeds, giving a portion that could be used to seed the next specimen.

The quality of the bicrystals and the ease with which they could be grown were found to depend on several factors - an optimum furnace temperature, the correct level of seeding, a uniform hot zone and well kept crucible. Specimen flaws were generally removed by a second run through the furnace; these appeared as non-planar boundaries, as boundaries non-parallel to the length and non-normal to the surface and as striations of slight misorientation in the grains.

A number of single crystals were grown in a similar way, but of unspecified orientation.

The Specpure (99.999% purity) copper was supplied by Johnson Matthey, whose analytic report is given in Appendix I. Before use all the copper bits were given a chemical polish with the following solution suggested by Teggart[233]:

1 part concentrated nitric acid
1 part concentrated phosphoric acid
1 part concentrated acetic acid
Used with an equal volume of water at 60°C.

3.3 The Determination of Orientation

The orientations were determined by the technique which uses the surface reflecting properties that develop as a result of etching. If certain crystallographic planes are preferentially attacked in the etching process, a regular stepped structure is produced, the faces of which act as a host of parallel mirror elements. The following solution, recommended by Barrett[234], was found to be satisfactory.

Etching Solution

1 part concentrated hydrochloric acid
1 part water
Mixture saturated with hydrated ferrous chloride

A light etch of 1 minute was usually sufficient to give reflections from the (100) planes. Strong reflections could be obtained by etching for longer periods, but this also produced weak reflections from the (110) planes. Certain changes in the composition of the etch were found to produce stronger (110) reflections.

An ex-R.A.F. astro-compass was adapted for use as a three circle goniometer. The specimen was suitably positioned on the face of the vertical circle and illuminated by a beam of parallel light. A large mirror with a transmission region at the centre was positioned normally in the beam so that the reflection of the illuminated specimen could be observed from a point near the beam axis and behind the goniometer. With this arrangement and a well etched specimen it was possible to determine the (100) reflecting positions to an accuracy of two degrees.

Growing [100] axial seeds was comparatively easy, since this is a preferred direction of growth, but it was difficult to produce square section seeds with the required angle of $22\frac{1}{2}^{o}$ between the face normal and the [010] direction. The misorientation was set by mounting the crucible on the goniometer and adjusting the seed in position using the (010) reflection and a small piece of mirror on the flat face of the crucible. It was essential to obtain the required misorientation at this stage, since it was not possible to adjust the seeds in the bicrystal

crucible. The orientation of the bicrystal was determined by positioning the specimen flat on the vertical circle, noting the reflecting positions for both grains and measuring the misorientation on a stereographic projection. Specimens were taken to be acceptable if the axial alignment and the misorientation of the grains were within 5° of the required orientation.

3.4 Preparation and Activation of the Specimens

The selected crystals were cut into 15 mm. lengths using a Metals Research spark cutter to give specimens 15 mm. × 15 mm. × 3mm. One of the large faces of each specimen was polished, either mechanically or by spark planing. Mechanically, the specimen was hand polished through the three finest grades of silicon carbide paper, using a paraffin oil lubricant, then through four stages on a mechanically rotating lap using diamond paste impregnated microcloths and a recommended commercial lubricant.

In order to relieve any residual strain, the specimens were given a few days pre-annealing treatment at a temperature in the range $400^{\circ}C$ to $500^{\circ}C$.

A uniform layer of the diffusant some 100 Å thick was deposited on the prepared surface of the specimen, by evaporation in the case of antimony-124 and silver-110 and by electrodeposition in the case of nickel-63. The evaporation was carried out in a laboratory made unit of conventional design (Plate 3) using the specimen holder assembly shown in Fig. 3. This assembly which was designed to prevent contamination of the evaporator with radioactive material, was readily replaceable and could be used to activate up to seven specimens at the same time. The silver in the form of 0.005" diameter wire and the antimony as small pellets were both found to

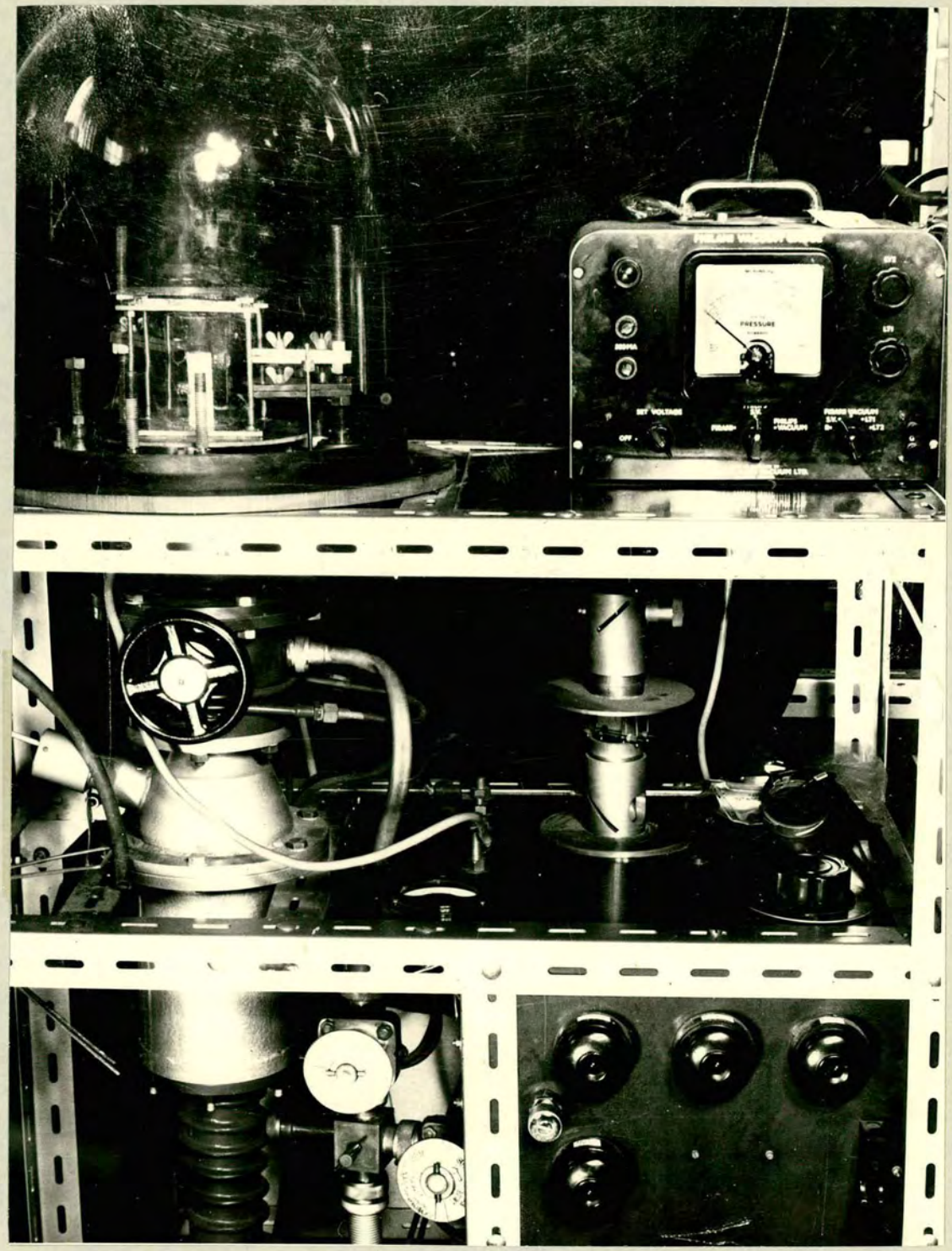

Plate 3. The evaporator unit.

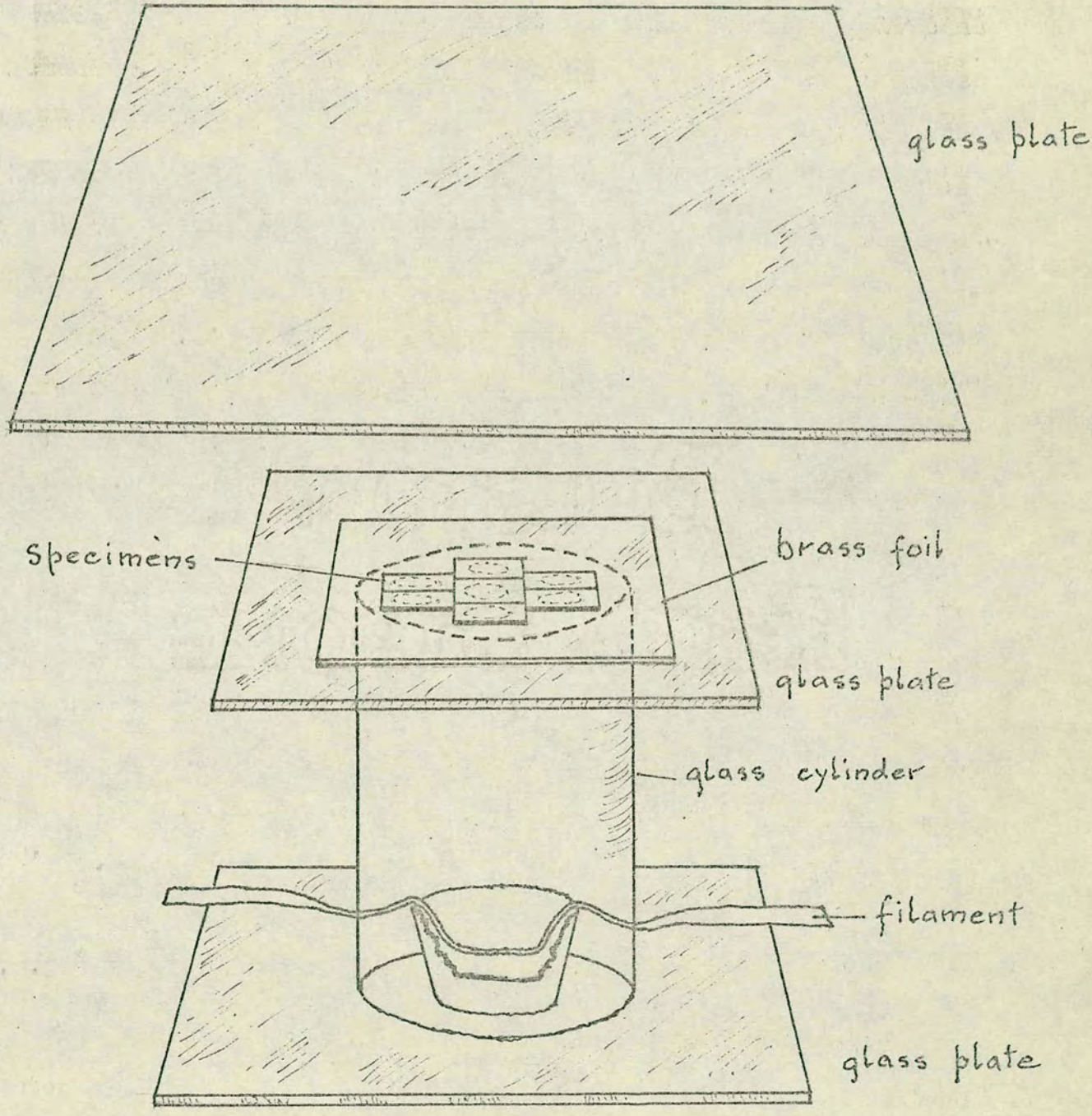

Fig. 3. Assembly for isotope evaporation.

evaporate cleanly from the molybdenum strip filament, shaped to give a high temperature at the source point. The weight of the active pieces ($\sim$ 3 gm.) was chosen so as to give a specimen-to-source distance sufficiently large ($\sim$ 12 cm.) to prevent film damage by excessive heat.

The electroplating of nickel, supplied as $NiCl_2$ in a dilute solution of HCl, caused a great deal of difficulty. Several plating solutions are recommended for the electrodeposition of nickel on to a copper surface and all of these when used with non-active nickel gave a good quality thin film. However, when nickel-63 was used, the result in each case was an irregular sooty deposit which was found to be radioactive. The current density, cell voltage and the solution composition were varied and the cell material was changed but this produced no improvement. The following plating solution was recommended by Maxim[235],

Ammonium sulphate	13.2 g.
Ammonium citrate	24.3 g.
Hydrazine hydrite	25 ml. of 50% solution
Ammonium hydroxide (.880)	50 ml.
Add distilled water to 1 litre.	

the $NiCl_2$ solution, having a nickel concentration of 2 mg./ml., to be diluted in the ratio of 10:1 with this electrolyte. When this was first tried a good nickel plating was obtained, however within a few days a black deposit was again appearing. Eventually this was overcome by recovering the nickel, mixing a fresh solution and immediately plating a number of specimens.

A layer of Specpure copper some 300 Å thick was evaporated over the active films so as to minimise the risk of the diffusant evaporating during the anneal.

It is to be noted that the diffusion direction was perpendicular to the common [100] tilt axis, a choice based on the familiarity and ease of specimen preparation and also on the several reports[146,153,162] that state little or no difference between the diffusivity in this direction

and that in the direction parallel to the tilt axis.

3.5 Specimen Annealing

The diffusion anneals were performed in an evacuated silica tube with the specimen contained in a split graphite crucible in close contact with a sheathed Pt/Pt 13% Rh thermocouple. The open end of the silica tube was closed by a brass end-piece assembly with vacuum seals for the thermocouple leads and with connections for the vacuum line and a Pirani gauge. The tube was evacuated by a high speed Metrovic DR1 rotary oil pump which gave a pressure of approximately 10^{-4} mm. Hg. The vacuum tube was placed in a furnace unit for the duration of the anneal. This unit consisted of an open ended silica tube which was wound with a Nichrome wire heating element and mounted horizontally in an asbestos casing well packed with asbestos wool. A specimen temperature of 1000°C could be reached with a power dissipation of 1.2 kilowatts.

A Sunvic RT2 controller was used to regulate the furnace temperature. This unit responds to a platinum resistance thermometer located on the heating element and functions by short-circuiting a resistance in series with the windings, the power levels being adjusted to give an optimum cycling period. Although the controller operates so as to produce a constant temperature on the furnace windings, the arrangement is most effective in producing a constant specimen temperature, and furthermore the controller scale can be calibrated in terms of specimen temperature if the furnace geometry is kept fixed. The specimen temperature, measured at regular intervals by the platinum thermocouple, potentiometer and moving coil galvanometer, was found to remain constant to within the 1°C accuracy of the thermocouple specification.

The anneals were started by inserting the vacuum tube into the matching furnace tube operating at the required temperature.

A record of the heating of the specimen was obtained by connecting the thermocouple output to a Sefram recorder. This was used to make the following correction to the annealing time, so as to allow for the heating-up period, where it was necessary. For a heating-up period from $t = 0$ to $t = t$, the effective time t_e at the annealing temperature T is defined by the relation

$$D(T)t_e = \int_0^t D(T')dt'$$

where the actual temperature at time t' is T'. If the activation energy Q is known approximately then this expression can be written in the form

$$t_e = \frac{\int_0^t \exp(-\frac{Q}{RT'})dt'}{\exp(-\frac{Q}{RT})}$$

and t_e determined graphically. The anneal was terminated by withdrawing the vacuum tube from the furnace.

The inside of the vacuum tube and the contents were monitored periodically for radioactive material. Although there was little evidence of evaporation of silver or nickel, a significant amount of antimony-124 was detected. To reduce this to a minimum, the annealing was carried out with the specimen contained between two matching pieces of thin flat quartz. In a few cases two single crystal specimens, with active faces touching, were annealed at the same time.

3.6 Mounting and Polishing of the Specimens

The annealed specimens were examined visually and prepared for autoradiography in the following way. Using the spark cutter the specimens were cut at right angles to both the boundary plane and the active face so as to give two equal bits. These were then mounted in the epoxy casting resin Araldite. To do this, they were placed in a 1½" diameter casting die, previously coated with a silicone release agent, standing upright on the cut faces with the edges accurately perpendicular to the base. The mixing (MY 753 resin + HY 951 hardner) pouring and curing of the Araldite was performed with care so that the casting was hard, free from air bubbles and in good contact with the specimen. After removal from the die the mount was polished mechanically, using the procedure already described, so producing the section required for autoradiography.

Those specimens that were annealed in pairs, were first mated together then the unit was cut in the same direction into two bits. The mating faces were highly polished and the specimens secured in two pairs of steel grips (~~Fig. 5~~ Plate 4), designed to achieve good contact. The mating was made so that the following specimen arrangements could be studied:

(i) one active face in contact with Araldite,

(ii) one active face in contact with a non-active face,

(iii) two active faces in contact.

Several undiffused specimens were mounted in arrangement (ii) for use in determining the function $\mu(\zeta)$.

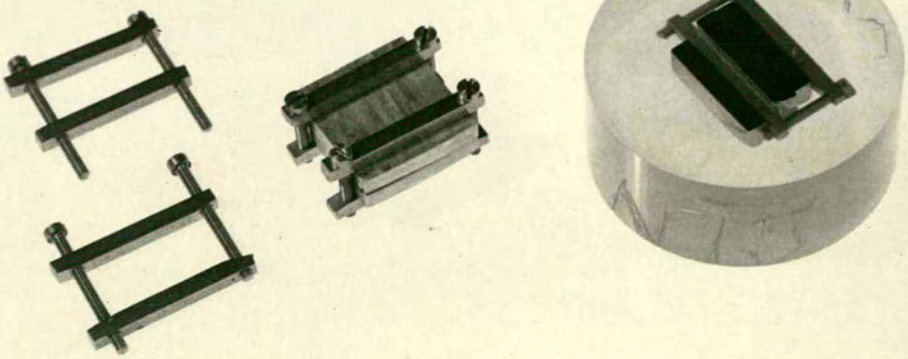

Plate 4. Steel grips, mated and mounted specimens.

3.7 Autoradiographic Image and Resolution

The increasing availability of radioactive isotopes has continually extended the application of autoradiography and during this development the technique has been reviewed regularly[238-241]. Its merit as an important means of detection is that it is non-destructive and that it allows not only an investigation of the spacial distribution of the tracer element, but also a study of the process or the mechanism that leads to the distribution, and on this account the method has been extremely valuable in biology and medicine. Although it is a particularly sensitive means of detection and location the disadvantage of the method is the difficulty of interpreting the data. The relationship between the density distribution on the autoradiograph and the concentration distribution of the tracer in the specimen is highly complex in all but a few cases. If the radiation of the tracer is of a very low energy, then the density distribution is an exact record of the tracer distribution on the surface examined, but when the radiation is of a high energy then the emulsion blackening at a point is due to radiation reaching it from within a region defined by the maximum range, and quantitative interpretation is not possible unless there is a degree of symmetry in the specimen. If the tracer variation is a two dimensional distribution then the prepared surface can be chosen so that all lines normal to it are of equiconcentration.

The tremendous simplification that this achieves makes an analysis of the problem a possibility, although there are few cases in which this has been attempted. Marshall et al.[242] determined

the total activity in uniform and non-uniform distributions in bone in this way using a calibration technique due to Dudley and Dobins[243]. Odeblad [244] has considered certain simple three dimensional distributions, cases of biological interest such as cell tissues, in the following way. The specimen was taken to be composed of structures of entities, generally of uniform concentration, such as the lamella, annulus, cylinder, with the axes normal to the surface, then a theoretical relationship between the radioactive content of each and the density distribution was proposed and tested. In most practical cases complications due to the energy effect are present to some degree of significance, although it is possible to reduce the effect either by arranging that the concentration distribution of the tracer element and its characteristic features are large in scale by comparison with the average range of the radiation, as for example in some diffusion studies, or by using sections of the specimen sufficiently thin to ensure that there is little contribution from long range radiation. Sections several microns thick are commonly used in biology and medicine but there are few reports of this with metal specimens[245, 246]. There have been a number of cases where the magnitude of this effect was large and where no allowance or correction was made for it; this has led not only to results that are unreliable but also to an unwarranted suspicion of the technique[180].

An important feature of the method is the resolution. This is a measure of the limiting source conditions which can be distinguished or defined by the film image. Stevens[247, 248] investigated this for a 4μ thick nuclear stripping emulsion using a Cobb-type photographic test chart toned with iodine-131 and found the limiting line

separation to be 2.3 microns. Doniah and Pelc[249] and Nadler and co-workers[250,251] examined several types of source - point, line, plane and cylindrical - and described the resolution in terms of the image spread from these, expressing it mathematically in terms of the specimen thickness, the film thickness and film contact. In the formulation the authors neglect the scattering and the absorption of the radiation, assume that the particle flux diminishes according to an inverse square law, and make oversimplifications of the effects associated with the energy distribution of the isotope radiation.

In choosing the experimental conditions for autoradiography, it is advisable to consider the resolution and examine how this is affected by the following factors.

(a) the type and energy of the isotope radiation,

(b) the density and the scattering and absorption properties of the specimen,

(c) the thickness of the specimen,

(d) the separation of the emulsion from the specimen surface,

(e) the thickness of the emulsion,

(f) the grain size of the emulsion,

(g) the dimensions of the examining aperture of the densitometer.

In the volume diffusion work the undistorted concentration distributions can be resolved only with the very low energy nickel-63, but to do this it is necessary to ensure favourable conditions for the factors (d) to (g), by choosing suitable film. The autoradiographic film that is available is with minor variations of three types:-

(i) a very thick, very large gain X-ray film suitable for use only in the coarsest of work;

(ii) a thick, large grain stripping film, for example, Kodak AR.50

with a 15μ thick emulsion on a 10μ thick gelatine backing and a grain size of 1μ in diameter.

(iii) a thin, small grain stripping film, for example Kodak AR.10 with a 5μ thick emulsion on a 5μ thick gelatine backing and a grain size of $\frac{1}{3}\mu$ in diameter.

The desired resolution can be achieved by using AR.10 film, with the emulsion in intimate contact with the specimen surface, for all but the smallest $(Dt)^{\frac{1}{2}}$ values. At this extreme an amount of image distortion occurs due to film thickness, convincingly demonstrated by the spread of the function $\mu(\varsigma)$ for nickel-63 in Table 1.

With silver-110 and particularly with antimony-124 it is not possible to resolve the undistorted tracer distribution because of the energy effect. Good film contact is also an important factor, but the improvements in the resolution that is achieved by using AR.10 film instead of AR.50 is marginal. The factors that determined the use of AR.10 film were the grain size and the dimensions of the examining aperture in the grain boundary case.

Although the concentration distribution cannot be resolved in an undistorted form, the image it produces can be measured with a high degree of precision, and it can be interpreted to give results of high accuracy. If the term resolution is used to describe these features, then it should be emphasised that this is not a direct measure of the source conditions, it is a measure of the method as a whole to determine the source conditions indirectly. In this case an indication of the resolution that is to be expected can best be obtained from the spread function $\mu(\ )$. This not only shows the combined effect of all the associated factors in the

required form but also illustrates the limiting source condition that can be determined in a given case. The spread functions for nickel-63, silver-110 and antimony-124 can be compared with the energies of the decay schemes by reference to Table 1 and Appendix 2.

3.8 Film Exposure and Processing

The film exposures were made using dry contact with the specimen, a technique originally developed by Lacassagne and Lattes[252], and carried out in a vacuum cassette similar to that of Sherwood[253]. In the light of a Wratten No. 1 Safelight, a $1\frac{1}{2}$" disc of film was cut and pealed from the glass plate, using a scalpel blade. With the specimen in the cassette, the film was placed emulsion side downwards in contact with the prepared surface and covered with two protective discs of thin polythene sheet. The cassette was closed by a soft rubber sheet and a brass ring seal, so that on evacuation the rubber deformed to press first on the specimen at the centre, and increase the contact radially outwards until a uniform pressure was exerted over the whole specimen. The vacuum system, composed of six cassettes, a Pirani gauge attachment and a needle valve air inlet, was evacuated by a slow speed rotary oil pump. In order to ensure uniform conditions of exposure the space between the prepared surface and the undeformed rubber sheet was arranged to be 2 cm. and the pressure in the cassette assembly was regulated to 10^{-2} mm. Hg. by the needle valve. These values had been found by trial to avoid pressure effects and also to give optimum film contact.

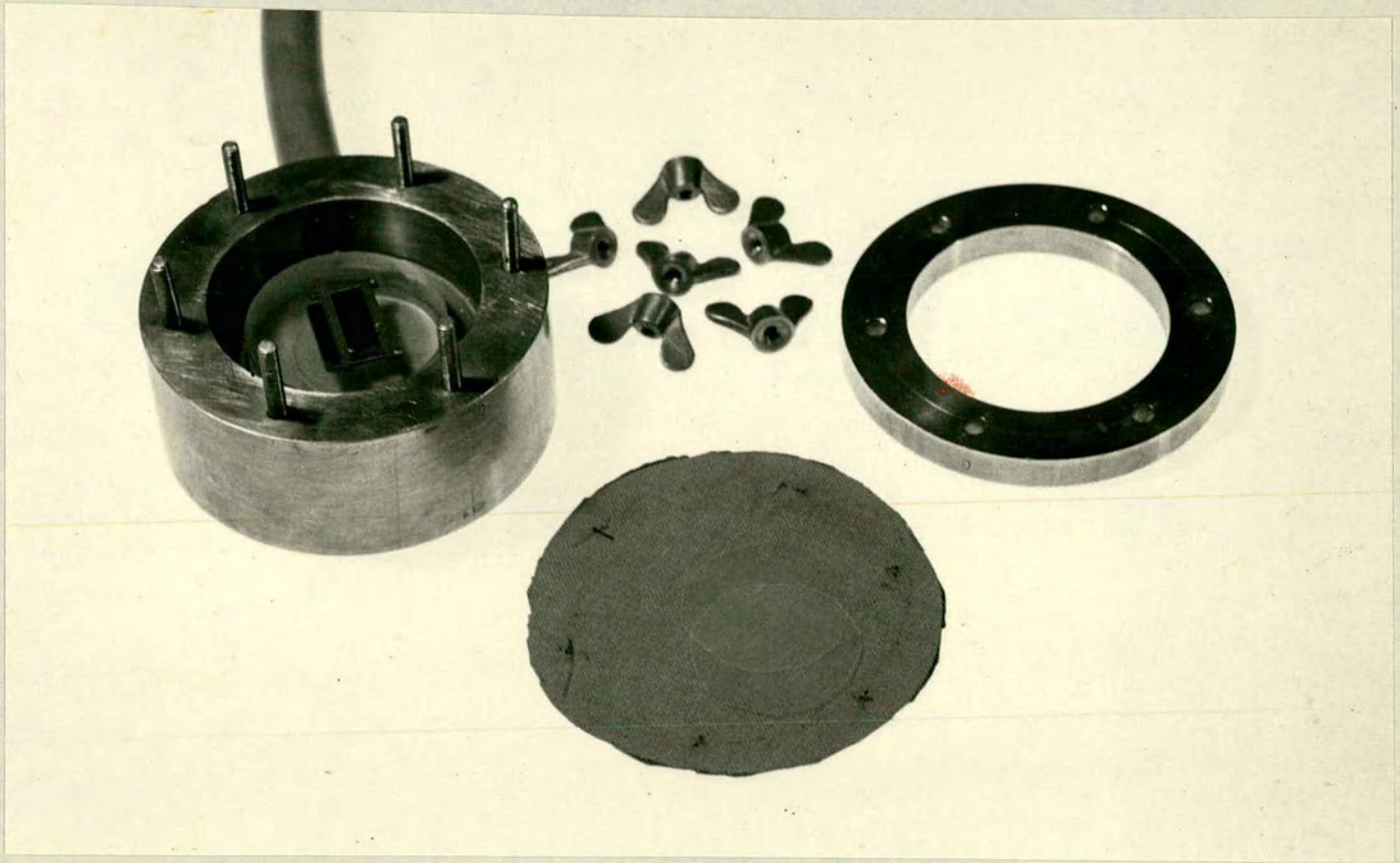

Plate 5. Vacuum cassette.

Excessively low pressures were found to cause mechanical damage to the AR.10 film. The exposure times that were necessary to produce the desired peak densities of approximately 0.6 above background, ranged from a few hours to a few days. The excessive film expansion that was produced by long periods of evacuation was taken to indicate hydration of the gelatine layer. Long exposures can also give latent image fading and reciprocity failure[254], but these were calculated to be minor effects.

Autoradiographic emulsions in general are very much less sensitive to γ-rays than to β-rays, and show a maximum response to particles of approximately 0.1 Mev. at diffuse incidence. For particles with energies greater than 0.5 Mev. the response falls to almost half the peak value. Although few data are available for the emulsions used, the characteristics of similar emulsions are given by Dudley[255] and others[239,240]. For AR.50 and AR.10 emulsions Hertz[256] has indicated that the relation between incident particle flux and film density remains linear up to film densities of 0.7 and 0.8 respectively.

The processing was done by mounting the exposed film between two perspex frames which secured it around the edge as shown in Plate 6. The film was developed for 5 minutes in Kodak I.D.19B solution, rinsed for 1 minute in distilled water, fixed for twice the clearing time in Kodak and fixing salt and washed for 30 minutes in running water. A water bath was used to maintain the solutions at 18°C. While being held under water the film was released from the frames and floated on to a clean glass plate which was withdrawn from the water so that the film was evenly spread out and free to contract uniformly, tacking to the plate

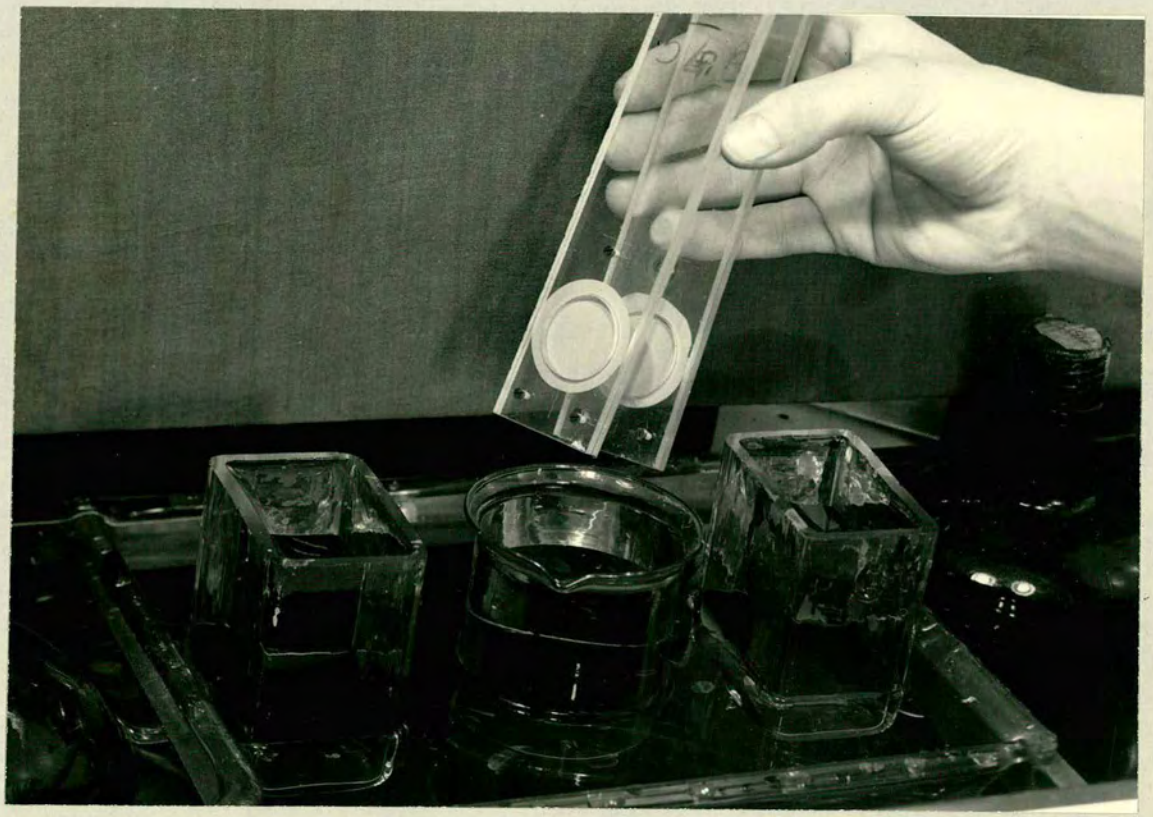

Plate 6. Film processing.

as it dried. After drying in a dust-free space, the film was examined for strain regions then numbered; the final value of the expansion was approximately 12 per cent. It should be added that satisfactory autoradiographs could not be produced unless the fluids and the containers were scrupulously clean, and unless the film was handled with the utmost delicacy at all stages.

3.9 The Measurement of Film Density

The density measurements were made using a Joyce-Loebl double beam automatic recording micro-densitometer. This instrument gives density values directly by making a comparison of the film with a linear density wedge.

Hunter and Driffield[225] defined density d as $d = \log_{10} (I_o/I)$ where I_o and I are the light intensity incident on and transmitted by the medium. When applied to photographic film, the quantity that is generally required is d_e the density above fog, or the additional blackening that results from the exposure and this is seen to be $d_e = \log_{10}(I'/I)$ where I' is the light intensity transmitted by an unexposed region of the film. This definition is not precise, because the transmitted light suffers an amount of scatter, and so the density value depends on whether I is taken as the directly transmitted light or as the total transmitted light. When the former is taken the value given is called the spectral density, and when the latter is taken it is the diffuse density. The optical system on most densitometers accepts light lying within a small angled cone and so the quantity measured is intermediate between the spectral and the diffuse density, but is expected to vary little

in fractional content at different density levels.

In the Joyce-Loebl instrument one beam of light is focussed on to an area of the emulsion and the transmitted fraction projected by an objective lens on to a viewing screen fitted with an adjustable slit. The intensity of the light that passes through the aperture is measured by a photomultiplier detection system. A second beam of light from the same source passes through the density wedge and falls on the same region of the photomultiplier. A rotating shutter chops the beams alternately and the difference that is detected in the photomultiplier output signal is amplified and used to drive a servo-motor which moves the wedge mounted in a sliding carriage with pen attachment, so that the light intensity of the reference beam is matched to that of the measuring beam. The motor-driven record table is linked to the specimen table by a lever arm of variable ratio, and as the specimen passes through the measuring beam, the changing densities are matched by the motion of the wedge. In this way the density of the speciman is recorded graphically as a function of position. Servo stability and response are achieved by means of a feedback signal adjusted to give critical damping of the pen and the speed of recording is variable and inversely proportional to the density gradient, features that aid the excellent reproducibility. There is a range of optical components and of mechanical linkage ratios to suit the scale of the image and the detail of the features can be displayed to advantage by the choice of density wedge.

The density distributions in most cases of volume diffusion were several hundred microns in extent and so although the

instrumental parameters were carefully selected by a series of trials, the adjustments were not critical. A coupling ratio of 200:1 allowing 1 cm. on the record to represent approximately 50μ on the film, produced a trace that displayed the main feature to advantage and also gave an adequate sample of the adjoining background. An optical magnification of x20 gave a projected image that was convenient in size for visual inspection and for slit adjustment. The slit height was limited only by irregularities in the film and was generally greater than five hundred microns, giving a slit area sufficiently large to allow a choice of slit widths and at the same time an adequate integration of grain effects. If the slit was too narrow then the trace showed excessive noise and if it was too wide, then distortion occurred. Slit widths for medium penetrations were approximately 10μ. The traces shown in Fig. 6 illustrate the wide range of penetrations covered and the three ways of mounting the specimen.

In a number of cases a larger lever arm ratio was necessary to determine the density distribution with sufficient accuracy. These included undiffused specimens or specimens where the penetration depth was small, especially when the tracer element was the very low energy isotope nickel-63. The film expansion of the autoradiograph was determined by comparing distances between the two images on the film with the corresponding distances on the specimen. In each case this large scale expansion ($\sim$ 1 cm.) was found to be uniform to within 1 per cent.

To determine the function $\mu(\xi)$, the undiffused specimens prepared using arrangement (ii) were examined under the microscope for good contact of the mating faces; a number of autoradiographs

were made of those specimens considered to be satisfactory and two or three traces taken from each. The density values were measured on each trace at 2μ, 5μ, 10μ and 20μ intervals over the range of the feature. Average values of the function were calculated from at least ten traces and an estimate of the accuracy was made. The average values were used in a computer program which calculated $\mu(\varsigma)$ values over the whole range at appropriate intervals - 1μ steps for nickel-63 and 1.5μ steps for silver-110 and antimony-124 - and stored these on magnetic tape for the subsequent calculations. An example of the experimental traces is given in Fig. 5 and values of the functions are tabulated in Table 1.

The grain boundary measurements were made using the Joyce Loebl Tec Ops Isodensitracer. This instrument consists of a modified microdensitometer controlled by an additional programmer unit. In one mode the microdensitometer scans and records in its normal way, and in the other it performs repeated scans covering a selected area of the specimen in a chosen number of steps, using a square aperture of small dimensions. For each scan of the specimen the density variation is represented on a corresponding straight line of the trace by a three symbol code applied by a solenoid activated pen. The code symbols, dots, line, blank in cyclic order signify an increasing density scale divided into equal increments. A density map of the scanned area is thus built up showing regions, each of a small density range, defined by contours corresponding to lines of equal density.

The distance moved between scans by the specimen and by the

pen assembly are variable, the ratio giving the transverse magnification of the trace and the density range of the wedge can be divided into 8, 16 or 32 increments.

The adjustment of the instrumental parameters was critical. Preliminary calculations indicated that the grain boundary diffusion region could be taken as triangular, on average some 300μ deep on a 150μ base, and that within this the concentration varied by three orders of magnitude. The range of the parameters indicated that it would be possible to scan the region in the required way, but the detail that was to be revealed and the exactness of the record would depend upon being able to reconcile the image characteristics with the instrumental factors. The minimum aperture was limited not only by the grain size of 0.5μ but also by the grain pattern, found to be simple with isolated grain for low energy radiations and complex with grain tracks in the case of high energy radiation.

The main consideration was that the size of the aperture should be consistent with the scale of the image features. A low energy tracer diffused at low temperatures for example gave a boundary width and a volume region depth that were both less than 50μ on the autoradiograph and the minimum size of aperture that could be used before excessive noise appeared on the isodensity trace was 6μ x 6μ, and for these conditions a small amount of distortion was found to occur in the trace. A correction can be made for this instrumental effect, provided it is not excessive, but there is an obvious limit to the image-aperture size ratio.

The final setting of the instrumental parameters was done by trial, the criterion being that the trace should be free from

noise and distortion and that it should display the complete feature in sufficient size and detail to make the required measurements.

The density wedge was chosen so that its full range was used, and the number of increments selected so that good contour definition was obtained, the specimen-to-record linkage was varied between 100:1 and 600:1 in both directions to suit the image and the speed of recording reduced well below the value where it was likely to produce distortion. The isodensity traces that are given in Fig. 7, each with instrumental parameters added, illustrate the wide range of conditions that have been used and indicate the limitations of the technique.

CHAPTER IV

INTERPRETATION OF THE EXPERIMENTAL DATA

4.1 The Density Distribution of the Volume Diffusion Zone

For volume diffusion in single crystals with diffusion taking place from a thin layer on a face into the body of a rectangular specimen, C the concentration per unit volume of the tracer element at a distance y from the face is given by equation (2.3)

$$C = \frac{C_o}{(\pi Dt)^{\frac{1}{2}}} \exp\left(-\frac{y^2}{4Dt}\right) \qquad (4.1)$$

If a surface perpendicular to the active face is prepared for autoradiography then the film image of the diffusion zone will show a density distribution that is some measure of the concentration distribution. If the effective radiation is of a very short range, it may be possible to assume that the density variation is directly proportional to the concentration variation so that the above equation can be written as

$$d = \frac{d_o}{(\pi Dt)^{\frac{1}{2}}} \exp\left(-\frac{y^2}{4Dt}\right) \qquad (4.2)$$

where d is the density at a distance y from the surface and d_o some constant. In the general case such a dependence cannot be assumed, for if the range of the particles is not negligible by comparison with the penetration depth, then the diffusion zone will produce an image on the film showing a degree of spread and having a density variation that depends upon the range of the particles. Blackburn and Brown[167] and Barry[92] discussing this in terms of resolution of the method, illustrate the magnitude

of systematic error that can arise from an uncritical application of equation (4.2).

A treatment of the problem using fundamental principles presents difficulties. For example, the particles reaching the surface at P in Fig. 4 can originate from any point within the diffusion zone nearer than some maximum distance. This distance is determined by the maximum energy associated with the disintegration schemes of the tracer element, and the stopping power of the specimen material. The contribution of the element of volume δv_1 to the number of emulsion grains developed at P, depends upon the number of particles reaching this point with an energy that can sensitize the film. This number is difficult to determine, depending upon such factors as concentration of the tracer in δv_1, the energies of the particles, the distance r_1 to P, the absorption and scattering properties of the specimen material, the emulsion thickness, characteristics and exposure time. A summation to account for all contributing elements of volume would be required to obtain the total density at P, and the effect of each one would be different. Lengthy and difficult computations involving factors not readily determined would be necessary to obtain the density distribution of the film due to some known concentration distribution. In the following treatment the use of factors of this sort is avoided, by introducing a function that combines the effect of all of these, and which is determined by one experiment.

Consider the prepared specimen to be made up of a series of elementary slices each with the same area as the active face, parallel to it and of a thickness $d\xi$. If $d\xi \rightarrow 0$ then the

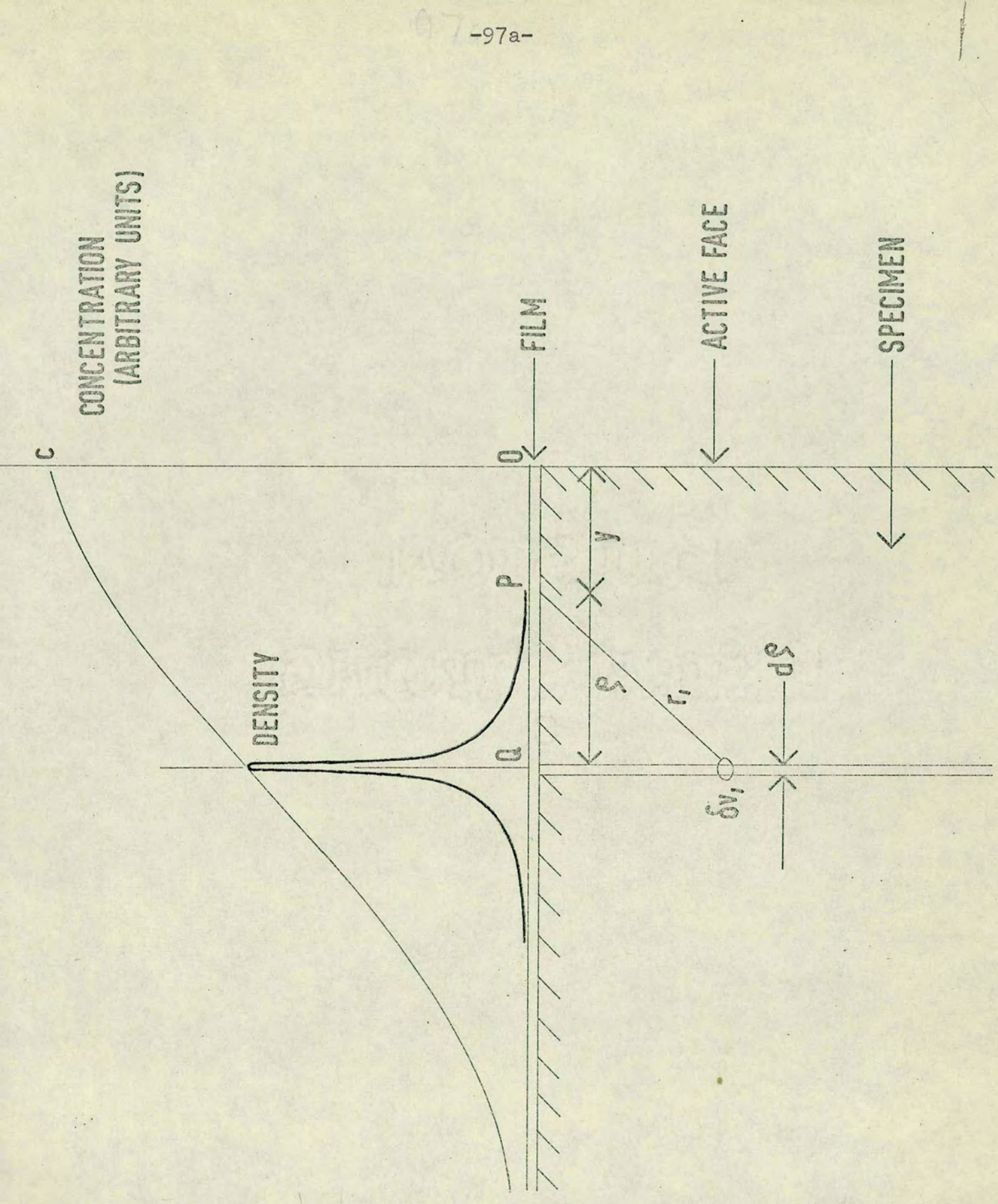

Fig. 4. Volume diffusion image spread.

concentration of the isotope in each slice can be taken as constant and given by equation (4.1). The radiations from a given element on reaching the surface will affect not only the grains in contact with that element, but also the grains in contact with adjoining elements. The density distribution or profile produced on the film by such an element will show a finite spread, and the complete density trace will be made up of the overlapping profiles of all such elements of the diffusion zone. If this overlapping is considerable, then a relative reduction of the film blackening of areas of high concentration and an increase of blackening of areas of low concentration will be expected to result.

Suppose the elementary slice at Q in Fig. 4 to be the only element containing the active isotope, and let C be the concentration per unit volume. If a film is laid in contact with the polished surface Oy, then upon developing, the distribution of the density about the source will be

$$\mu(\xi)C\,d\xi$$

where ξ is measured from Q, $C\,d\xi$ is a measure of the strength of the source and $\mu(\xi)$ is a measure of the density distribution produced by an infinitely thin plane source of unit strength.

Now take the element at Q to be an element of the diffusion zone. The contribution of the source at Q to the resulting density of the film in contact with the point at P, a distance ξ from Q and a distance y from the origin is

$$\mu(\xi)\,C\,d\xi\ .$$

Now the concentration at Q is given by equation (4.1), so that

the contribution of Q to the density at P can be written as

$$\mu(\xi)\,\frac{C_o}{(\pi Dt)^{\frac{1}{2}}}\exp\left[-\frac{(y+\xi)^2}{4Dt}\right]d\xi$$

and the total resulting density d at P is found by summing the contribution of all such elements from -y to $+\infty$

$$d = \int_{-y}^{\infty} \frac{C_o}{(\pi Dt)^{\frac{1}{2}}}\,\mu(\xi)\exp\left[-\frac{(y+\xi)^2}{4Dt}\right]d\xi \qquad (4.3)$$

Since it is sufficient to know the distribution of relative density due to the diffusion zone, $C_o/(\pi Dt)^{\frac{1}{2}}$ can be taken as a normalizing factor and $\mu(\xi)$ can be taken as a measure of the density distribution from an infinitely thin plane source of any uniform concentration contained within the body of the specimen material.

Equation (4.3) was used to produce the density distribution for a given $(Dt)^{\frac{1}{2}}$ value, the y intervals being chosen so as to give a well defined curve. The integral was evaluated by an application of Simpson's Rule which selected the ξ intervals of integration to suit the variation of the integrand; in this, the function $\mu(\xi)$ was used in the numeric form, the values of which were determined in the way described in Section 3.9. In the earlier stages a Ferranti Sirius computer was used, but most of the calculations were performed on an English Electric KDF9. A set of such curves were produced with the $(Dt)^{\frac{1}{2}}$ values chosen so as to give a generous selection within the range covered experimentally. These curves were used to determine D by matching the experimental trace as detailed in Section 4.3.

4.2. The Density Distribution of the Grain Boundary Zone

The image spread that occurs in grain boundary diffusion can be treated in a similar way. In this case the concentration distribution varies in two dimensions and so the elements of constant concentration are rod sources parallel to the active face.

Take Fig. 1 to represent the section of a diffused specimen prepared for autoradiography, with the free active surface $O\xi$ and the grain boundary $O\eta$ both normal to it, and with the contours of constant concentration as indicated.

The exact solution of Suzuoka is given by equation (2.9)

$$C(\xi,\eta,\beta) = \frac{K}{(\pi Dt)^{\frac{1}{2}}}\left[\exp\left(-\frac{\eta^2}{4}\right)+\frac{1}{4}\int_1^{\Delta}\left(\frac{\eta^2}{\sigma}-2\right)\exp\left(-\frac{\eta^2}{4\sigma}\right)\operatorname{erfc}\left(\frac{\xi}{2}+\frac{\sigma-1}{2\beta}\right)\frac{d\sigma}{\sigma^{3/2}}\right]$$

$$= C_1(\eta) + C_2(\xi,\eta,\beta) \quad . \qquad (4.4)$$

Consider the boundary diffusion zone to be made up of an assembly of rod-like elements of cross-sectional area da and perpendicular to the prepared surface. The contribution of the source at $Q(\xi',\eta')$ to the film density at $P(\xi,\eta)$ is

$$\mu'(\zeta)\, C\, da$$

where $\mu'(\zeta)$ is the spread function due to an elementary rod source of unit strength, Cda a measure of the source at Q and

$$\zeta = \left[(\xi-\xi')^2 + (\eta-\eta')^2\right]^{\frac{1}{2}} \quad .$$

The total resulting density at P, $d(\xi,\eta)$ is found by summing the contribution of all such elements over some region A determined by range considerations, that is

$$d(\xi, \eta) = K' \int^{A} \mu'(\zeta)\, C(\xi', \eta', \beta)\, da$$

where K' is some constant, or alternatively with appropriate limits and $da = d\xi'\, d\eta'$

$$d(\xi, \eta) = K' \iint \mu'(\xi - \xi', \eta - \eta')\, C(\xi', \eta', \beta)\, d\xi'\, d\eta' \tag{4.5}$$

Since it is usually desirable to make grain boundary measurements with the effect of the volume diffusion removed, subtracting the volume density contribution gives the resulting distribution $d'(\xi, \eta)$ which may be written as

$$d'(\xi, \eta) = K' \iint \mu'(\xi - \xi', \eta - \eta')\, C_2(\xi', \eta', \beta)\, d\xi'\, d\eta' \tag{4.6}$$

where $C_2(\xi', \eta', \beta)$ is the grain boundary diffusion term in equation (4.4), and this may conveniently be used as an expression of relative density with $K'K$ a normalizing constant.

The method was applied as follows. A value of β was assumed, and the concentration C_2 was calculated at points forming a grid over the triangular area of the diffusion zone, with a point separation of approximately 1.5μ. The values were calculated using the Laplace quadrature method and stored on magnetic tape for each required β value. The accuracy of the Laplace quadrature was checked over the range of each parameter against a Simpson's Rule formula so as to determine the required normalization factors; the integration was achieved with a small number (6 to 12) of sampling points at all except the highest β values. The film density at a point was calculated by performing the required convolution of the calculated concentration distribution with the $\mu'(\zeta)$ function.

To do this a two-dimensional numerical integration was performed over an area of the grain boundary region defined by the range of the $\mu'(\zeta)$ function. As a first stage the density distribution down the grain boundary was calculated and compared with the experimental variation to obtain a β value by matching as detailed in section 4.4.

The function $\mu'(\zeta)$ was not determined directly. Experimentally it was possible to obtain an infinitely thin rod source of activity by evaporating on to a polished surface with a thin ruled line on it, polishing away the unwanted activity, then mating a copper blank. The density distribution produced by this source however, was too small to be measured with sufficient accuracy. The required distribution was determined from the distribution $\mu(\zeta)$ obtained from the infinitely thin plane source of activity, used in the volume diffusion case. The two are related as follows. Imagine the plane source to be made up of a series of rod or strip-like elements of length Δx then if $\mu(d_i)$ is the density at a point distance d_i from the plane source and $\mu'(r_j)\Delta x_{ij}$ is the contribution of the element Δx_{ij} at a distance r_j from the point then

$$\mu(d_i) = k \sum^{j} \mu'(r_j)\, \Delta x_{ij} \qquad (4.7)$$

where k may be taken as unity since it is only relative densities that are required, and the summation is carried out for a set of distances r_j, chosen for use throughout, and covering the values zero to maximum particle range. The function $\mu(\zeta)$ was obtained as previously described and its value determined at points d_i suitable for use in the above equation. If the

distances d_i are chosen to be the same as the r_j distances, then a set of simultaneous equations is obtained from which the required values $\mu'(r_j)$ are obtained by inversion of the matrix of the coefficients Δx_{ij}. A high density of points was chosen at small ρ values and a low density at high ρ values, the total number being limited to approximately 70 by the demands of matrix inversion on the storage capacity of the KDF9 computer core. The values obtained were then used to determine the complete $\mu'(\rho)$ function in the same numeric form as the $\mu(\rho)$ function and these data stored on magnetic tape for use in the convolution calculations. The spread of the $\mu'(\rho)$ distribution is less at corresponding points than that of the $\mu(\rho)$ distribution, but extends to the same maximum range. For Kodak AR.10 film the half-height values are 17μ and 30μ respectively for antimony-124, 7μ and 16μ for silver-110 and 4.5μ and 6μ for nickel-63.

It is emphasised that the spread function should be interpreted as the result not only of the energy effect, but of all the factors that produce an image spread. With nickel-63 for example the particle energies are very low, but the $\mu(\rho)$ distribution is not correspondingly narrow; the reason for this is the effect produced by film thickness. Preferably the spread function should also include the instrumental effect due to the image-aperture size ratio; this can be taken into account to some extent by using the aperture conditions appropriate to the isodensity traces in determining $\mu'(\rho)$.

4.3 The Determination of D

To determine the volume diffusion coefficient for a given temperature, the density curves computed from equation (4.3) were compared in turn with the experimental density trace obtained from the microdensitometer. Corrections were applied to the y scale to allow for film expansion and lever arm ratio calibration, and the adjustment of the density scale was made by normalizing at several points in the region of the peak density. Matching was considered to be acceptable when it was possible to obtain a good fit of the experimental trace along its length after achieving superposition of the characteristic features - the origin and the peak and background densities. It was then possible to assign a $(Dt)^{\frac{1}{2}}$ value to the experimental trace and to quote an error due to the uncertainty in matching. A matching process of this sort was carried out on a number of traces from a given specimen. In a very few cases the experimental trace could not be fitted satisfactorily by the computed curves and it was discarded. The random variation that was present on the traces obtained from AR.50 film did not impair matching to any serious extent. This instrumental noise is associated with a film grain effect that varied with the energy of the isotope in a way that is illustrated in the graphs.

4.4 The Determination of D'

The grain boundary diffusion coefficients were determined as follows. The density distribution down the boundary and in the volume diffusion zone were obtained from the isodensity trace. The penetration measurements were made with the aid of a D-mac

x-y plotter with digital output. These were graphed together and the volume density distribution subtracted from the grain boundary distribution. The resulting curve was then matched with the density curve calculated from equation (4.6). The matching requires consideration. The origins must be carefully identified and the η scales appropriately adjusted, the backgrounds must be carefully determined and the curves finally normalized at some point or over some region in the following way. If the form of the two curves were the same then normalization would not be critical; however, this was found not to be the case in the near surface region. Normalization was carried out clear of the point at which the curves were expected to diverge, and a fit could be achieved over a reasonable length of the curve. The fit towards the tail was less satisfactory on account of the difficulty in determining the exact background value. A number of examples of matching are given in Fig. 8. These also show the β values of the computed curve and the β value assigned to the experimental curve.

In the case of nickel-63 three additional β values were obtained by assuming a concentration-density equivalence. The contact angle ϕ was measured at a number of η values on the isodensity trace, and the β value corresponding to this determined from the calculated concentration distributions stored on magnetic tape by means of a supplementary computer programme. This did not always correspond closely with the β value obtained from the approximate expression of the Whipple solution[228]. A β value was also obtained by matching the contours on the isodensity traces with curves of equiconcentration obtained from

the stored distributions. Another β value was obtained by a method analogous to the sectioning technique. The total amount of diffusant $\bar{C}$ in a section was taken to be proportional to the integrated density measured along the corresponding line on the isodensity trace, and an appropriate penetration plot was used to give a value of the quantity $\frac{\partial \ell n \bar{C}}{\partial y^{6/5}}$. A self-consistent β value was obtained by using the relation quoted in Section 2.3.4.

$$\beta = \frac{1}{Dt}\left(\frac{\partial \ell n \bar{C}}{\partial(\eta \beta^{-\frac{1}{2}})^{6/5}} \Big/ \frac{\partial \ell n \bar{C}}{\partial y^{6/5}}\right)^{5/3}$$

$\frac{\partial \ell n \bar{C}}{\partial(\eta \beta^{-\frac{1}{2}})^{6/5}}$ being taken from the calculated values given by Suzuoka[160].

In the case of silver-110 the matching was repeated with density distributions calculated by using C_2, the boundary concentration term given by the Whipple solution (equation (2.8)).

CHAPTER V

RESULTS AND DISCUSSION

5.1 Summary of the Results

Table 1 gives an abridged form of the spread functions $\mu(\zeta)$ determined from sandwich-type specimens as described in Section 3.9. The $\mu'(\zeta)$ functions are shown alongside the $\mu(\zeta)$ functions from which they were derived as described in Section 4.2. The table, which gives the widths at the tenth-heights for each curve, illustrates that the differences are more marked in the lower half of the curves. An example of the experimental traces is shown in Fig. 5.

The results of the initial volume diffusion measurements of antimony-124 into copper single crystals using AR.50 film and given in Tables 2 and 3 and Fig. 6.

Table 2 illustrates the results that were obtained from the matching of individual traces for a few specimens with penetration depths typical of the range covered. The average values have been calculated from each set of results and the quoted errors correspond to the 95°/o reliability limit. Table 3 shows the average result for each of the penetrations used. The calculated values have been obtained by using the corresponding mechanical sectioning results of Inman and Barr, and the errors also refer to the 95°/o reliability limit. The graphs of Fig. 6 show that there is good agreement between the experimental trace and the computed curve taken to match it. Table 4 gives the results for the volume diffusion of nickel-63 and silver-110 obtained in the same way, but using the bicrystal specimens, most of which were mounted in

Table 1

The spread function: skeleton data

Fraction of peak height	Widths of the spread functions in microns							
	Antimony-124			Silver-110			Nickel-63	
	A.R.10		A.R.50	A.R.10		A.R.50	A.R.10	
	$\mu(\varsigma)$	$\mu'(\varsigma)$	$\mu(\varsigma)$	$\mu(\varsigma)$	$\mu'(\varsigma)$	$\mu(\varsigma)$	$\mu(\varsigma)$	$\mu'(\varsigma)$
1.0	0	0	0	0	0	0	0	0
0.9	8.4	1.6	12	3.5	1.0	9	2.4	1.8
0.8	13.4	3.0	18	6.2	1.3	13	3.2	2.7
0.7	18.0	6.6	28	9.2	1.8	17	4.1	3.4
0.6	22.2	10.6	36	15.4	2.7	20	5.0	4.1
0.5	29.4	15.5	54	16.8	4.0	30	5.8	4.8
0.4	40.0	18.4	84	21.6	6.0	36	7.4	5.5
0.3	55.4	22.2	126	30.6	10.0	55	8.6	6.6
0.2	83.2	31.2	204	41.2	14.0	80	10.6	8.3
0.1	166.0	46.0	376	128.0	20.4	170	13.8	11.2
0	750.0	750.0	1000	2200.0	2200.0	2000	30.0	30.0

Table 2

Volume diffusion data: individual antimony-124 results

Specimen number	14/1	12/1	11/1	11/2	13/1	13/3
Specimen arrangement	(ii)	(ii)	(iii)	(ii)	(iii)	(iii)
Uncertainty in matching	Autoradiograph plate/trace number and observed $(Dt)^{\frac{1}{2}}$ value in cm 10^{-4}					
	± 8	± 6	± 6	± 6	± 5	± 5
	14/4 152 14/5 150 14/6 150 15/7 150 15/8 152 15/9 154	5/4 80 5/5 82 5/6 76 8/10 80 8/11 82 8/12 84 8/13 82	18/4 60 18/5 56 21/4 60 21/5 58 21/6 58 23/2 53 23/3 55	32/1 38 32/2 38 32/3 40 29/4 40 29/5 42	40/1 15 40/2 16 40/3 15 41/4 19 41/5 18 41/6 19 38/7 16 38/8 15 38/9 17	44/1 10 44/2 8 44/3 8 42/7 8 42/8 6 42/9 10 45/4 7 45/5 7 45/6 8
Average $(Dt)^{\frac{1}{2}}$ value	151 ± 3	81 ± 2	57 ± 2	40 ± 2	17 ± 2	8 ± 1
$(Dt)^{\frac{1}{2}}$ value calculated from sectioning results	150 ± 5	78 ± 3	59 ± 2	39 ± 2	20 ± 1	10 ± 1

Table 3

Volume diffusion data: summary of antimony-124 results

Specimen number	Specimen arrangement	T°C	t sec 10^{-4}	Observed $(Dt)^{\frac{1}{2}}$ cm.10^4	Calculated $(Dt)^{\frac{1}{2}}$ cm.10^4	D cm^2 sec^{-1}. 10^{12} Present Results	D cm^2 sec^{-1}. 10^{12} Previous Results
14/1	(i)	795	26.214	147 ± 4	150 ± 5	825 ± 45	860 ± 45 (1)
14/1	(ii)	795	26.214	151 ± 3	150 ± 5	870 ± 40	860 ± 45 (1)
4/4	(i)	700	110.880	121 ± 3	119 ± 4	132 ± 10	127 ± 15 (1)
5/5	(i)	651	222.840	98 ± 3	96 ± 4	43 ± 3	40 ± 3 (1)
12/1	(i)	856	2.406	79 ± 2	78 ± 3	2600 ± 150	2500 ± 150 (1)
12/1	(ii)	856	2.406	81 ± 2	78 ± 3	2730 ± 150	2500 ± 150 (1)
11/3	(iii)	896	1.542	80 ± 1	84 ± 3	4150 ± 100	4600 ± 250 (1)
11/1	(ii)	743	11.028	57 ± 2	59 ± 2	295 ± 20	312 ± 20 (1)
11/1	(iii)	743	11.028	57 ± 2	59 ± 2	295 ± 20	312 ± 20 (1)
11/2	(ii)	743	4.920	40 ± 2	39 ± 2	325 ± 20	312 ± 20 (1)
11/2	(iii)	743	4.920	37 ± 2	39 ± 2	280 ± 30	312 ± 20 (1)
13/1	(iii)	663	7.458	17 ± 2	20 ± 1	39 ± 4	53 ± 3 (1)
13/3	(iii)	560	31.266	8 ± 1	10 ± 1	2.1 ± 0.5	3.3 ± 0.5 (2)

(1) Inman and Narr[266].

(2) Barr[265].

Table 4

Volume diffusion data: additional results

T°C	Specimen number	$(Dt)^{\frac{1}{2}}$ cm 10^4	D cm^2 sec^{-1} $.10^{12}$ Present Results	Previous Results
		Nickel-63		
676	N16	5.7 ± 1	0.42 ± 0.15	0.25 (2)
703	N4	11.2 ± 1	0.90 ± 0.16	0.55 (2)
698	N15	13.2 ± 1.5	0.80 ± 0.16	0.53 (2)
750	N3	24.5 ± 2	4.3 ± 0.5	2.3 (1)
750	N12	25.5 ± 2	3.0 ± 0.5	2.3 (1)
803	N9	36.4 ± 3	12.7 ± 2	8.3 (1)
800	N13	50.3 ± 3	11.7 ± 2	8.3 (1)
818	N14	17.6 ± 1	17.9 ± 2	12.8 (1)
823	N11	25.0 ± 2	18.1 ± 3	15.6 (1)
850	N1	33.5 ± 2	32.5 ± 4	26.8 (1)
Activation Energy (k cal/mole)			54 ± 3	56.5 (1)
Pre-exponential Factor (cm^2/sec.)			1.1 $\pm^{0.9}_{0.4}$	2.7 (1)
		Silver-110		
543	W19	6.8 ± 1	0.34 ± 0.05	0.36 (3) 0.18 (4)
593	W4	12.6 ± 1	1.2 ± 0.2	1.7 (3)
593	W8	17.5 ± 2	1.2 ± 0.2	1.0 (4)
		Antimony-124		
605	S28	23 ± 5	16 ± 5	12.0 (5)
626	S27	28 ± 4	24 ± 4	20.3 (5)
650	S15	26 ± 2	39 ± 5	38.5 (5)
680	S20	26 ± 2	78 ± 9	78.8 (5)
721	S23	40 ± 2	185 ± 20	193 (5)

(1) Mackliet[259]
(2) Mackliet extrapolated D
(3) Morrison[112] Observed D
(4) Mercer[258] extrapolated D
(5) Inman and Barr[266].

Table 5

Grain Boundary diffusion data: summary of results

T°C	t sec 10^{-4}	Specimen	$(Dt)^{\frac{1}{2}}$ cm 10^{4}	β	cm^2 D' sec^{-1} 10^{6}	D'/D 10^{-5}
				Nickel-63		
676	78.0	N16	5.7	190 ± 30 200 ± 30 200 ± 30 240 ± 30	1.8 ± 0.4	43 (1) (3) (6)
703	138.2	N4	11.2	54 ± 10 45 ± 10 60 ± 10 55 ± 8	2.0 ± 0.5	24 (1) (3) (6)
698	214.8	N15	13.2	55 ± 10 45 ± 10 55 ± 10 45 ± 8	2.4 ± 0.6	28 (1) (3) (6)
750	216.3	N12	25.5	7 ± 2 5 ± 2 6 ± 2 5 ± 2	2.5 ± 0.6	7.4 (1) (3) (6)
750	138.2	N3	24.5	8 ± 2 8 ± 2 8 ± 2 5 ± 2	2.6 ± 0.6	7.7 (1) (3) (6)
803	103.7	N9	36.4	19 ± 4 6 ± 3 10 ± 4 11 ± 2	32 ± 6.0	27.5 (1) (3) (6)
800	216.0	N13	50.3	1.9 ± 0.4 1.5 ± 0.4	4.5 ± 1.0	3.9 (1)
818	17.28	N14	17.6	3.6 ± 0.8 3.0 ± 0.5 2.0 ± 1.0	4.3 ± 1.0	2.4 (1) (3)
823	34.56	N11	25.5	3.0 ± 0.8 2.5 ± 0.5 2.8 ± 0.5	6.2 ± 2.0	3.1 (1) (3)
850	34.65	N1	35.3	1.5 ± 0.5 1.0 ± 0.3	7.6 ± 2.5	2.1 (1)

Activation Energy = 26 ± 2 kcal/mole

Pre-exponential Factor = $0.9 \begin{smallmatrix} + 1.5 \\ - 0.3 \end{smallmatrix}$ $cm^2/sec.$

Table 5 (Continued)

T°C	t sec 10^{-4}	Specimen	$(Dt)^{1/2}$ cm 10^4	β	D' $cm^2\ sec^{-1}$ 10^6	D/D 10^{-5}
				Silver-110		
543	138.2	W19	6.9	1500 ± 500	14 ± 6	41.2 (4)
			5.0	1900 ± 300	6.5 ± 3	120 (5)
				1600 ± 250		(2)
593	127.4	W4	12.6	125 ± 35	8 ± 2	62
			11.0	150 ± 40	6.0 ± 2	50 (5)
				150 ± 30		(2)
593	266.1	W8	17.5	150 ± 50	12 ± 4	105
			15.7	175 ± 40	9.6 ± 3	80 (5)
				150 ± 40		(2)
640	138.7	W3	24.0	26 ± 6	10 ± 2	25
				27 ± 6		(2)
642	243.2	W7	31.5	22 ± 5	11 ± 2	28
				22 ± 5		(2)
698	20.74	W5	18.0	23 ± 4	25 ± 4	16
				23 ± 4		(2)
690	37.41	W16	24.0	13.5 ± 3	20 ± 4	13
				13.5 ± 3		(2)
718	8.64	W18	16.8	17 ± 4	37 ± 7	11
				18 ± 3		(2)
719	4.75	W17	12.5	18 ± 4	30 ± 6	9
				18 ± 4		(2)
757	2.36	W12	13.5	12.5 ± 3	52 ± 15	6
				13.5 ± 3		(2)
Activation Energy = 26 ± 2 kcal/mole Pre-exponential Factor = $15 \pm {}^{10}_{3}$ cm^2/sec.						
				Antimony-124		
605	32.08	S28	19.1	255 ± 50	230 ± 60	190
626	32.14	S27	25.5	145 ± 30	270 ± 80	130
650	17.28	S15	25.7	80 ± 16	320 ± 60	82
650	23.16	S16	29.8	60 ± 14	280 ± 60	73
680	4.32	S18	18.5	72 ± 15	420 ± 120	50
680	8.64	S20	26.1	49 ± 15	400 ± 120	50
700	8.66	S25	32.8	27 ± 7	440 ± 120	35
700	10.37	S26	35.9	34 ± 7	600 ± 120	50
720	4.76	S22	30.3	27 ± 7,	630 ± 160	30
721	8.64	S23	40.8	21 ± 6	670 ± 160	30
Activation Energy = 21 ± 3 kcal/mole Pre-exponential Factor $23 \pm {}^{20}_{8}$ cm^2/sec.						

(1) Angle of contact measurement
(2) Whipple model
(3) Limited contour fitting
(4) Result from one measurement
(5) Result using extrapolated D
(6) Integrated concentration measurement.

$\partial = 5.10^{-8}$ cm.

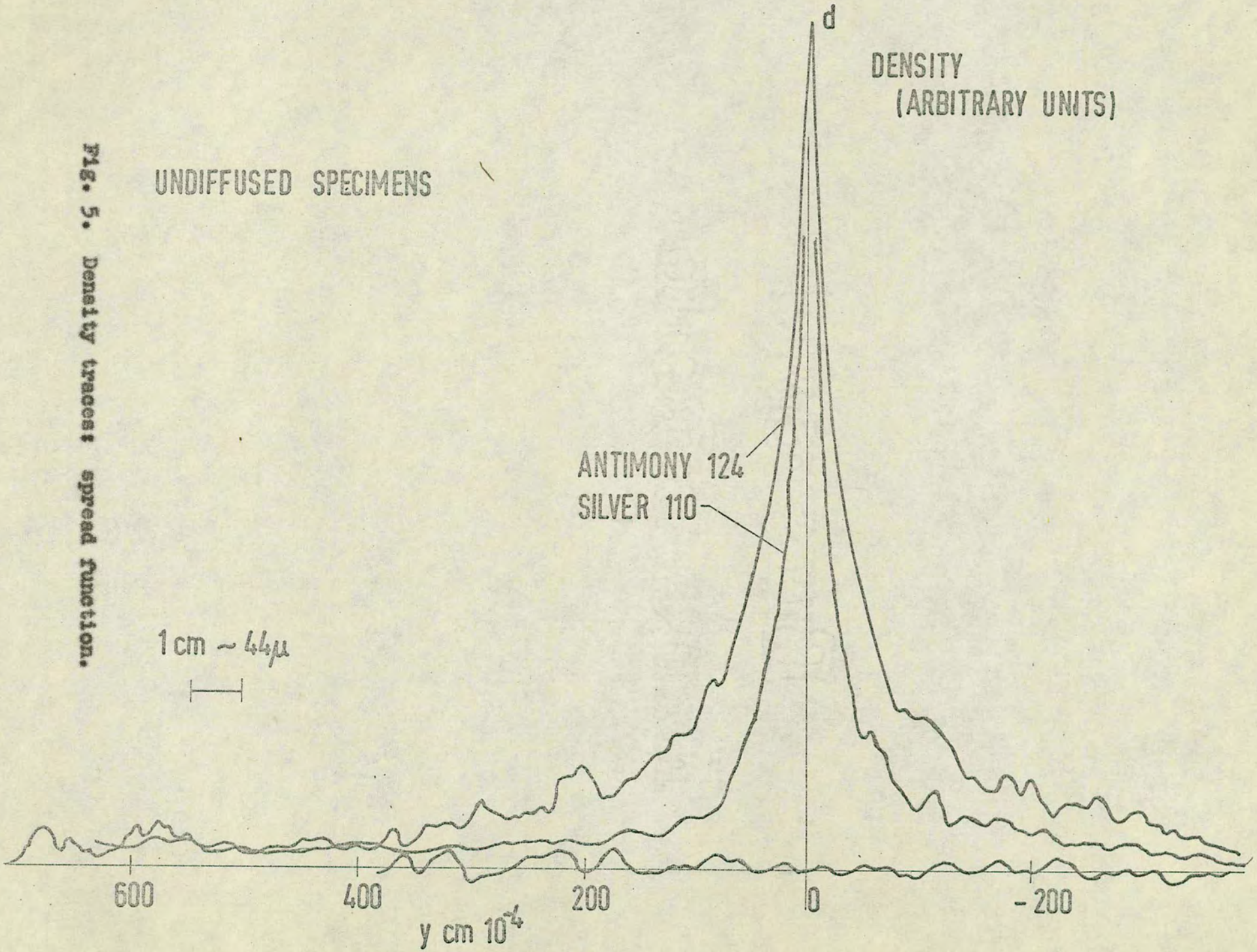

FIG. 5. Density traces: spread function.

arrangement (1), and AR.10 film. Arrhenius plots for the results are shown in Fig. 9.

The grain boundary diffusion results shown in Table 5, are average values obtained from two or three individual results. The diffusion coefficients were calculated from the boundary penetration measurements, taking δ equal to 5.10^{-8} cm. and plotted against the reciprocal of the absolute temperature in Fig. 10.

5.2 Reliability of the Results

The error that is quoted for the individual results is the uncertainty in matching and for the average results it is the standard deviation in those cases where there is a sufficient number of observations and where there is not, it is the mean error. Additionally there are a number of cases where a comparison can be made between the average values obtained from two specimens annealled for different times at the same temperature. This is a more realistic measure of the accuracy since it also indicates the effect of time dependent factors. For volume diffusion an examination of the quoted errors indicates a consistency between the uncertainty in matching, the error in the average value and the results from different anneals at the same temperature. In the grain boundary case there are insufficient individual observations to allow such a comparison, also the agreement between the results obtained from specimens annealled at the same temperature is less satisfactory. In this section the respective contributions of the several sources of error is examined and the possibility of undetected systematic variation is explored.

5.2.1 Sources of Error

In most of the anneals the temperature was held constant to $\pm$ 1.5°C, and the effect of this on the diffusion coefficients calculated from the relation

$$\frac{dD}{D} = \frac{Q}{RT^2}\, dT$$

is approximately 3°/o at the mid-point of the temperature range. This assumes that the temperature of the specimen is exactly the same as that of the thermocouple, but Mallard et al.(260) point out that this may not hold if radiation is the primary means of thermal communication, and add that this effect together with errors in calibration and reading of the thermocouple could give rise to a temperature variation of 3°C which would produce an error of 6°/o in the diffusion coefficient.

The heating-up correction described in Section 3.5 was necessary only in a few cases, but the maximum error that can arise from this, or from uncorrected anneals of several days duration, is approximately 0.2 per cent.

If the surface prepared for autoradiography is not normal to the grain boundary and to the active surface then the error is similar to the one that results from misalignment of the specimen in the sectioning technique. A misalignment of 6 degrees produces a 0.5°/o error in the penetration measurement, but the effect that this produces in the matching cannot be calculated in this way. Considering the precautions described in Section 3.4 the total error from this source is estimated to be less than 1 per cent.

Despite the precautions that were taken, evaporation of antimony-124 during the anneal appears to have occurred. The

volume diffusion results of S27 and S28 show this as a distortion in the near surface region of the trace, but this effect is not detected at higher temperatures. The effect tends to furnish a high value for the diffusion coefficients; in these cases it was estimated at 10 to 15 per cent, and there seems to be no reason for the grain boundary results to be effected very differently.

The effect of film expansion and lever arm ratio (Section 3.9) on the accuracy of the penetration measurements is small ($\sim 10^{o}/o$), but in the grain boundary case where the parameters are dimensionless, the $(Dt)^{1/2}$ factor itself shows an error of approximately $5^{o}/o$ at high and $20^{o}/o$ at low temperatures, and this is estimated to produce an error in the matching process of $10^{o}/o$ and $20^{o}/o$ respectively in D'.

The calculated density values are affected by errors in the spread function and additionally, in the grain boundary case, by the $(Dt)^{1/2}$ value. If the spread function errors are random then the effect will be reduced in the convolution; however if the errors are systematic, then it will be exaggerated. $\mu(\zeta)$ and $\mu'(\zeta)$ were determined with the greatest of care so that the error arising from this is estimated to be less than 2 per cent. The effect that the error in the $(Dt)^{1/2}$ value produces on the density values is known from trials not to be large, but it is a systematic variation.

In the matching process itself the factors that contribute to the total uncertainty in matching are mainly the fixing of the origin, determining the background value and the grain noise of the experimental trace, but any artifact in the trace, especially in the region of the peak density or near the origin is liable to cause a mismatch. An extended defect in the film generally resulted in a failure to match the experimental trace; this was readily

detected with volume diffusion, but with grain boundary traces, the matching was much less critical.

A correction for thermal expansion was not applied, the comparison with other results being made on this basis. With good quality mechanical sectioning results[265] this was found to give coefficients that are 2°/o low and activation energies that are 1°/o high.

For volume diffusion the combined effect of all these sources gives an error in D which varies from less than 10°/o at large penetrations to 25°/o at very small penetrations. For grain boundary diffusion the combined effect is larger and varies not only with the penetration but also with other conditions. The error in D' can be as low as 15°/o, but for conditions described in Section 5.3 as unfavourable, it can be as great as 75 per cent. These estimates are in substantial agreement with the errors quoted in the tables and apart from the low temperature results, agree also with the scatter of the points on the Arrhenius plots.

5.3 Discussion of the Method

There are certain basic features that must be examined when assessing any new method of measurement. The method should be based on principles that are scientifically sound and the analysis that is employed should be mathematically correct, also the technique should offer some advantage over existing methods, and the results should be reproducible to the existing standard of accuracy.

An expedient test is to compare the results produced by the method with those obtained by a tried and accepted method over the range of experimental conditions that is common to both. Outside the common range the results should be compared with theoretical predictions and failure to find agreement at any stage demands that a careful reassessment be made.

Although the analysis in the present application is based on a calibration procedure and not derived from fundamental principles, it appears that the mathematical basis of the method is quite sound and further that there are no limitations imposed by the calibration. This is certainly true at large penetrations, but at low penetrations obvious limitations exist with most methods. In this case the function $\mu(\zeta)$ also corresponds to a diffusion condition of zero penetration, and since this is measured directly it is possible in principle to measure diffusion penetrations down to this limiting value. In practice the smallest $(Dt)^{1/2}$ value that can be measured is the one which produces a density distribution that can be resolved from $\mu(\zeta)$, allowance being made for the error spread in $\mu(\zeta)$ and in the experimental trace.

5.3.1 Volume Diffusion

In the volume diffusion measurements the agreement that is found between the experimental trace and the computed curve taken to match it and between the observed results and the calculated results shown in the tables is sufficiently good to confirm that the method can be accepted as reliable over a wide range of the experimental conditions. There are some results however that do not show agreement with quoted value, and there are some assumptions that require careful scrutiny.

One assumption that has been made throughout this work is that film expansion does not vary with density, at the low densities used, and that the expansion over the image region is the same as that over the large region between the images used to determine

its value. There has been no attempt to verify this assumption, but if it was substantially incorrect then the results would not have shown the agreement observed.

In the derivation of equation (4.3) it was assumed that the scattering of the particles is the same at all points. This requires that the diffusion zone is situated within an extended solvent material and this condition cannot be fully satisfied. With unmated specimens mounted in arrangement (1) the scattering within the Araldite is different from the scattering within the copper and so the density traces are very different in the region which corresponds to the Araldite, and will show a small effect in the copper near surface region. Although this has no significant effect on the matching process at large penetrations, it becomes increasingly serious at lower penetrations. There would appear to be no reason however why this difficulty should not be largely overcome by a correction.

For specimens mounted in arrangement (1) it is possible to identify the origin with a point on the trace where the characteristic change in density is taken to result from the copper-Araldite interface. For specimens mounted in arrangement (11), although the origin cannot be identified with any point on the trace, matching is possible along the whole length of the curve. It is in arrangement (111) where both of the advantages are combined and where the spread of the trace is much larger, that the highest accuracy is to be expected. This is especially desirable for measuring the lowest penetrations.

Volume diffusion of all but the smallest penetrations

($(Dt)^{1/2} > 10\mu$) can be measured by this method with comparative ease. Because of the advantage of repeated autoradiography the method can achieve an accuracy that appears to be comparable with the sectioning technique. In this range of penetrations, the method is not critically dependent upon the energy of the tracer isotope or the choice of stripping film. For $(Dt)^{1/2} < 8\mu$ the large image spread of the very high energy isotope offers an advantage in measurement over the very low energy isotope, but this is offset to an extent by the poorer dispersion of the calculated curves. Very low penetrations ($(Dt)^{1/2} < 2\mu$) have not been measured, but the accuracy in this range is expected to be much less than the microtechniques that are available[261].

Despite a few deficiencies in detail there would appear to be no serious violation of the scientific principles in this application of autoradiography to volume diffusion. This is contrasted with previous applications[216, 262-264] where the basic assumption that the density distribution was directly proportional to the concentration distribution was erroneous. The graphs of Fig. 6 show these two distributions to be quite different, although there is a similarity between a portion of the density curve and the concentration curve. This can be found by superposition of the two curves, in Fig. 6, taking the peaks to correspond. This feature has been used to determine diffusion coefficients[92,167]. To do this equation 4.2 was applied, the peak density was chosen as origin and the background was adjusted to a suitable value. This introduces a systematic error, which becomes increasingly serious

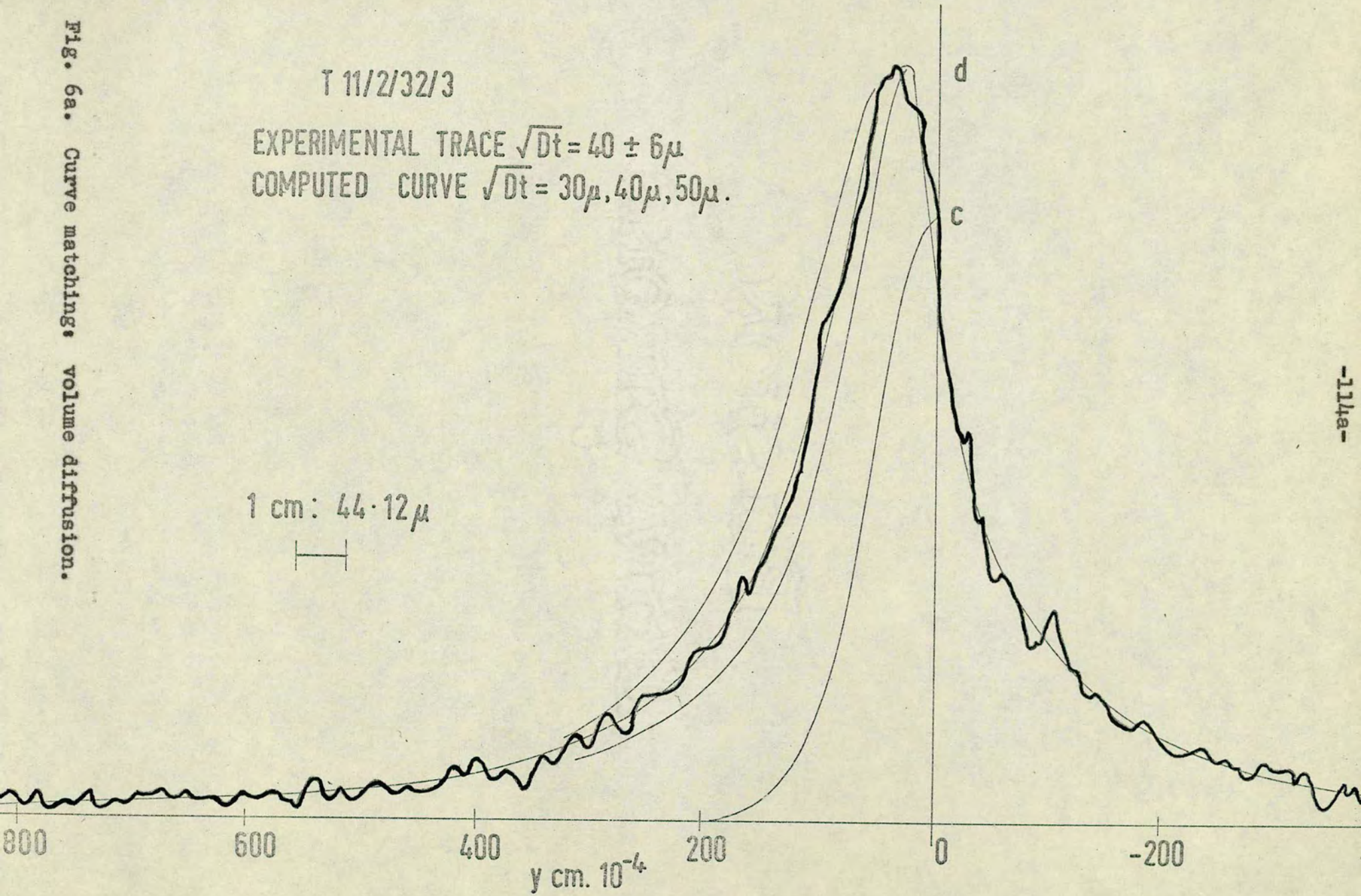

Fig. 6a. Curve matching: volume diffusion.

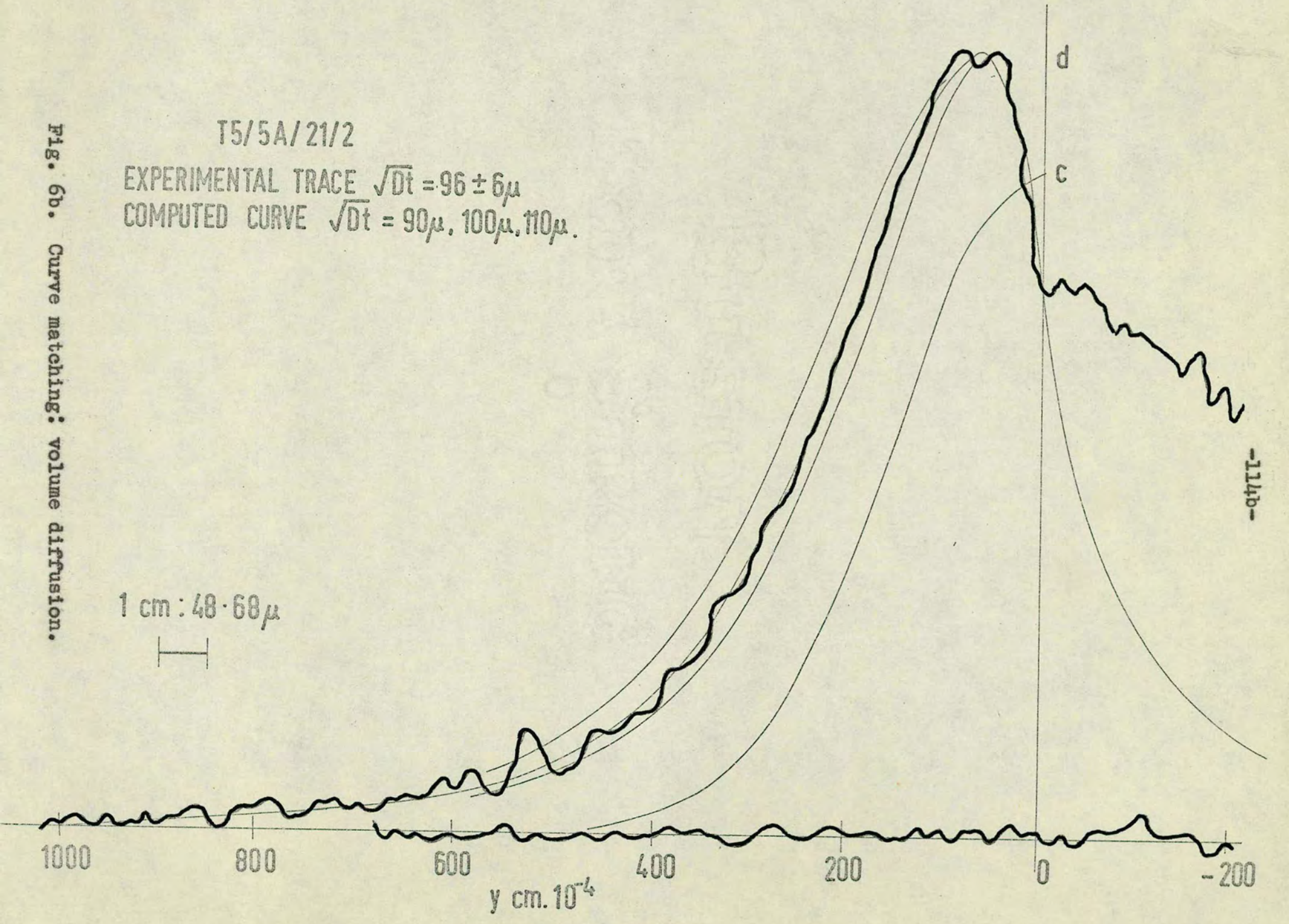

Fig. 6b. Curve matching: volume diffusion.

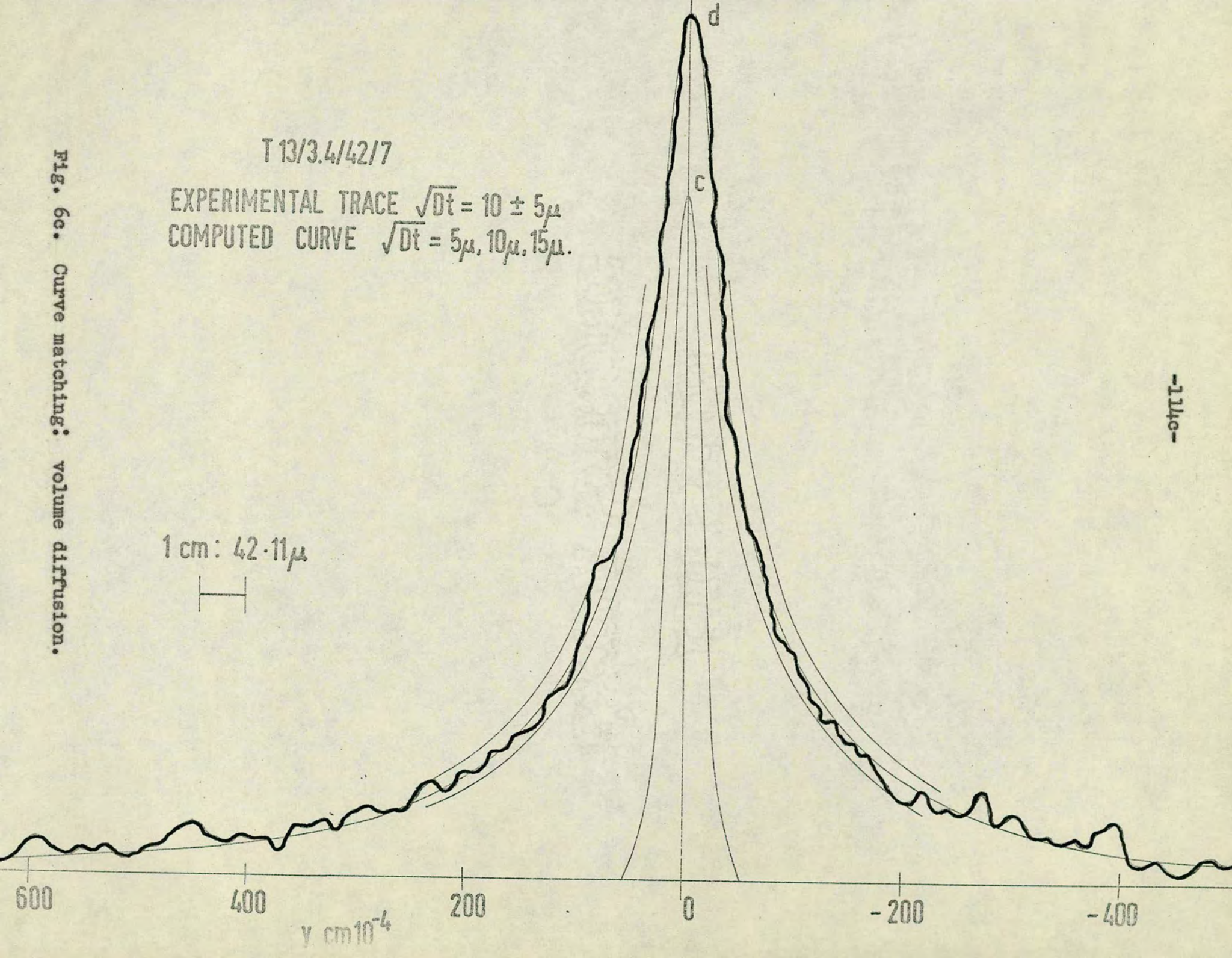

Fig. 6c. Curve matching: volume diffusion.

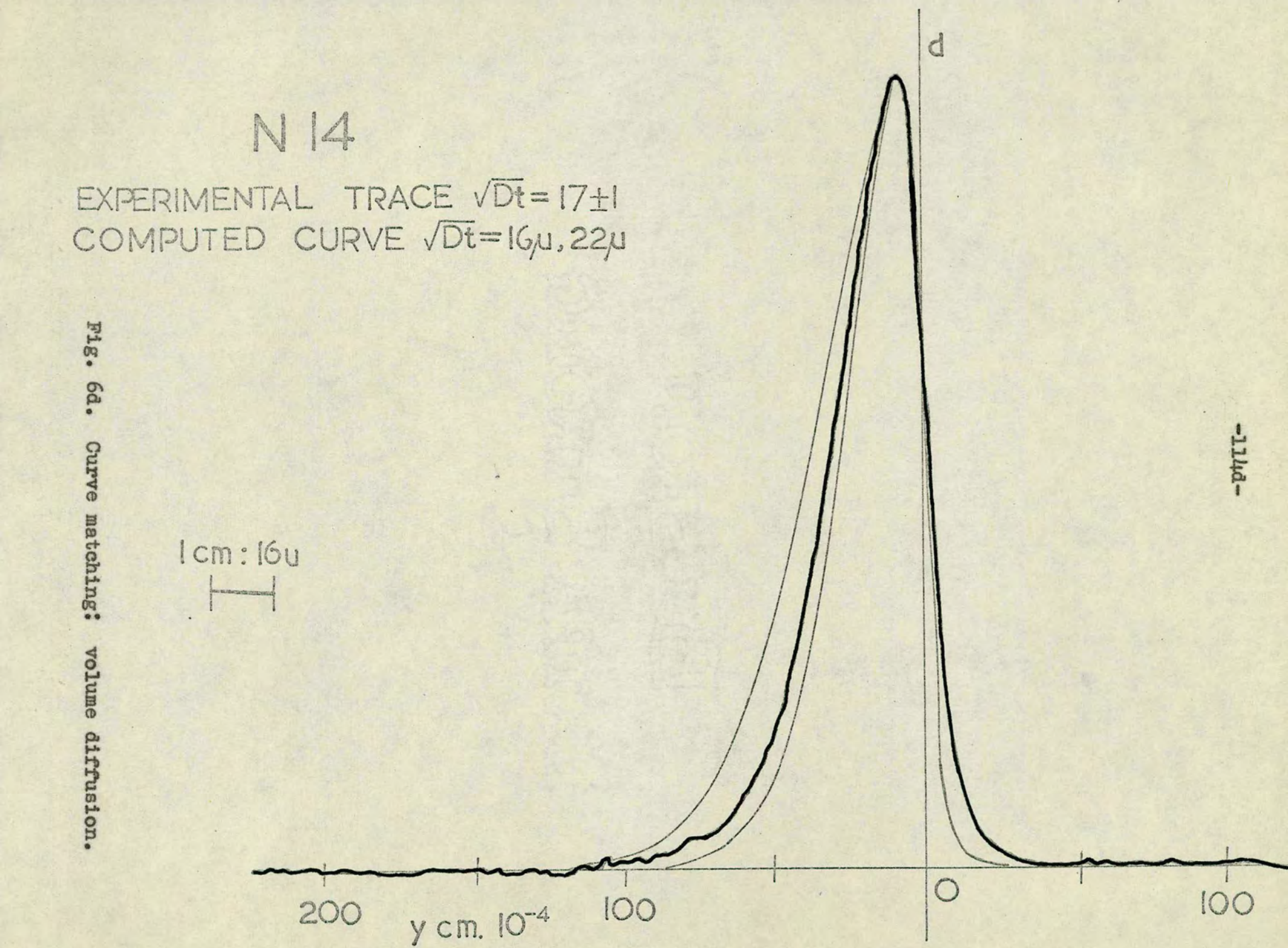

Fig. 6d. Curve matching: volume diffusion.

below medium penetrations - $(Dt)^{1/2}$ 50μ in the case of antimony-124 and $(Dt)^{1/2}$ 30μ in the case of silver-110. This procedure has been critically discussed by Barry[92], who in using it for the comparison of two simultaneously diffused specimens (one with and one without additional mechanical straining) achieves a correction by calibrating the observed $(Dt)^{1/2}$ values against calculated $(Dt)^{1/2}$ values. In this work it is also suggested that the spread function be used in analytic form and an expression for this is given; this, however, is of no advantage in the present case for two reasons. The numeric form avoids the calculations that are necessary with the analytic form, and it is also much more accurate. The several attempts to fit the spread function curves in the present work did not give sufficiently good agreement over the complete range.

5.3.2. Grain Boundary Diffusion

The difficulties in determining D', the grain boundary diffusion coefficient, are proportionately greater because to do this D, the volume diffusion coefficient, must first be determined. The volume penetrations are generally small (mean $(Dt)^{1/2}$ value $\sim$ 18μ) so this is not a minor consideration. However the difficulty is minimized by the procedure applied, which subtracts away the volume diffusion contribution, and gives little weight to the volume diffusion region, though it does employ the $(Dt)^{1/2}$ value as a parameter of prime importance. The additional complications that arise in the grain boundary case are very much affected by the energy of the tracer radiation and by the features of the measuring instrument. It is therefore instructive to discuss the application and the

limitations of the method in terms of these two factors - referred to as the energy effect and the instrumental effect - and the matching process.

If the effective radiation is of very high energy then the resulting image spread produces a decrease in the density of the grain boundary feature relative to the volume density, thus reducing the bulk and the length of the trace outside the volume region available for matching. This relative decrease is so great at low temperatures where the volume penetration is small and boundary content low, that the boundary feature cannot be adequately detected at normal exposures (Fig. 8(e)). At high temperatures where the volume penetration is large and this relative decrease consequently less, the image spread is still sufficient to produce an apparent decrease in the normally low β values. For antimony-124 annealing temperatures are restricted to the range 600°C to 720°C by the limiting β values of 300 (Fig. 7(f)) and 16 (Fig. 7(g)) respectively.

If the effective radiation is of very low energy then the density and the concentration distributions are the same, and β values from less than one to several thousand can in principal be observed, in practice however this range is limited by an instrumental effect due to the size of the examining aperture, the minimum dimensions of which are determined by the instrumental response to the image features and by a film grain effect (Section 3.9). If the image is small, an instrumental convolution occurs, and although this can be taken into account to some extent in determining the spread function $\mu'(\zeta)$, the effect imposes an obvious limit at low temperatures. Fig. 7(a) shows that the

limiting features are the boundary width and the volume penetration. At higher temperatures instrumental effects become negligible and the isodensity trace allows an investigation of the exact detail of the concentration distribution over a fairly wide range of β values. Good quality traces with β values as low as 1 allow annealing temperatures as high as 850°C with nickel-63 which is well outside the limit ($\beta \sim 8$) of the sectioning technique. Instrumental effects do not occur with antimony-124, but can be expected to give some effect with silver-110 at very low temperatures.

In the matching process the most favourable value of β in each of the systems was found to be intermediate within the ranges covered, at the point where the trace shows a fairly deep volume penetration, a deep boundary penetration and a fairly broad boundary zone. At low β values the required density difference is determined by subtraction from curves, both of which are varying rapidly as in Fig. 8(a) and this gives poor accuracy. A number of factors affect the accuracy at high β values especially in the case of a low energy isotope as in Fig. 7(a). The narrow width of the image introduces a larger instrumental effect, the inaccuracy in the small $(Dt)^{1/2}$ value gives a larger error in determining the η scale and the quick fall-off of the volume density to background value makes this uncertain feature more significant.

A qualitative examination of the isodensity traces indicates a certain amount of detail of the concentration distribution. The region of depletion near the surface associated with the thin source model is immediately apparent. Surprisingly the effect is most prominent in the case of antimony-124, where

the high energy radiations would be expected to mask it. It is also present in the case of nickel-63 but not with silver-110. The result of surface diffusion towards the boundary is noted by the difference in the adjacent and the distant peak density of the volume diffusion zone, this is evident to a very large extent with silver-110 and to a very small extent with antimony-124 over the whole temperature range in both cases. These observations are in agreement with the results of the boundary matching, where antimony-124, nickel-63 and silver-110 show good, fair and bad matching in the near surface region with the Suzuoka model, and where the improved matching of silver-110 with the Whipple solution is taken to result from source depletion by active surface diffusion.

Antimony-124 and silver-110 illustrate the difference between the Suzuoka and the Whipple distributions. The depletion feature in the vicinity of the volume diffusion zone is shown most clearly on the isodensity trace. No quantitative measurements of the difference have been made using the two dimensional data. In the boundary penetration measurements the difference is shown clearly in the matching of specimen W4. When the curves are normalized over a region well removed from the surface, the difference between them is small but sufficient to indicate the better agreement with the experimental curve. Nearer the surface the better agreement is very convincing.

The limitations of the method are marked in the case of antimony-124. Here the extremely high energy of the radiations not only restricts the application to a modest range of β

values but also impairs the accuracy seriously. Nickel-63 is basically a severe test of the method, for not only is this the isotope of lowest energy, but its volume diffusion coefficients are also extremely low, here, therefore, maximum instrumental effect will be observed. Silver-110 is a very favourable case for the method, witness the very large range of D'/D values; also its energy range and its diffusivity are very near average. For most isotopes the range of application is therefore as great as can be expected from any other method. The particular deficiency of the method is that the form of $u'(\zeta)$ may vary with the chosen setting of the aperture and this may be difficult to determine exactly. It should also be noted that the application does not make a thorough investigation of the composite grain boundary diffusion model. The result of subtracting-off the volume diffusion effect and further giving reduced weight to the volume diffusion region in the matching process is that the relationship between the two components, C_1 the volume diffusion contribution and C_2 the grain boundary diffusion contribution, tends to lose its validity.

An examination of the matching curves however shows that the agreement within the volume diffusion region is good for antimony-124 and nickel-63. For silver-110 the experimental diffusion that has occurred resembles the Whipple diffusion conditions, but the surface conditions correspond to the Suzuoka solution and so the relation between the factors C_1 and C_2 cannot be expected to correspond exactly.

The particular merit of the method is that it allows a study of the detail of the concentration distribution of the

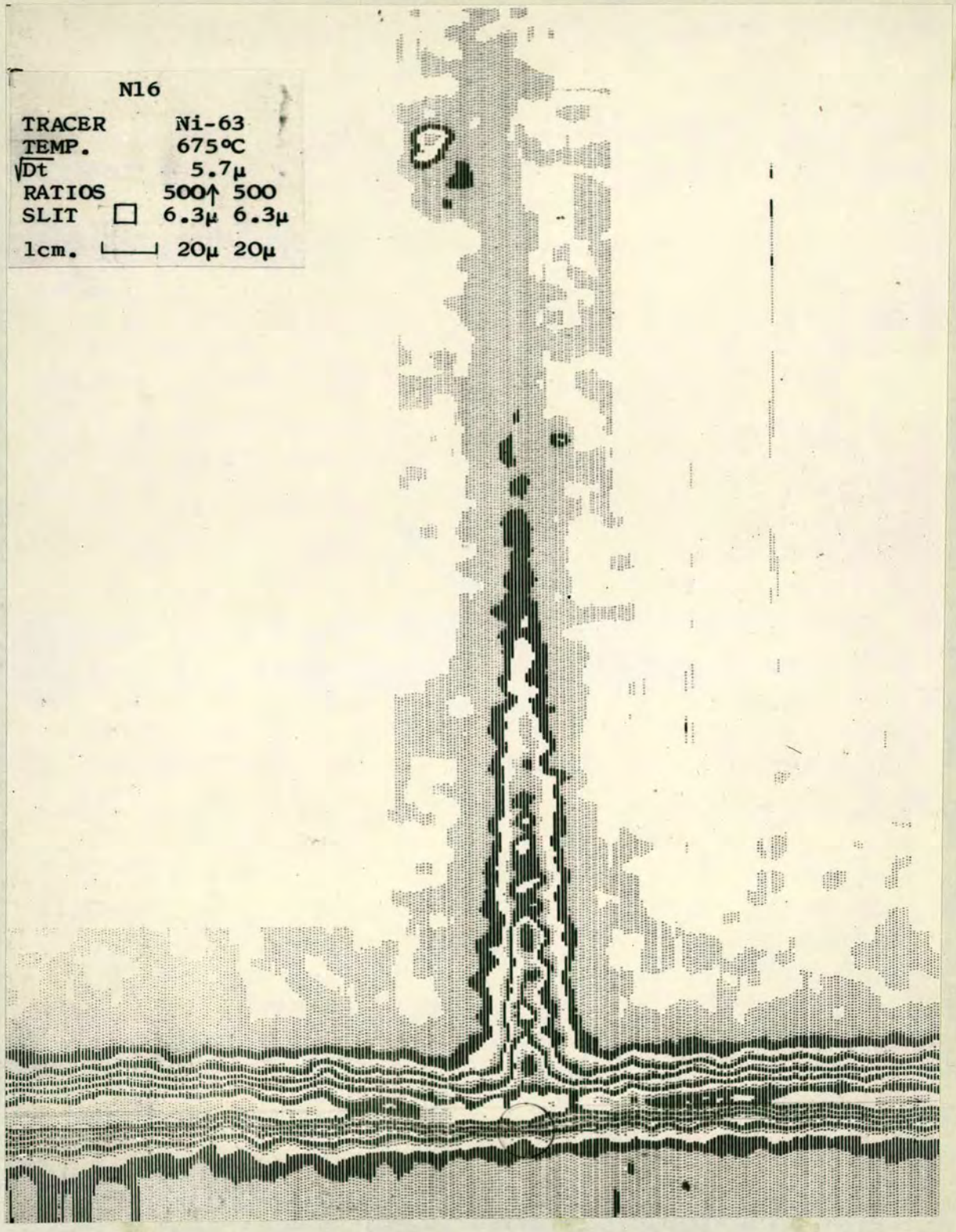
N16
TRACER Ni-63
TEMP. 675°C
√Dt 5.7μ
RATIOS 500↑ 500
SLIT □ 6.3μ 6.3μ
1cm. 20μ 20μ

Fig. 7(a).

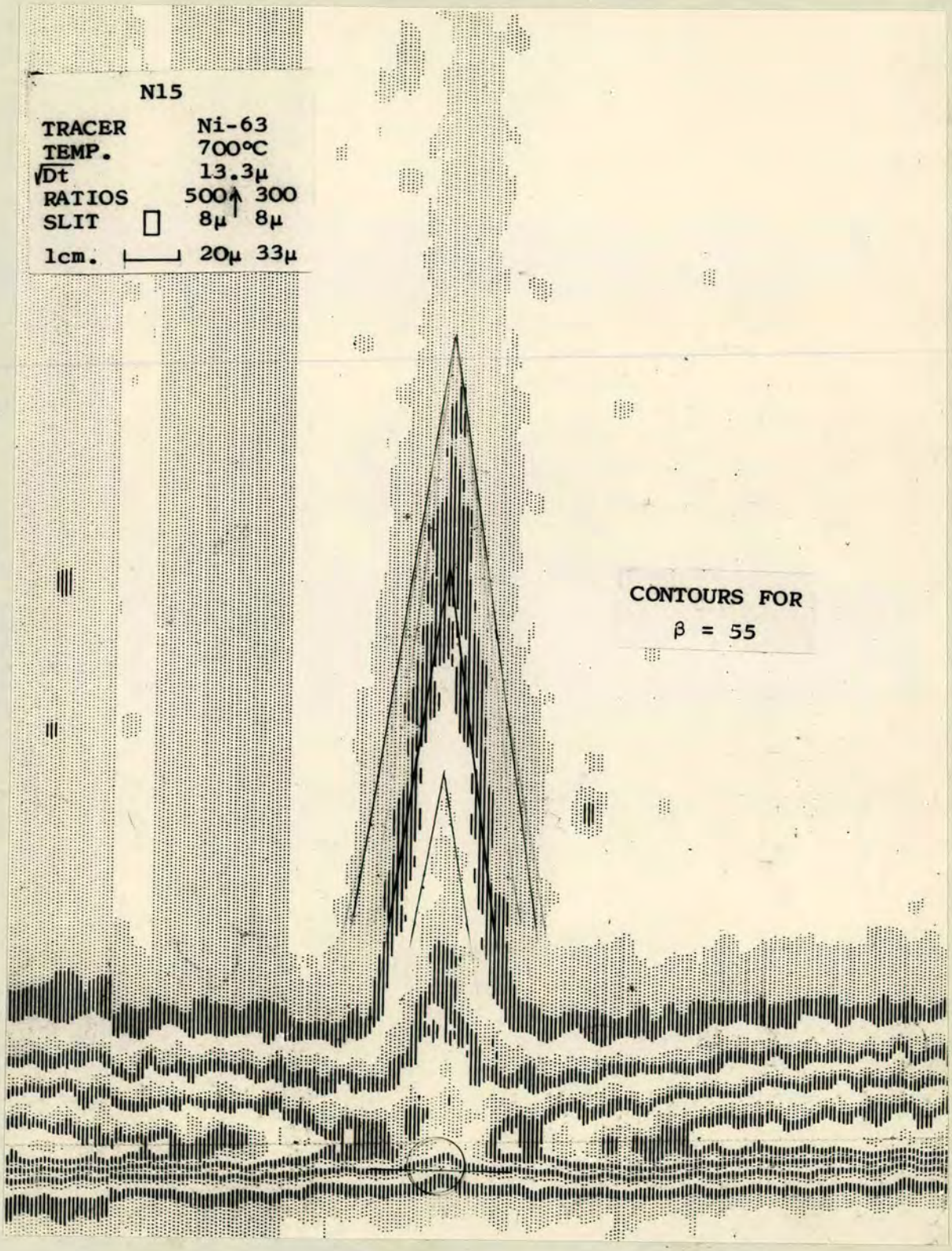
N15
TRACER Ni-63
TEMP. 700°C
√Dt 13.3μ
RATIOS 500 300
SLIT 8μ 8μ
1cm. 20μ 33μ
CONTOURS FOR
β = 55

Fig. 7(b).

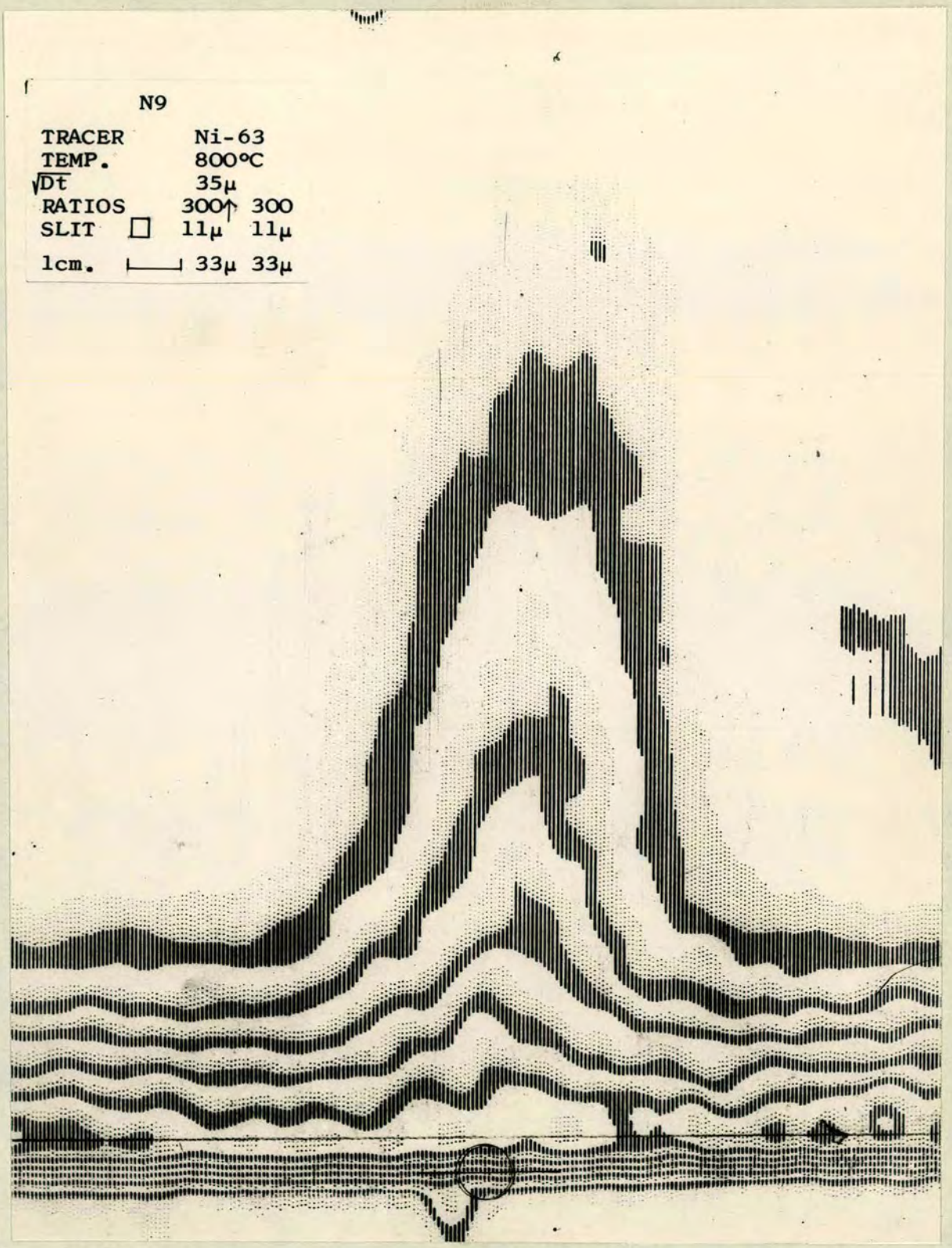
N9
TRACER Ni-63
TEMP. 800°C
√Dt 35μ
RATIOS 300↑ 300
SLIT □ 11μ 11μ
1cm. 33μ 33μ

Fig. 7(c).

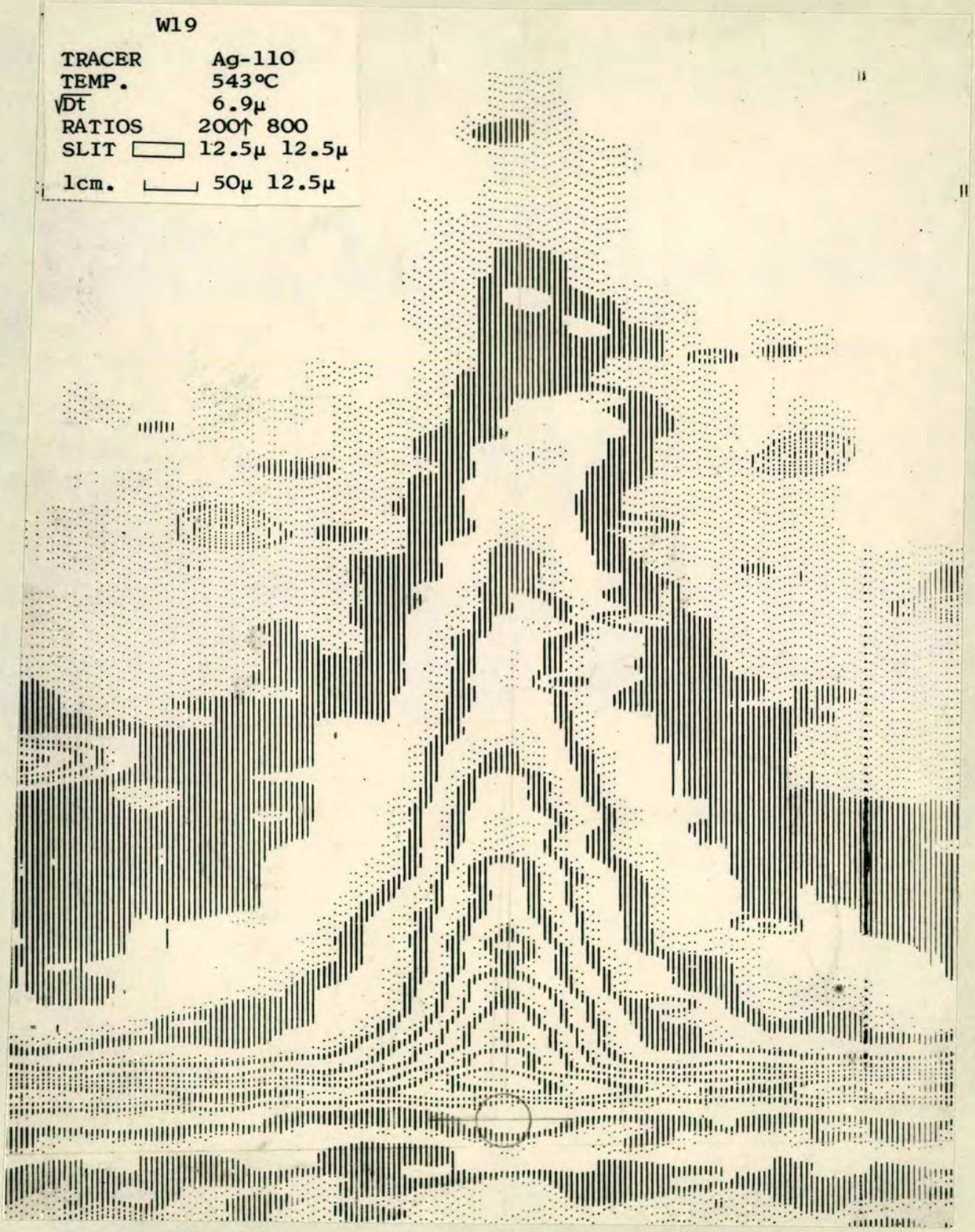
W19
TRACER Ag-110
TEMP. 543°C
√Dt 6.9μ
RATIOS 200↑ 800
SLIT 12.5μ 12.5μ
1cm. 50μ 12.5μ

Fig. 7(d).

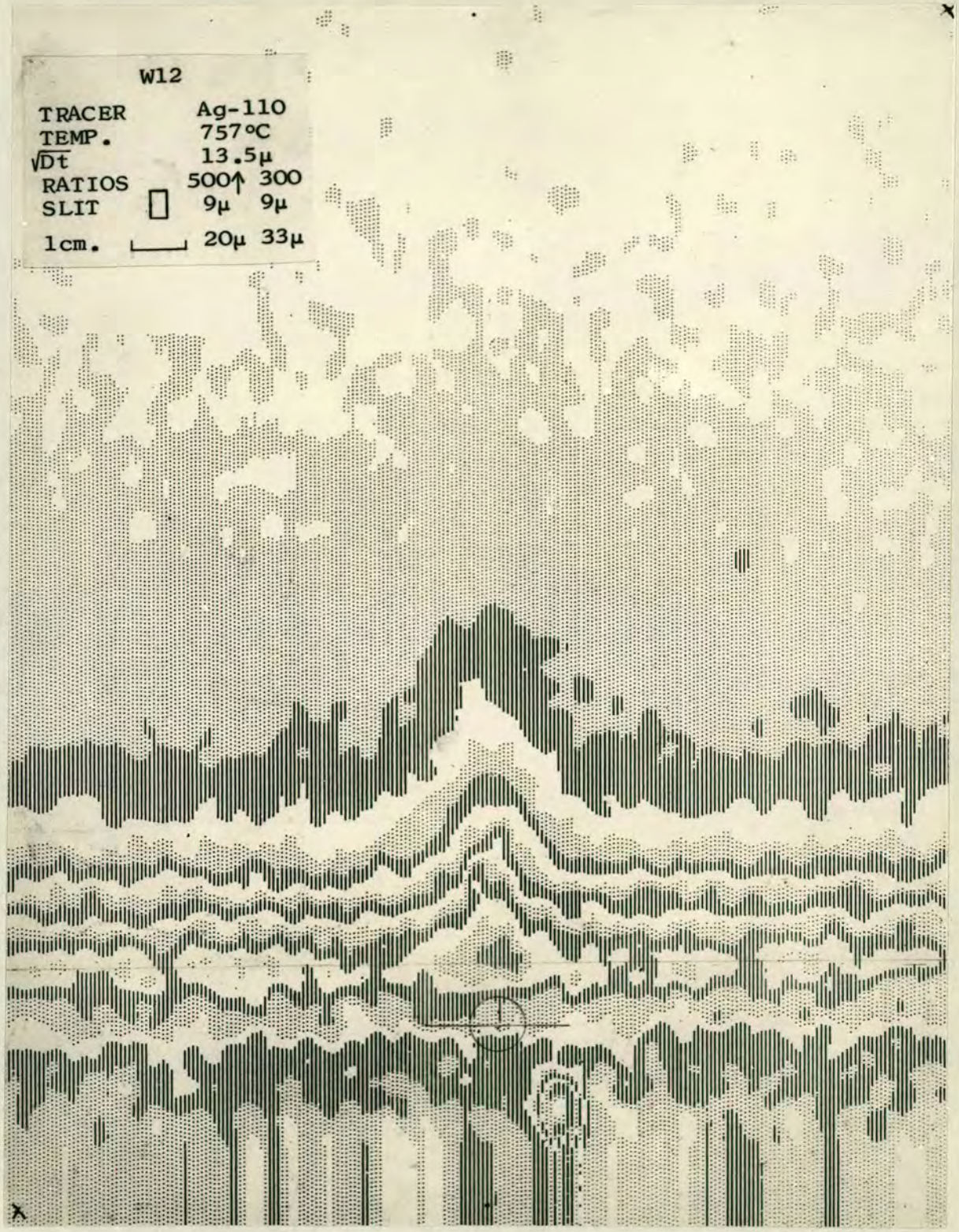
W12
TRACER Ag-110
TEMP. 757°C
√Dt 13.5μ
RATIOS 500↑ 300
SLIT 9μ 9μ
1cm. 20μ 33μ

Fig. 7(e).

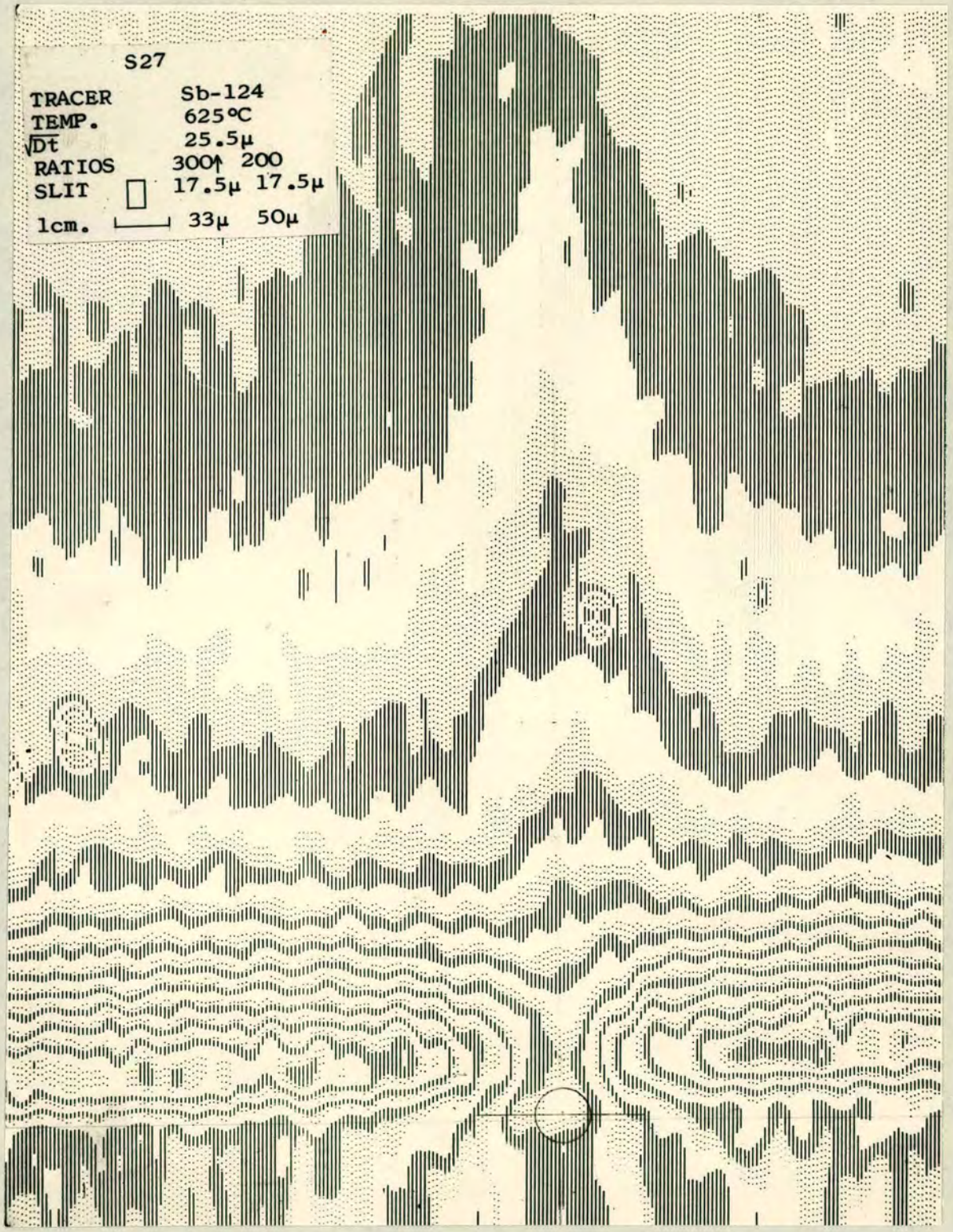
S27
TRACER Sb-124
TEMP. 625°C
√Dt 25.5μ
RATIOS 300↑ 200
SLIT 17.5μ 17.5μ
1cm. 33μ 50μ

Fig. 7(f).

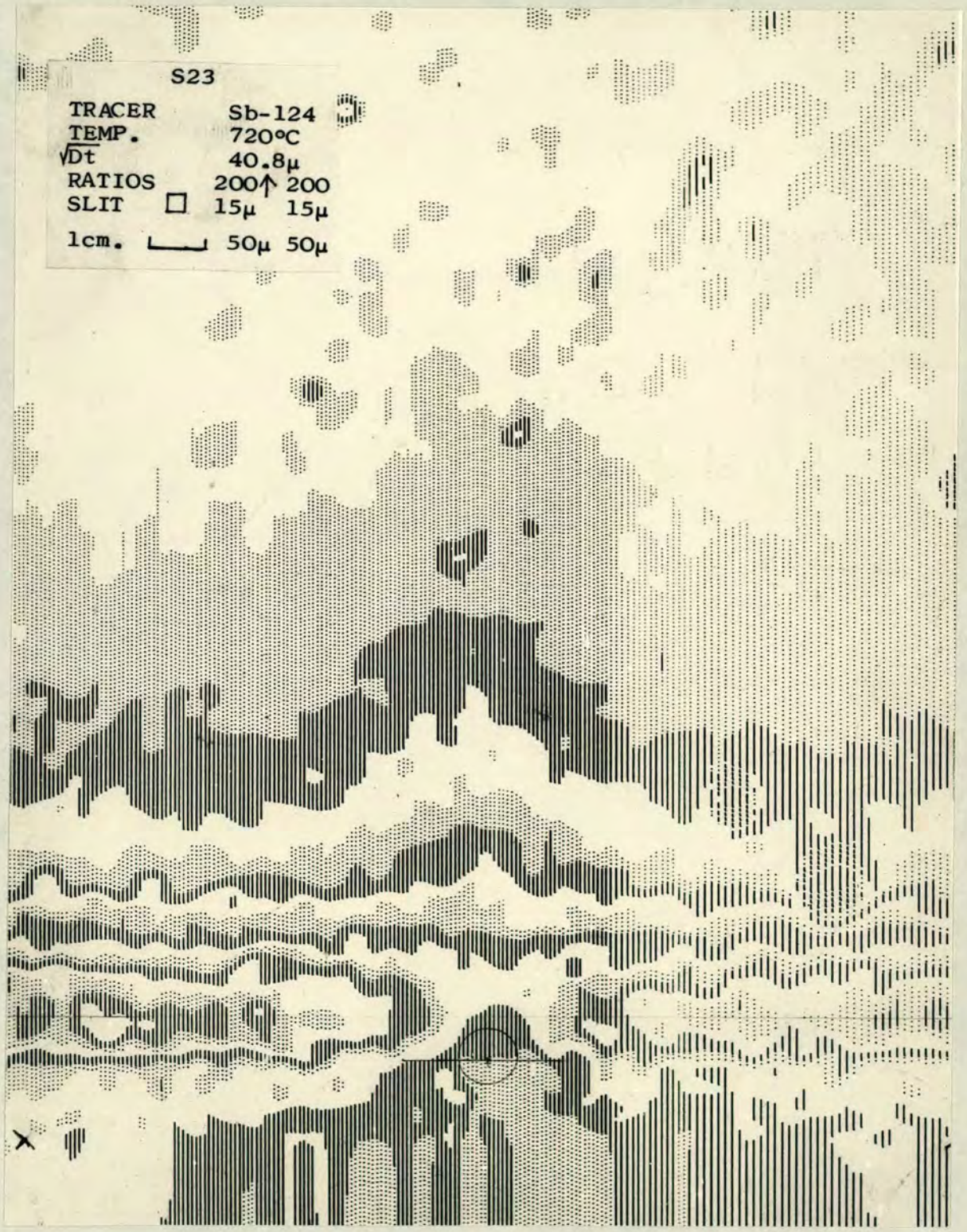
S23
TRACER Sb-124
TEMP. 720°C
√Dt 40.8μ
RATIOS 200↑ 200
SLIT □ 15μ 15μ
1cm. ⌊⌋ 50μ 50μ

Fig. 7(g).

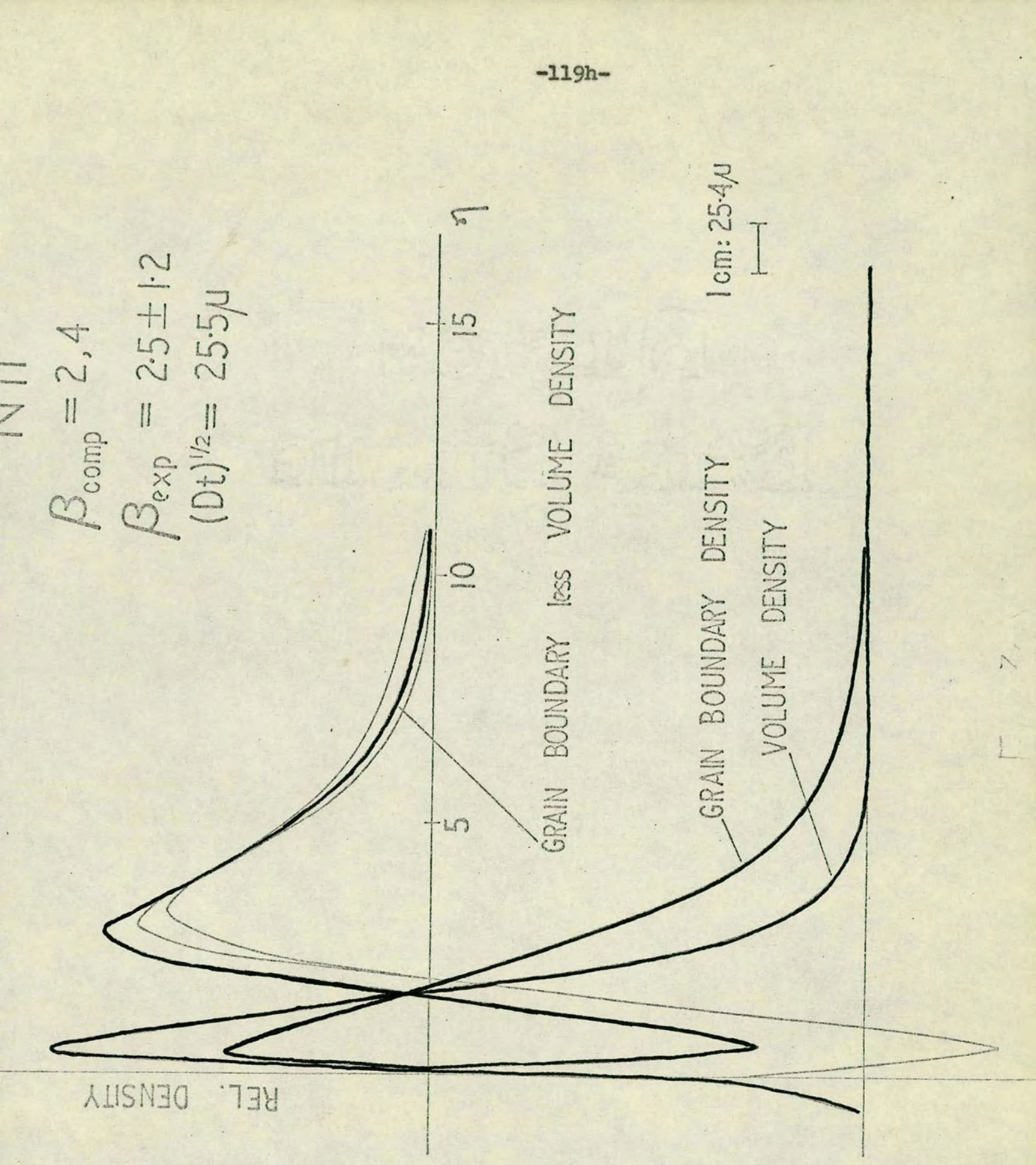

Fig. 8a. Curve matching: boundary trace.

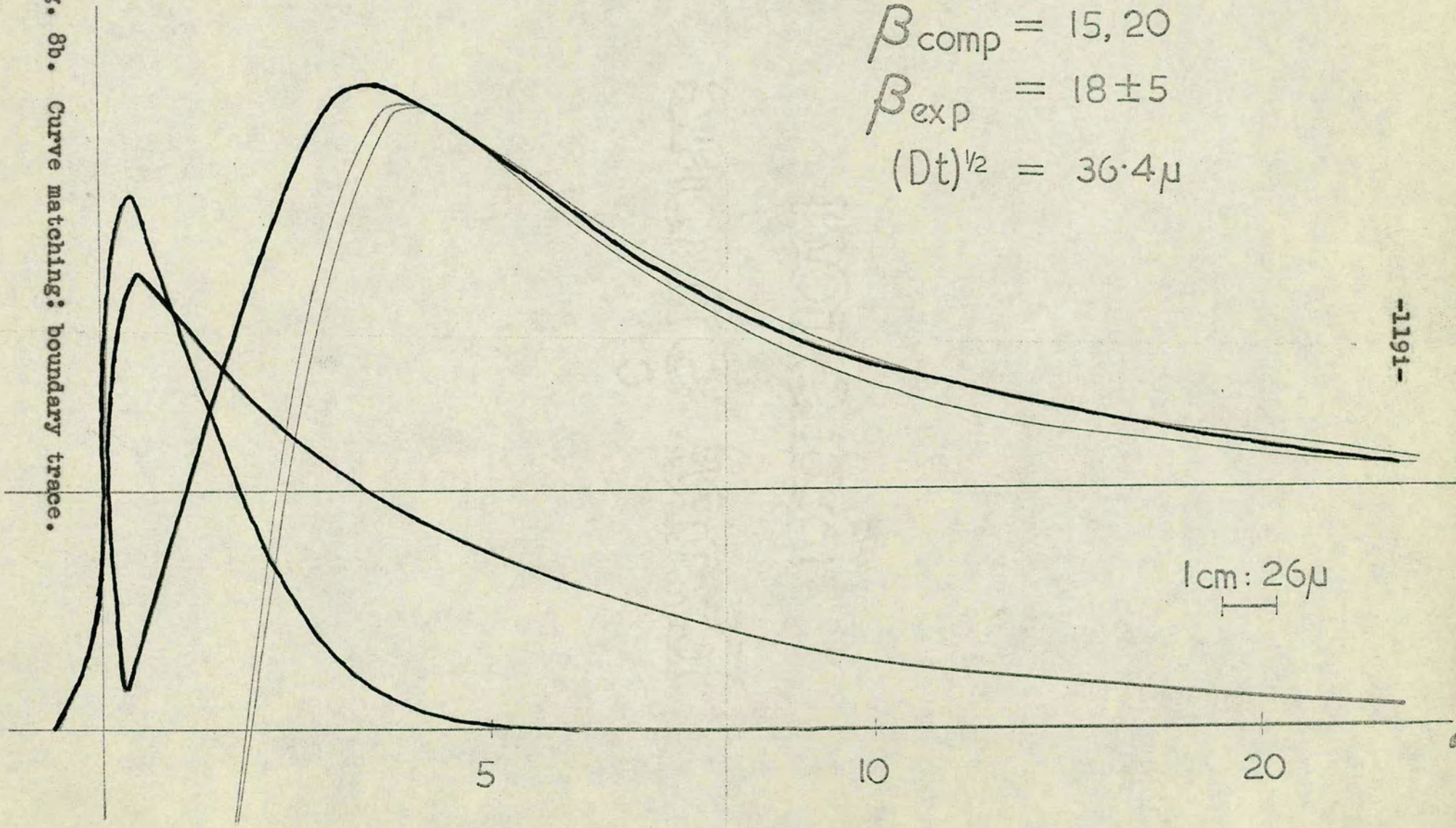

Fig. 8b. Curve matching: boundary trace.

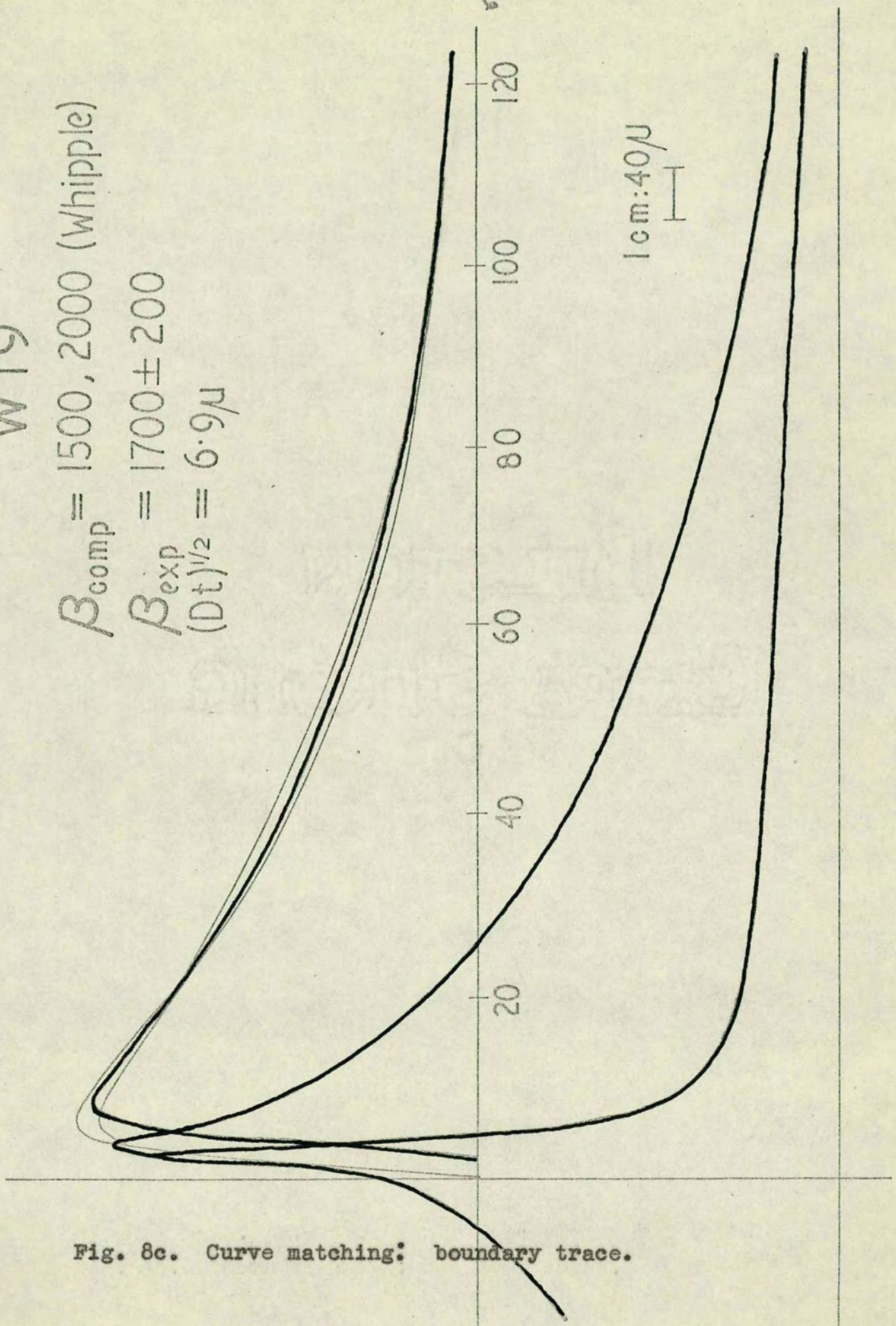

Fig. 8c. Curve matching: boundary trace.

W4

β_{comp} = 150(Whipple), 160(Suzuoka)

β_{exp} = 140 ± 25

$(Dt)^{1/2}$ = 12·6μ

Fig. 8d. Curve matching: boundary trace.

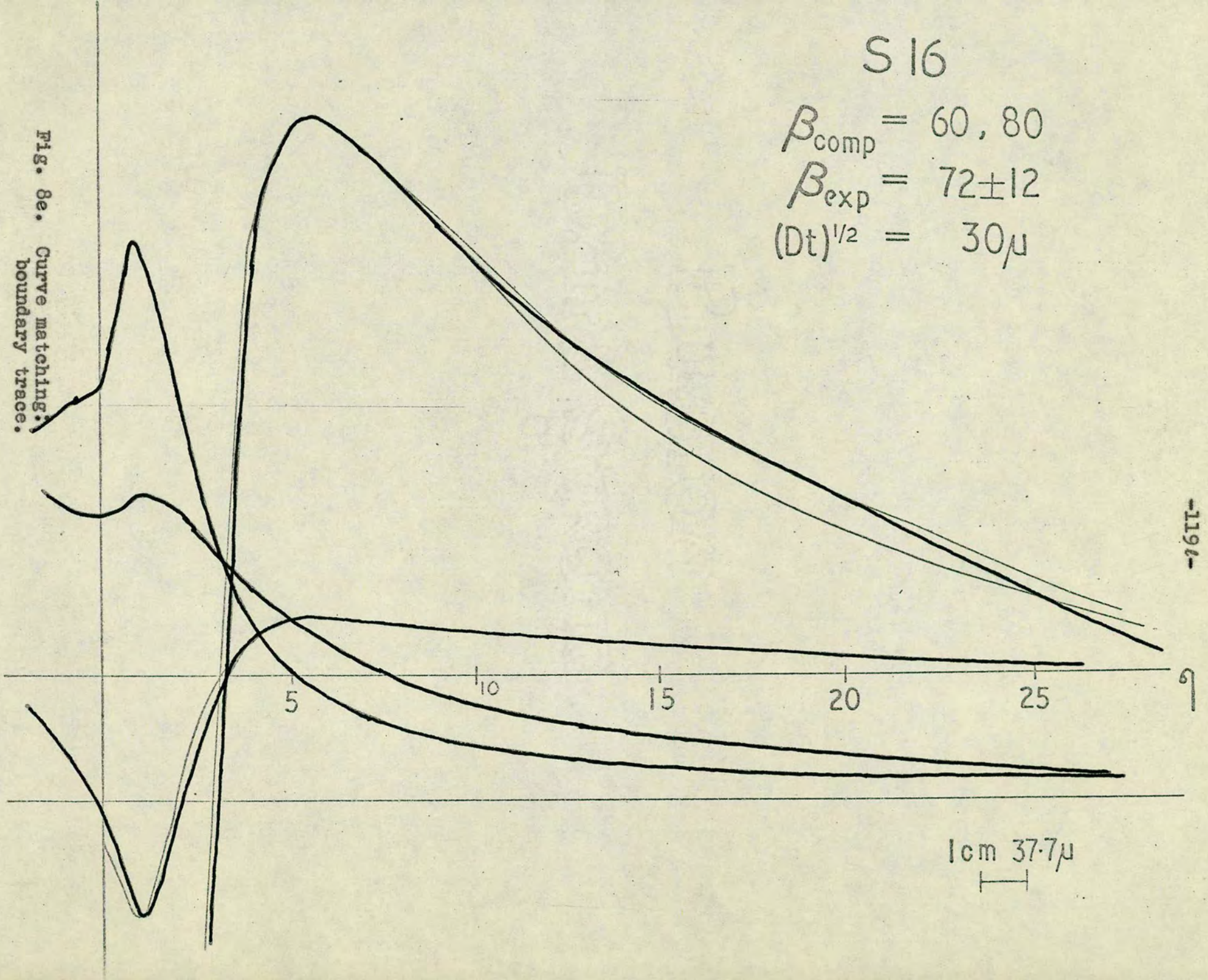

Fig. 8e. Curve matching: boundary trace.

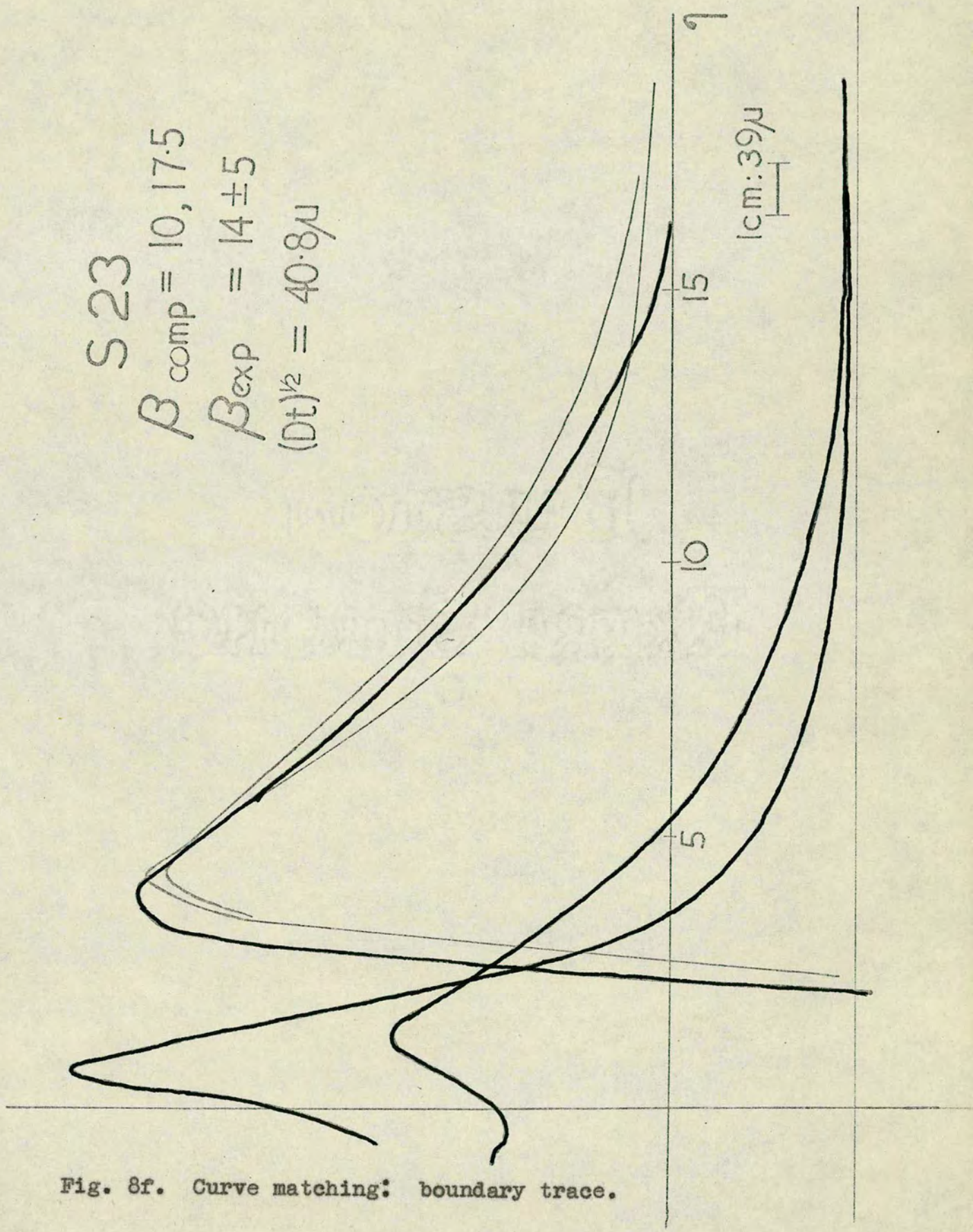

Fig. 8f. Curve matching: boundary trace.

grain boundary region for tracer diffusion conditions. This feature is not achieved in any other method. Microprobe analysis allows a detailed study but not in tracer concentrations and the sectioning of polycrystals allows a study of tracer diffusion but this represents multi-variate grain boundary conditions (see Section 2.4).

5.4 Discussion of the Results

The principal aims of this work have been to develop the method and to determine the range of conditions over which it could be applied. In order to achieve both of these aims, results of a certain minimum standard have been produced, but it should be noted that with further attention a significant improvement in the quality of many of these could be achieved. The grain boundary results, in particular, have been obtained from two isodensity traces, where six would probably be recommended.

5.4.1 Volume Diffusion Results

It is only in the case of nickel-63 that the results do not show close agreement with quoted values. Although the image spread was significantly less, the film distances and the other experimental conditions were not greatly different from those in the other two cases. The temperature range of Mackliet's[259] results, 742°C to 1076°C, is slightly higher, but the only real difference between the experiments is in the method of measurement. Mackliet measured the residual activity in the specimen, after the removal of each section by an end-window Geiger tube with a mica window 1.9 mg./cm^2 thick. The mean range of the 0.067 Mev β-particles is 2.6 mg./cm^2 and so the effect of absorption in the process of detection is a major consideration. With autoradiography the equivalent effect is known to be accurately incorporated in the spread function and taken into account in subsequent measurements. The difference between the results is about 15% at the high temperatures, but increases to about double this at low temperature; this is not much greater than the errors quoted in this work, although Mackliet quotes an error of a few per cent. Both sets of results show no departure from linearity in the Arrhenius plots.

Within the common range, the silver-110 results agree with those of Mercer[258], and at low temperatures they differ only slightly near the point of departure from linearity with those of Morrison[112]. The enhancement observed by Morrison was taken to result from diffusion along dislocations, and

interpreted using the Hart-Mortlock analysis to give an activation energy of 40 kilocalories per mole for the process.

The results in the case of antimony-124 agree with those obtained by mechanical sectioning[266]. The one result at a much lower temperature lies below the extrapolated Arrhenius plot. This is in fair agreement with the deviation obtained by Barr[265] using a chemical sectioning method. Following section 1.4.4 this might be taken to indicate the inherent curvature of the Arrhenius plot suggested by Le Claire[70], but the magnitude of the deviation appears to suggest more than this.

5.4.2 Grain Boundary Results

There are few results from previous investigations that can be quoted. Further, the differences in the experimental conditions and in the methods of interpretation do not allow an exact comparison. The extensive measurements of Austin and Richard on the diffusion of nickel into copper at 750°C, using the microprobe analyser, thick source conditions and the Whipple solution give $1.8.10^{-6}$ and $2.0.10^{-5}$ cm^2 per sec. for D' from boundary penetration and contact angle measurements respectively and 6.10^{-12} cm^2 per sec. for D using the Matano analysis. The results obtained in this work show considerable concentration dependence and do not give consistency between the different types of measurement. The corresponding results in this case are $2.5.10^{-6}$ and $3.0.10^{-12}$ cm^2 per sec. for D' and D respectively.

The corresponding D' value of Yukawa and Sinnott[150]

obtained by another autoradiographic method is some 20 times smaller, but these results are criticised quite generally. The results for silver-110 show good agreement with those of Achter and Smoluchowski, obtained by metallography, $Q' = 24$ kca. per mole and poor agreement with those of Blackburn and Brown[167], $Q' = 32$ kcal. per mole and $D_o' = 450$ cm^2 per sec. obtained by autoradiography assuming concentration-density equivalence and the Fisher solution.

The several types of measurement made on each of the nickel-63 specimens use quite different features of the distribution, and so the good agreement that is found between these, recommends the consistency of the method. The integrated concentration results show less agreement at the extremes of the β range; this is due to a deficiency in this method of analysis which gives a $\frac{\partial \ell n \bar{C}}{\partial(\eta \beta^{-\frac{1}{2}})^{6/5}}$ value that is dependent upon the average value of the range of the observations. In the present measurements the range averages were low and this leads to a marked increase in the above quantity at high β values and a decrease at low β values relative to the near constant values that correspond to higher range averages. The N9 result shows both a boundary coefficient enhanced by a factor of seven and normal volume diffusion. There was one feature only in which this specimen differed from all others, the thickness of this specimen was approximately 1.5 mm by comparison with the normal 3 mm, and the boundary penetration was more than 75% of this distance; there was however no evidence of tracer material on the distant face.

The consistency that is found in an Arrhenius plot can be an indication of the quality of the results. Fig. 10 shows that the consistency is good, and that the scatter of the points is less than might be expected from the variations found in previous work. In each case the results could be described as linear over a large part of the temperature range with increasing departure from linearity at low temperatures. Over each linear region the ratio Q'/Q is approximately 0.5. The theoretical values that have been suggested for this ratio range from 0.4 to 0.7 for a vacancy mechanism and the experimental values show a spread even greater than this. Hoffman and Turnbull[152] found this ratio to be 0.44 for silver self-diffusion in low angle boundaries and suggested that Q' might be associated with only the activation energy of movement, on the assumption that all the vacancies necessary for the process were already formed in the boundary dislocation pipes. Following the same argument Gertsriken[168] suggested that the ratio should be 0.67, while Klotsman[174] quotes the value 0.3 to 0.4 as established for polycrystals.

The possible causes of the departure from linearity should be examined. The effects already discussed could produce a combined error of approximately 70 per cent but this cannot explain the magnitude nor the systematic nature of the variation. The first possibility to examine is whether the instrumental factor is more serious than has been estimated; if this were so it would give an effect much greater with nickel-63 and much less with antimony-124 than is observed, and it is unlikely to account for the many fold enhancements observed with silver-110 at the lowest temperatures.

Departure from linearity in the volume diffusion results would produce a corresponding effect on the boundary diffusion results, and in the case of silver-110 the temperature coincidence of this is marked. Fig. 10 shows that the use of linearly extrapolated volume diffusion coefficients throughout the matching process reduces the effect, but the indication is that this factor does not account for all the enhancement, and moreover volume enhancement is not detected in the nickel-63 or antimony-124 measurements. Kaygorodov and coworkers[176,177], investigating grain boundary impurity diffusion in polycrystalline silver at very low temperatures, report a similar non-linearity in the measurements below 300°C but, as stated in Section 1.6.4, the significance of this is obscured because high temperature extrapolated D values are assumed and the analysis, based on the Fisher solution, is inadequate.

The matching does not indicate any serious breakdown in the grain boundary equations, but a full-scale matching process might well be required to show this. For silver-110 at the lowest temperatures the traces show an anomalous excess or pile-up of activity in the boundary near the surface, and although no explanation can be given for this, the source of the excess can only be the free surface. This and other features suggest that surface diffusion be examined as the cause of the enhancements, but for this to be the sole cause would require that surface diffusion be equally active in comparable cases with each isotope, and this appears not to be the case.

If the enhancement was the result of a change in some

fundamental boundary property or in boundary width or boundary structure, then this would be expected to produce a departure from linearity that occurred at much nearer the same temperature in each case than is observed. Changes in other related factors should be examined to determine if these could produce boundary conditions sufficiently different at low temperatures to cause this large effect.

At low temperatures the volume, the boundary and the lateral penetrations are very much less, and so if there is no corresponding reduction in the thickness of the deposited layer, then the concentrations are all greatly increased. Although the average concentration in the volume diffusion zone is still less than 1%, the increase in the boundary slab may be much greater. The indication of a tracer pile-up in the isodensity trace of specimen W19 (Fig. 7(d)) might, for example suggest a boundary saturation. If this possibility is pursued then the effect on the boundary diffusion process of the several concentration dependent factors - solubility, segregation and associated aspects of chemical diffusion - should be examined. The effect of segregation has been discussed by Gibbs,(274) who suggests that the boundary diffusion parameter is given by $A = \alpha D'\delta$, where α is a segregation factor, and not by $D'\delta$ as indicated in all the solutions. For self diffusion $\alpha = 1$ but for impurity diffusion α is defined by the following equation due to McLean, which relates the concentrations on the inside and on the outside of the boundary slab faces for equilibrium segregation to the boundary

$$C' = \frac{C \exp \Delta F/RT}{1 + C \exp \Delta F/RT} = \alpha C ,$$

where ΔF is the solute-boundary binding energy. For a weakly-segregating impurity $\alpha = \exp \Delta F/RT$ and writing $\Delta F = \Delta U - T\Delta S$ the Arrhenius equation for the process is obtained as

$$A = D_o' \delta \exp(-\Delta S/R) \exp -(Q_s - \Delta U)/RT .$$

Gibbs suggested that ΔU can account for the difference between the impurity and Q_s the self diffusion activation energy. The main objection to this interpretation is that the conditions in the boundary region are not representative of equilibrium segregation, and on this account A may not be an accurate measure of the segregation effect although the effect itself may well be a real one. Brandon[211] has observed segregation directly in the boundary of a W-5% Rh specimen using the field ion microscope, and Aust[273] and coworkers, studying solute induced hardening near boundaries in zone refined Pb, Sn and Zn, suggest that solute clustering at the boundaries may have important implication on segregation effects. Murray and Machlin[269] have examined the solubility of nickel in silver by measuring the grain boundary diffusion and suggest that the results indicate a greatly increased solubility and migration therein, but this again seems an over-simplification and the results are not conclusive. For our purpose it is to be noted that solubility decreases at lower temperatures.

It might be suggested that the reduced demand of the adjoining grains at low temperatures increases the concentration gradient to an extent that produces enhanced boundary flow. Lowering

+ Preliminary results

a Inman and Barr[266]

b Mercer[258]

- - - extrapolation of results.

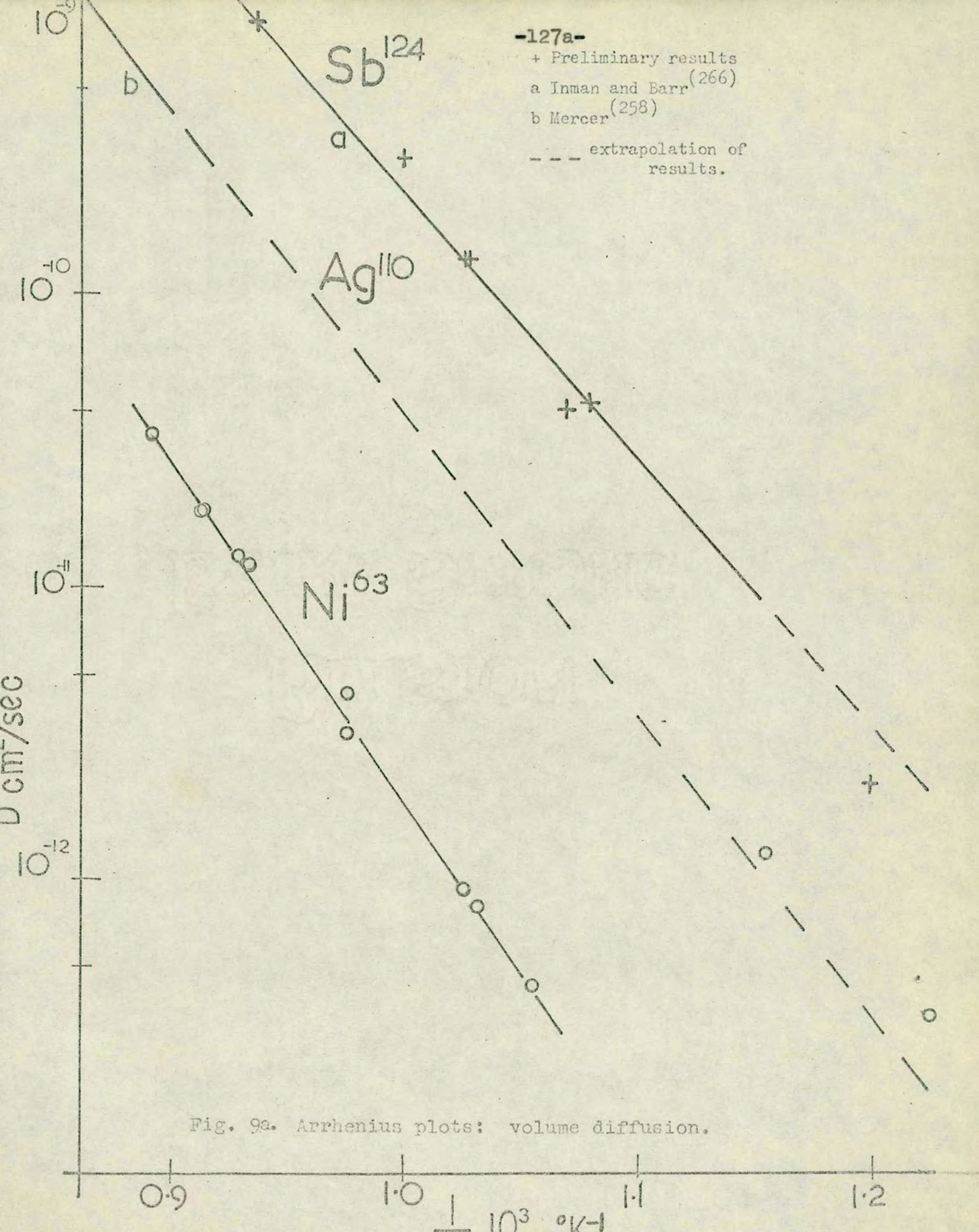

Fig. 9a. Arrhenius plots: volume diffusion.

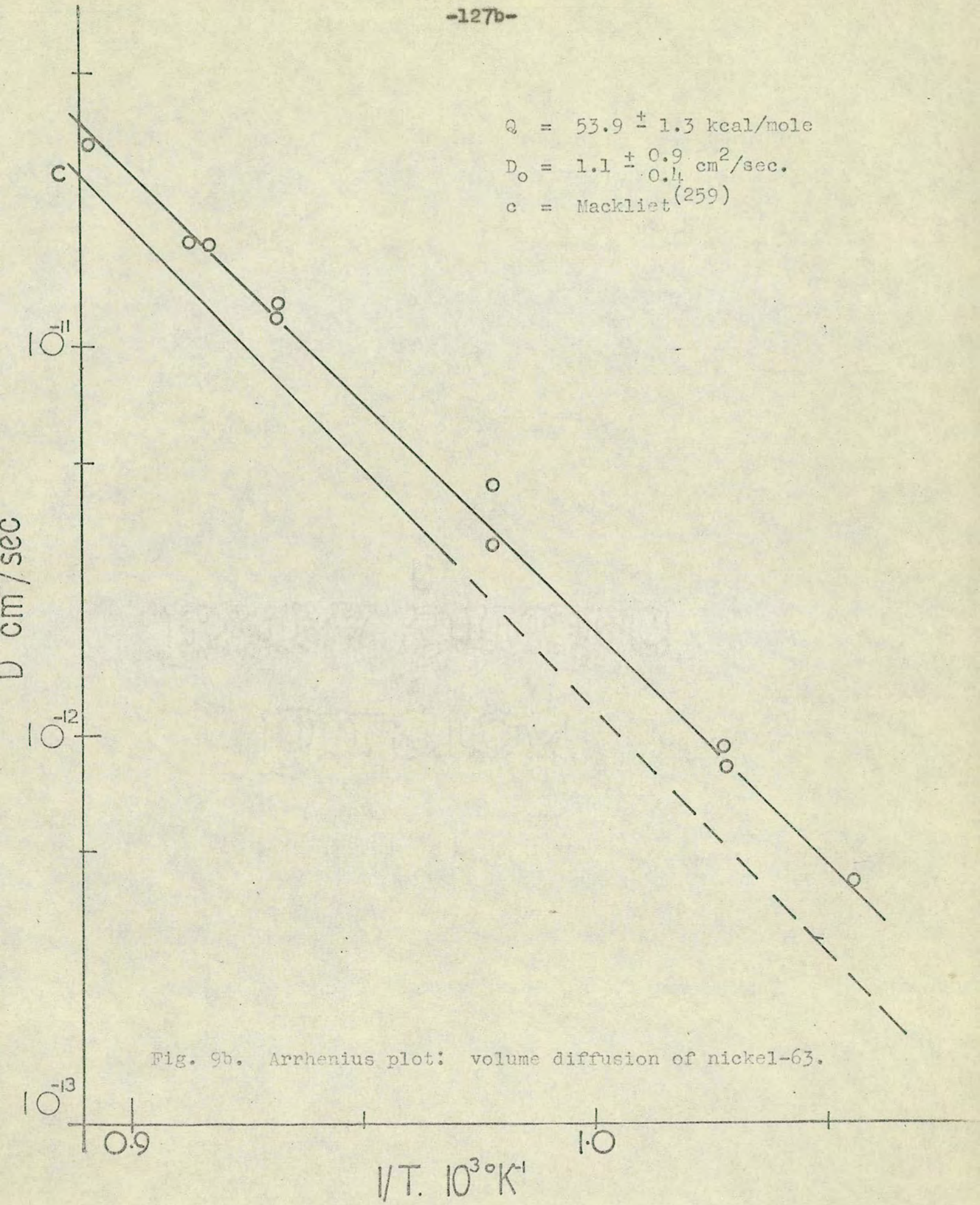

Fig. 9b. Arrhenius plot: volume diffusion of nickel-63.

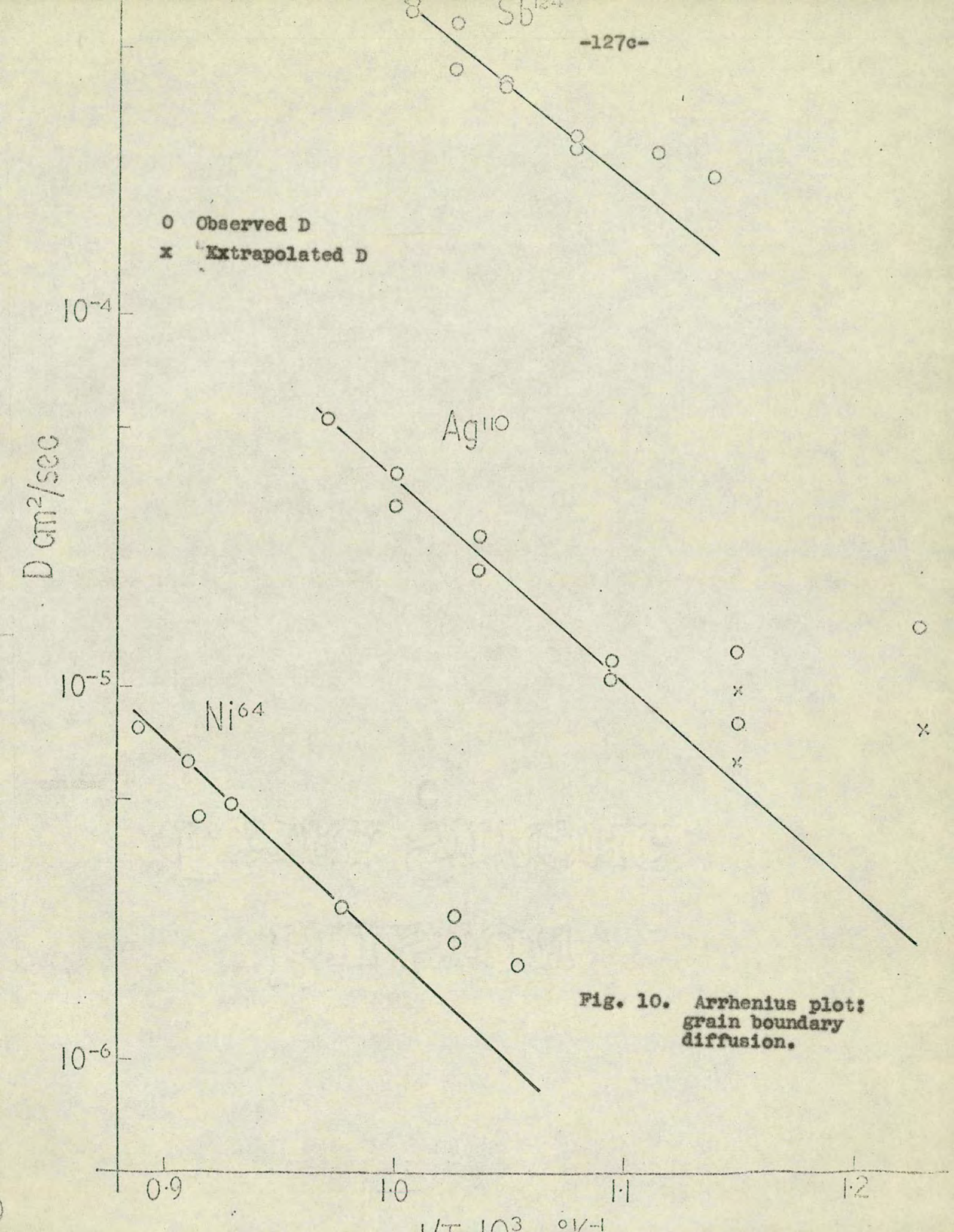

Fig. 10. Arrhenius plot: grain boundary diffusion.

the temperature to the point where lateral diffusion becomes negligible could, on this supposition, produce increasing diffusion coefficients and only below this point would true unimpeded grain boundary diffusion be observed. This is not dissimilar to the proposal contained in the Smoluchowski model to account for the orientation dependence.

An examination of the departures from linearity in Fig. 10 indicates that the effect is related significantly to some property of the diffusing atom. If the enhancement is entirely an impurity effect such as segregation then this would not occur in a similar study of self-diffusion. If the result of self-diffusion studies was merely to reduce the effect, then the other contributing factors would have to be identified by control experiments.

5.5 Conclusions

The measure of agreement that is found when the results produced in this work are compared with those obtained by mechanical sectioning and other methods, confirms that this application of the method of autoradiography to the measurement of volume diffusion is sound and reliable over a wide range of tracer diffusion conditions.

The method when applied to the measurement of grain boundary diffusion can produce an accurate density map sufficient in detail to allow the investigation of the characteristic features of the boundary concentration distribution and the validity of the mathematical solutions over a wide range of tracer diffusion conditions. The results assessed on the basis of consistency

indicate a fair degree of reliability in the method. Although a certain reservation should be attached to the low temperature results, the departure from linearity that is observed in the Arrhenius plots is less likely to indicate a deficiency in the method than it is to prove a real effect.

5.6 Improvements and Suggestions for Future Work

The Isodensitracers that were used in this work were standard models supplied for general purpose use, and so an immediate improvement in the quality of the isodensity traces and in the range of application could be achieved by using a model specifically designed for small-scale work.

It is clear that a full-scale two-dimensional comparison of the experimental distribution with the theoretical distribution should be used to examine the validity of the solutions in much greater detail and guided by this, the process of matching extended to cover a more representative area of the grain boundary region.

The observed discrepancy between the theoretical distribution and the experimental distribution in the near surface region is clearly related to the amount of surface diffusion, and so a full analysis can not always be made with the present solutions. A solution which unifies the effects of volume, grain boundary and surface diffusion is obviously required, but this could also be of limited value since the surface diffusion coefficient is generally unknown and difficult to determine. A model of this sort has been studied by Stark[270], but this has been applied to the diffusion of tracer material through a thin metallic slab by grain boundary

diffusion in order to examine the surface diffusion effect. This is a refinement of the method proposed by Hendrickson and Machlin[155] which follows the treatment of Wüttig and Birnbaum[113] for the corresponding case of dislocation diffusion. An expression is derived for the mass accumulated on the distant face and this has been solved for the two cases of zero and infinite surface diffusion. The difference between the accumulated amounts in the two cases is found to be similar to the contribution from direct lattice diffusion and from this it has been concluded that, for a relatively short diffusion time, the effects of surface diffusion are not significant. A unified model for diffusion controlled sintering has been proposed by Johnson[271] from which the three diffusion coefficients can be obtained and preliminary results for iron and copper show good agreement with those measured by other techniques.

On the basis of the present results the directions along which the investigation should be extended are clearly defined.

It is important that the measurements in each case should be extended to lower temperatures so that a more exact form of the departure from linearity can be determined. This feature might prove to be an indication of low temperature boundary processes. The enhancements that are observed indicate that the grain boundary penetration remains large, but that the boundary concentrations become small, and autoradiography is possibly the least unfavourable method of detection under these conditions.

An attempt should be made to obtain a quantitative measure of the surface diffusion effect. One way of doing this would be

to vary the width of the active film, measured in the x-directions, in a way that affected the amount of surface tracer material available for diffusion towards the boundary entrance. In the case of silver-110 this would mean film widths less than 0.5 mm in extent. Complementary to this, the active film could show a break across this strip, so that the only boundary diffusion to occur would be a surface diffusion contribution.

It is equally important that the result of specimen N9 should not be dismissed. The possibility of an ehnancement effect due to specimen thickness could easily be investigated by a diffusion anneal of a number of specimens of varying thickness. If this should prove to be real, then it could simply indicate violation of the boundary conditions of the Sucuoka model but it would not be prudent to dismiss the possibility of some change in the diffusion properties with very thin specimens. Such a change would demand a careful reappraisal of the method of Hendrickson and Machlin[155] which, when used with specimens 300μ thick, was found to show high values, in particular the result for nickel-63 diffusing in silver[269] could be reconciled only by assuming a 100% boundary solubility limit. Boundary migration has also been reported[272] as the cause of enhancements as great as fifty fold, and this would seem to be particularly relevant to the case of thin specimens, but more important, it could well be taken to emphasise the basic requirement of grain boundary diffusion investigations, namely well defined and well controlled experimental conditions.

Throughout this work the crystallographic orientation of the specimens has been kept constant in order to simplify the interpretation of the results (see section (1.7)) but it should be emphasised that the diffusivity is so greatly dependent upon the orientation that this remains one of the most powerful means of studying the phenomenon. An intriguing prospect would be an investigation of the effect of grain orientation on the low temperature anomaly.

ACKNOWLEDGEMENTS

I wish to express my sincere gratitude to Professor N. Feather, F.R.S., and Professor W. Cochran, F.R.S., for allowing me to use the facilities of the Natural Philosophy Department of the University. It is also a pleasure to acknowledge the encouragement and advice given by Professor A.F. Brown.

My thanks are due to U.K.A.E.A., Harwell, for the award of a maintenance grant and to the University of Edinburgh for a Research Fellowship.

Mr. Hardie, School of Building Science, University of Newcastle and Joyce-Loebl & Co. Ltd. are thanked for the use of isodensitracers.

REFERENCES

1. Fick, A., 1855, Ann. Phys. Lpz., 94, 59.
2. Spring, W., 1878, Bull. Acad. Roy. Belg., 45, 746.
3. Roberts-Austen, W.C., 1896, Phil. Trans. Roy. Soc. A, 187, 383.
4. Roberts-Austen, W.C., 1891, Proc. Roy. Soc. A, 59, 281.
5. Arrhenius, S.A., 1889, Z. Phys. Chem., 4, 226.
6. Mehl, R.F., 1936, Trans. AIME, 122, 11.
7. Mehl, R.F., 1937, J. Appl. Phys., 8, 174.
8. Barrer, R.M., Diffusion in and through Solids, Cambridge University Press, 1941.
9. Seith, W., 1955, Diffusion in Metallen, Springer, Berlin.
10. Jost, W., 1952, Diffusion in Solids, Liquids and Gases, Academic Press.
11. Smithells, C.J., 1949, Metals Reference Book, Butterworth, London.
12. Matano, C., 1933, Jap. J. Phys., 8, 109.
13. Boltzman, L., 1894, Ann. Phys. Lpz., 53, 959.
14. Grube, G. and Jedele, A., 1932, Z. Electrochem., 38, 799.
15. Darken, L., 1948, Trans. AIME, 174, 184.
16. Kirkendall, E.O., 1942, Trans. AIME, 147, 104.
17. Smigelskas, A.D. and Kirkendall, E.O., 1947, Trans. AIME, 171, 130.
18. Bardeen, J., 1949, Phys. Rev., 76, 1403.
19. Seitz, F., 1948, Phys. Rev., 74, 1513.
20. Le Claire, A., 1953, Progress in Metal Physics, 4, 265, Butterworth, London.
21. Manning, J.R., 1967, Acta Met., 15, 817.
22. Meyer, R.O. and Slifkin, L.M., 1966, Phys. Rev. 149, 556.
23. Manning, J.R., 1959, Phys. Rev., 116, 69.

REFERENCES (Contd.)

24. von Hevesay, G., Keil, A., Seith, W., 1932, Z. Physik, 79, 197,

25. Seith, W., 1933, Z. Electrochem., 39, 538.

26. Le Claire, A., 1949, Progress in Metal Physics 1, 306, Butterworth, London.

27. Lazarus, D., 1960, Solid State Physics, 10, 71, Academic Press.

28. Shewman, P.G., 1963, Diffusion in Solids, McGraw-Hill.

29. Peterson, N.L., 1969, Solid State Physics, 22, 409. Academic Press.

30. Nachtrieb, N.H. and Hardler, G.S., 1954, Acta Met. 2, 797,

31. Pearson, K., 1905, Nature, 77, 294.

32. Lord Rayleigh, 1880, Phil. Mag., 10, 73.

33. von Smoluchowski, M., 1906, Bull. Acad. Cracovie, p. 203.

34. Chandrasekhar, S., 1943, Rev. Mod. Phys. 15, 1.

35. Markov, A.A., 1912, Wahrscheinlichkeitsrechnung, Leipzig.

36. Crank, J., 1956, The Mathematics of Diffusion, Clarendon Press.

37. Rice, S.A., 1958, Phys. Rev. 112, 804.

38. Manley, O.P., 1960, J. Phys. Chem. Solids, 13, 244.

39. Barrer, R.M., 1941, Trans. Faraday Soc., 37, 590.

40. Wert, C. and Zener, C., 1949, Phys. Rev. 76, 1169.

41. Glasstone, S., Laidler, K.J. and Eyring, H., 1941, The Theory of Rate Processes, McGraw-Hill.

42. Zener, C., 1952, Imperfections in Nearly Perfect Crystals, p. 289, John Wiley and Sons, New York.

43. Vineyard, G., 1957, J. Chem. Solids, 3, 121.

44. Pound, G.M., Bitler, W.R. and Paxton H.W., 1960, Phil. Mag. 6, 473.

45. Glyde, H., 1967, Rev. Mod. Phys. 39, 373,

46. Mundy, J.N., Barr, L.W. and Smith, F.A., 1966, Phil. Mag. 14, 785.

47. Le Claire, A.D., 1966, Phil. Mag. 14, 1271.

48. Fumi, F.G., 1955, Phil. Mag., 46, 1007.

REFERENCES (Contd.)

49. Brooks, H., 1954, Impurities and Imperfections, p. 1, Amer. Soc. for Metals, Cleveland.

50. Amar, H., 1962, J. Appl. Phys., 33, 666.

51. Lomer, W., 1959, Progress in Metal Physics, Vol. 8, p. 255, Butterworth, London.

52. Bardeen, J. and Hemming, C., 1950, Imperfections in Nearly Perfect Crystals, p. 261, Amer. Soc. for Metals, Cleveland.

53. Le Claire, A.D. and Lidiard, A.B., 1956, Phil. Mag., 1, 518.

54. Mullen, J.G., 1961, Phys. Rev., 124, 1723.

55. Howard, R.E., 1966, Phys. Rev., 144, 650.

56. Compaan, K. and Haven, Y., 1958, Trans. Faraday Soc. 54, 1498.

57. Manning, J.R., 1964, Phys. Rev., 136, A1758.

59. Ebisuzaki, Y., Kass, W.J. and O'Keeffe, M., 1967, Phil. Mag., 15, 1071.

60. Wert, C., 1950, Phys. Rev., 79, 601.

61. Schoen, A.H., 1958, Phys. Rev. Letters, 1, 138.

62. Tharmalingam, K. and Lidiard, A.B., 1959, Phil. Mag. 4, 899.

63. Mullen, J.G., 1961, Phys. Rev. 121, 1649.

64. Barr, L.W. and Munday, 1965, Diffusion in bcc Metals, p. 171, Am. Soc. Metals.

65. Bonanno, F.R. and Tomizuka, C.T., 1965, Phys. Rev., 137, A1264.

66. Mott, N.F. and Gurney, R.W., 1950, Electronic Processes in Ionic Crystals, Chapter11, Oxford Univ. Press.

67. Friauf, R.J., 1962, J. Appl. Phys. Suppl. 33, 494.

68. Lidiard, A.B., 1960, Phil. Mag., 5, 1171.

69. Howard, R.E, and Manning, J.R., 1967, Phys. Rev. 154, 561.

70. Le Claire, A.D., 1962, Phil. Mag., 7, 141.

71. Nowick, A.S. and Dienàs, G.J., 1967, Phys. Stat. Sol., 24, 461.

72. Seeger, A. and Schumacher, D., 1967, Mater. Sci. Engng., 2, 31.

REFERENCES (Contd.)

73. Wang, C.G., Seidman, D.N. and Balluffi, R.W., 1968, Phys. Rev., 169, 553.

74. Stoehe, T.G. and Dawson, H.J., 1968, Phys. Rev. 166, 621.

75. Seeger, A. and Mehrer, H., 1968, Phys. Stat. Sol., 29, 231.

76. Makin, S.M., Rowe, A.H. and Le Claire, A.D., 1957, Proc. Phys. Soc., 70, 545.

77. Simons, R.O. and Balluffi, R.W., 1962, Phys. Rev., 125, 862.

78. Le Claire, A.D., 1965, Diffusion in bcc Metals, p.3, Am. Soc. Metals.

79, Lundy, T.S. and Pawel, R.E., 1969, Trans. AIME, 245, 283.

80. Peart, R.F., 1967, Phys. Stat. Sol., 20, 545.

81. Seitz, F., 1950, Imperfections in Nearly Perfect Crystals, p. 3, J. Wiley & Sons.

82. Simons, R.O. and Balluffi, R.W., 1963, Phys. Rev., 129, 1533.

83. Seitz, F., 1950, Acta Cryst., 3, 355.

84. Broom, T. & Hamm, R.K., 1958, Vacancies and Other Point Defects in Metals and Alloys, p. 41, Inst. of Metals, London.

85. Bradshaw, F.J. and Pearson, S., 1957, Phil. Mag. 2, 379.

86. Kinchin, G.H. and Pease, R.S., 1955, Rep. Progress Physics 18, 1.

87. Denny, J., 1956, Bull. Amer. Phys. Soc., 1, 335.

88. Blewitt, T.H., 1956, Bull. Amer. Phys. Soc., 1, 130.

89. Seitz, F., 1952, Adv. in Physics, 1, 43.

90. Mott, N.F., 1952, Phil. Mag., 43, 1151.

91. Dienes, G.J. and Vineyard, G.H., 1957, Radiation Effects in Solids, Chapter 4, Interscience Publishers Inc.

92. Barry, B.E., 1969, M.Sc. Thesis, University of Edinburgh.

93. Lomer, W.M., 1958, Vacancies and Other Point Defects in Metals and Alloys, p. 79, Inst. of Metals, London.

REFERENCES (Contd.)

94. Dienes, G.J. and Damask, A.C., 1958, J. Appl. Phys. 29, 1713.

95. Arndt, B.A. and Hines, R.L., 1961, J. Appl. Phys. 32, 1913.

96. Blewitt, T.H. and Coltman, R.R., 1954, Acta Met. 2, 549.

97. Thomson, N. and Wadsworth, N.J., 1958, Adv. in Physics 7, 72.

98. Guinier, A., 1959, Solid State Physics, 9, 293.

99. Overhauser, A.W., 1953, Phys. Rev., 90, 393.

100. Swalin, R.A., 1957, Acta Met., 5, 443.

101. Lazarus, D., 1954, Phys. Rev., 93, 973.

102. Mott, N.F., 1936, Proc. Cambridge Phil. Soc., 32, 281.

103. Alfred, L.C.R. and March, N.H., 1957, Phil. Mag., 48, 985.

104. Fujiwara, H., 1958, J. Phys. Soc. Japan, 13, 935.

105. Rothman, S.J. and Peterson, N.L., 1967, Phys. Rev., 154, 558.

106. Ghate, P.B., 1964, Phys. Rev., 133, A1167.

107. Peterson, N.L. and Rothman, S.J., 1965, ANL-6568, Argonne Nat. Lab., Argonne, Illinois.

108. Le Claire, A.D., 1964, Phil. Mag., 10, 641,

109. March, N.H. and Murray, A.M., 1961, Proc. Roy. Soc. A261, 119.

110. Gibbs, G.B., 1961, Ph.D. Thesis, University of Reading.

111. Turnbull, D. and Hoffman, R.E., 1954, Acta Met., 2, 419.

112. Morrison, H., 1965, Phil. Mag., 12, 985.

113. Wuttig, M. and Birnbaum, H.K., 1966, Phys. Stat. Sol., 11, 363.

114. Hart, E.W., 1957, Acta Met., 5, 597.

115. Lidiard, A.B. and Tharmalingam, K., 1959, Disc. Faraday Soc. 28, 64.

116. Harrison, L.G., 1961, Trans. Faraday Soc., 57, 1191.

118. Lothe, J., 1960, J. Appl. Phys., 31, 1077.

119. Li, J.C.M., 1961, J. Appl. Phys. 32, 525.

REFERENCES (Contd.)

120. Love, G.R., 1964, Acta Met., 12, 731.

121. Geguzin, Ya Ye., Kovalev, G.N. and Ratner, A.M., 1960, Phys. Met. Metallag., 10, 45.

122. Amer, H. and Drew, J.B., 1964, J. Appl. Phys. 35, 533.

123. Shewman, P.G., 1963, J. Appl. Phys., 34, 755.

124. Suzuoka, T., 1965, J. Phys. Soc. Japan, 20, 1259.

125. Mullins, W.W., 1959, J. Appl. Phys., 30, 77.

126. Reviere, J.C., 1969, Bull. Inst. Phys., 20, 85.

127. Lundy, T.S., and Pagett, R.A., 1968, Trans. AIME, 242, 1897.

128. Ellis, W.P. and Nachtrieb, N.H., 1969, J. Appl. Phys. 40, 472.

129. Mortlock, A.J., 1967, The Near-Surface Diffusion Anomaly in Gold, Oak Ridge Nat. Lab. Dept. ORNL-4141 (July 1967).

130. Dushman, S. and Kohler, L.R., 1924, unpublished research, see reference 143, p. 634.

131. Clausing, P., 1927, Physica, 7, 193.

132. Rhines, F.N. and Wells, C., 1939, Amer. Soc. Metals, 27, 625.

133. Scheil, E. and Schiesse, K.E., 1949, Z. Naturforsch. 4a, 524.

134. Voce, E. and Hallowes, A.P.C., 1947, J. Inst. Metals, 73, 323.

135. Achter, M.R. and Smoluchowski, R., 1949, Phys. Rev., 76, 470A.

136. Achter, M.R. and Smoluchowski, R., 1951, Phys. Rev. 83, 163

137. Achter, M.R. and Smoluchowski, R., 1951, Physics of Powder Metallurgy, p. 77, McGraw-Hill.

138. Achter, M.R. and Smoluchowski, R., 1951, J. Appl. Phys., 22, 1260.

139. Turnbull, D., 1949, Phys. Rev., 76, 471A.

140. Fensham, P.J., 1950, Australian J. Sci. Res. A3, 105.

141. Barnes, R.S., 1950, Nature, 166, 1032.

142. Fisher, J.C., 1951, J. Appl. Phys., 22, 74.

143. Hoffman, R.E. and Turnbull, D., 1951, J. Appl. Phys. 22, 634.

REFERENCES (Contd.)

144. Flanagan, R. and Smoluchowski, R., 1952, J. Appl. Phys. 23, 785.

145. Smoluchowski, R., 1952, Phys. Rev., 87, 482.

146. Couling, S.R.L. and Smoluchowski, R., 1954, J. Appl. Phys. 25,1538.

147. Haynes, C.W. and Smoluchowski, R., 1955, Acta Met., 3, 130.

148. Shirn, G.A., Wajda, E.S. and Huntington, H.B., 1953, Acta Met., 1, 513.

149. Wajda, E.S., Shirn, G.A. and Huntington, H.B., 1955, Acta Met. 3, 39.

150. Yukawa, S. and Sinnott, M.J., 1955, J. Metals, 7, 996.

151. Whipple, R.T.P., Phil. Mag., 45, 1225. (1954).

152. Turnbull, D. and Hoffman, R.E., 1954, Acta Met., 2, 419.

153. Hoffman, R.E., 1956, Acta Met. 4, 97.

154. Okkerse, B. Tiedema, T.J. and Burgers, W.G., 1955, Acta Met. 3, 300.

155. Hendrickson, A. and Machlin, E.S., 1954, Trans. AIME, 200, 1035.

156. Borisov, V.G. and Lyubov, B. Ya., 1958, Fiz. Metallov. i Metallovedenie, 1, 298.

157. Levine, H.S. and MacCallum, C.J., 1960, J. Appl. Phys. 31, 595.

158. Geguzin, Y.Y., Kovalev, G.M. and Ratner, A.M., 1960, Phys. Met. and Metallog., 10, 45.

159. Suzuoka, T., 1961, Trans. Japan Inst. Metals, 2, 25.

160. Suzuoka, T., 1964, J. Phys. Soc. Japan, 19, 839.

161. Suzuoka, T., 1961, Trans. Japan Inst. Metals, 2, 176.

162. Austin, A.E. and Richards, N.A., 1961, J. Appl. Phys., 32, 1462.

163. Austin, A.E. and Richards, N.A., 1962, J. Appl. Phys. 33, 3569.

164. Stark, J.P. and Upthegrove, W.R., 1963, Office of Naval Research Report, Task No. NR 031-611.

165. Okkerse, B., 1955, Acta Met., 2, 551.

166. Gertsriken, C. and Revo, A., 1961, Ukrain. Fiz. Zhur., 6, 398.

REFERENCES (Contd.)

167. Blackburn, D.A. and Brown, A.F., 1962, Radioisotopes in the Physical Sciences and Industry, p. 145, International Atomic Energy Agency, Vienna.

168. Gertsriken, S.D., 1957, Naukoviy Shchoricknik KDU, Kiev, 394.

169. Arkharov, V.I., Klotsman, S.M., Timofeyev, A.N. and Rusakov, I.I. 1958, Metallurgiya i Metalloved, Moscow, Izd. Akad. Nauk. S.S.S.R.

170. Klotsman, S.M. and Orlov, A.N., 1959, Sb. Issled po Zharoprochn. Splavan 3, Moscow, Izd. Akad. Nauk. S.S.S.R.

171. Bokshteyn, D.K., Belaschchenko, D.K. and Zhukhovitskiy, A.A., 1962, Fiz. Tverd. Tel., 4, 1728.

172. Panteleyev, V.A. and Metrikin, V.S., 1967, Fiz. Metal. Mettaloved, 23, 1065.

173. Klotsman, S.M., Timofeyev, A.N. and Trakhtenberg, I. Sh., 1963, Fiz. Metal. Metalloved, 16, 895.

174. Klotsman, S.M., Timofeyev, A.N. and Trakhtenberg, I. Sh., 1967, Fiz. Metal. Metalloved., 23, 257.

175. Borisov, B.T., Golikov, V.M., and Shcherbedinskiy, G.V., 1964, Fiz. Metal. Metalloved, 17, 881.

176. Kaygorodov, V.N., Rabovskiy, Ya.A. and Talinskiy, V.K., 1967, Fiz. Metal. Metalloved., 24, 117.

177. Kaygorodov, V.N., Rabovskiy, Ya.A. and Talinskiy, V.K., 1967, Fiz. Metal. Metalloved, 24, 661.

178. Zhukhovitsky, A.A., 1956, Peaceful Uses of Atomic Energy, p. 63, Atomic Energy Commission, Washington.

179. Johnson, D.L., 1969, J. Appl. Phys., 40, 192.

180. Tomisuka, C.T., 1959, Methods in Experimental Physics, Vol. 6, p. 364, Academic Press.

181. Le Claire, A.D., 1951, Phil. Mag., 42, 74.

182. Makin, S.M., 1960, Radio isotopes in the Physical Sciences and Industry, Vol. 1, p. 217, UNESCO Conference at Copenhagen.

183. Rosenhain, W., and Humphrey, J.C.W., 1913, J. Iron Steel Inst., 87, 219.

184. Beilby, G., 1911, J. Inst. Metals, 6, 5.

185. Hargreaves, F. and Hill, R.J., 1929, J. Inst. Metals, 41, 257.

REFERENCES (Contd.)

186. Chalmers, B., 1937, Proc. Roy. Soc. A, 162, 120.

187. Burgers, J.M., 1939, Proc. Kon. Ned. Acad. v. Wet, Amsterdam, 42, 239.

188. Burgers, J.M., 1940, Proc. Phys. Soc., 52, 23.

189. Bragg, W.L., 1940, Proc. Phys. Soc., 52, 54.

190. van der Merwe, T.H., 1950, Proc. Phys. Soc., 63A, 616.

191. Frank, F.C., 1950, Symposium on Plastic Deformation of Crystalline Solids, p. 150, Carnegie Inst. of Tech., Pittsburg.

192. Read, W.T. and Shockley, W., 1950, Phys. Rev., 78, 275.

193. Vogel, F.L., Pfann, W.G., Corey, H.E. and Thomas, E.E., 1953, Phys. Rev., 90, 489.

194. Weinberg, F., 1959, Progress in Metal Physics, Vol. 8, p. 105, Pergamon Press.

195. Zener, C., 1946, Trans. AIME, 167, 155.

196. Kê, T.S., 1947, Phys. Rev., 72, 41.

197. Aust., K.T. and Chalmers, B., 1952, Seminar on Metal Interfaces p. 153, Detroit, Amer. Soc. Metals.

198. Mott, N.F., 1948, Proc. Phys. Soc., 60, 391.

199. Kê, T.S., 1949, J. Appl. Phys., 22, 274.

200. Orowan, E., 1947, Proc. Iron and Steel Inst. West of Scotland, 54, 45.

201. Walter, J.L., and Cline, H.E., 1968, Trans. AIME, 242, 1823.

202. Friedel, J., Cullity, B. and Crussard, C., 1953, Acta Met., 1, 79.

203. Frank, F.C., 1958, cited by S. Ranganathan, Acta Crystallogr. 21, 197.

204. Li, J.C.M., 1961, J. Appl. Phys., 32, 525.

205. Brandon, D.G., 1966, Acta Met., 14, 1479.

206. Fletcher, N.H. and Adamson, P.L., 1966, Phil. Mag., 14, 99.

207. Bollmann, W., 1967, Phil. Mag., 16, 363.

208. Bollmann, W., 1967, Phil. Mag., 16, 383.

REFERENCES (Contd.)

209. Kronberg, M.L. and Wilson, F.H., 1949, Trans. AIME, 85, 501.

210. Dunn, C.G., 1950, Annual AIME Meeting, San Francisco.

211. Brandon, D.G., Wald, M., Southow, M.J. and Ralph, B., 1963, J. Phys. Soc. Japan, 18, Suppl. 11, 324.

212. Ralph, B. and Brandon, D.G., 1963, Phil. Mag., 8, 919.

213. Garber, R.I., Dranova, Zh.I. and Mikhailovski, I.M., 1968, Soviet Physics J.E.T.P. 27, 381.

214. Ishida, Y., Hasegawa, T. and Nagata, F., 1969, J. Appl. Phys. 40, 2182.

215. Braunovic, M. and Haworth, C.W., 1969, J. Appl. Phys. 40, 3459.

216. Bokstein, S.Z., Kishkin, S.T. and Moroz, L.M., 1957, Radio-isotopes in Scientific Research, Vol. 1, p. 232, UNESCO Conference, Paris.

217. Bokstein, B.S., Magidson, I.A. and Svetlov, I.L., 1958, Fiz. Metal Metalloved, 6, 1040.

218. Borisov, V.T. and Golikov, V.M., 1956, Zavodskaia Laboratorica No. 2.

219. Le Claire, A.D., 1958, Colloque sur la Diffusion a l'Etat Solid, Symposium at Saclay, France. North-Holland Publ. Co., Amsterdam (1959).

220. Cottrell, A.H., 1948, Theoretical Structural Metallurgy, Chap. 12, Arnold and Co.

221. Dehlinger, U., 1936, Z. Phys., 102, 633.

222. Lamm, O., 1943, Arkiv. Kemi mineral Geol., 17A, No. 9.

223. Crank, J., 1956, The Mathematics of Diffusion, Oxford Univ. Press.

224. Einstein, A., 1905, Ann. Physik, 17, 549.

225. Borisov, V.G., Golikov, V.M., Ljubov, B.Y. and Shtsherbendisky, G.V., 1957, Radio isotopes in Scientific Research, Vol. 1, p. 212, UNESCO Conference, Paris.

226. Wood, V.E., Austin, A.E. and Milford, F.J., 1962, J. Appl. Phys., 33, 3574.

227. Maneri, C.C. and Milford, F.J., 1961, Report ARL 48, Contract AF33 (616)-6265, Aeronautical Research Laboratory, Air Force Research Division.

REFERENCES (Contd.)

228. Le Claire, A.D., 1963, Brit. J. Appl. Phys., 14, 351.

229. Johnson, W.A., 1943, Trans. Met. Soc. AIME, 147, 331.

230. Azaroff, L.V., 1961, J. Appl. Phys., 32, 1658.

231. Huntingdon, H.B. and Seitz, F., 1949, Phys. Rev., 76, 1728.

232. Langmuir, I.J., 1934, Franklin Inst., 217, 543.

233. Teggart, W.J.McG., 1956, The Electrolytic and Chemical Polishing of Metals, Pergamon Press, London.

234. Barratt, C.S., 1953, The Structure of Metals, p. 194, McGraw-Hill, New York.

235. Private Communication from P.S. Maxim, 26 January, 1967.

236. Buckley, H.E., 1952, Crystal Growth, Chapman and Hall.

237. Tanenbaum, M., 1959, in Methods of Experimental Physics, Vol. 6, Part A, Chap. 2.4, p. 86, Academic Press, New York.

238. Hertz, R.H., 1951, Nucleonics 9, 24.

239. Yagoda, H., 1949, Radioactive Measurements with Nuclear Emulsions, Chapman and Hall.

240. Boyd, C.A., 1955, Autoradiography in Biology and Medicine, Academic Press, New York.

241. Autoradiography of Diffusable Substances, 1969, Ed. Roth, Ll.J. and Stumpf, W.E., Academic Press.

242. Marshall, J.H., Rowland, R.E. and Jowsey, J., 1959, Radiat. Res., 10, 213.

243. Dudley, R.A., and Dobyns, B.M., 1949, Science, 109, 327.

244. Odeblad, E., 1956, Acta Radiol., Stockh., 45, 323.

245. Micha el, A.B., Leavitt, W.Z., Bever, M.B., and Spedden, H.R., 1951, J. Appl. Phys., 22, 1403.

246. Rogers, G.T., and Glanville, D.E., 1962, J. Inst. Met., 90, 354.

247. Stevens, G.W.W., 1948, Nature, 161, 432.

248. Stevens, G.W.W., 1950, Brit. J. Radiol., 23, 723.

REFERENCES (Contd.)

249. Doniach, I. and Pelc, S.R., 1950, Brit. J. Radiol., 23, 184.

250. Nadler, N.J., 1951, Canad. J. Med. Sci., 28, 182.

251. Gross, J., Bogoroch, R., Nadler, N.J. and Lebond, C.P., 1951, Amer. J. Roent. Rad. Therapy, 65, 420.

252. Lacassagne, A. and Lattes, J., 1924, Compt. Rend. Soc. Biol., 90, 352.

253. Sherwood, H.F., 1947, Rev. Sci. Inst., 18, 80.

254. Mees, C.E.K., 1954, The Theory of the Photographic Process, MacMillan, New York.

255. Dudley, R.A., 1954, Nucleonics, 12, 24.

256. Private Communication from R.H. Hertz (3 November, 1964).

257. Hurter, F. and Driffield, V.C., 1890, J. Soc. Chem. Ind., 9, 445.

258. Mercer, L., 1955, Ph.D. Thesis, Leeds University.

259. Mackliet, C.A., 1958, Phys. Rev., 109, 1964.

260. Mullard, W.C., Gardner, A.B., Bass, R.F. and Slifkin, L.M., 1963, Phys. Rev., 129, 617.

261. Pawel, R.E. and Lundy, T.S., 1968, J. Electrochem. Soc., 115, 233.

262. Forestieri, A.F. and Girifalco, L.A., 1959, J. Phy. Chem. Solids, 10, 99.

263. Revo, A.L., 1961, Phys. Metal. Metallog., 11, (5), 77.

264. Mortlock, A.J. and Tomlin, D.H., 1956, Proc. Phys. Soc. Lond. B., 69, 250.

265. Barr, L.W., 1959, Ph.D. Thesis, Edinburgh University.

266. Inman, M.C. and Barr, L.W., 1960, Acta Met., 8, 110.

267. Katz, L. and Penfold, A.S., 1952, Rev. Mod. Phys., 24, 28.

268. Handbook of Mathematical Functions, 1965, Ed. Ambramowitz, A. and Stegun, I.A., Dover Publications Inc., New York.

REFERENCES (Contd.)

269. Murray, G.T. and Machlin, E.S., 1964, J. of Metals, 65, 274.

270. Stark, J.P., 1969, J. Appl. Phys. 40, 3101.

271. Johnson, D.L., 1969, J. Appl. Phys., 40, 192.

272. Pampillo, C.A. and De Recca, N.W., 1969, J. Materials Sci.(G.B.), 4, 985.

273. Aust. K.T. Hanneman, R.E., Niessen, P. and Westbrook, J.H., 1968, Acta Met., 16, 291.

274. Gibbs, G.B., 1966, Report RD/B/N600, Berkeley Nuclear Laboratories, C.E.G.B. (G.B.).

APPENDIX 1

Purity of Metals

a) Copper strip: Specpure grade, supplied by Johnson, Matthey & Co. Ltd., Laboratory Report No. 39312. Spectrographic analysis revealed the presence of the following impurities.

Element		Estimate of quantity present (parts per million)
Silver		3
Iron		2
Chromium) Magnesium)	each element less than	1
Silicon)		

Oxygen — Oxygen was sought by a vacuum fusion method but was not detected.

The following elements were specifically sought but not detected.

Aℓ, As, Au, B, Ba, Bℓ, Bi, C, Co, Cs, Ga, Ge, Hf, Hg, In, Ir, K, Li, Mn, Mo, Na, Nb, Ni, Os, P, Pℓ, Pd, Pt, Rb, Re, Rh, Ru, Sb, Sℓ, Sn, Sr, Ta, Te, Ti, Tℓ, V, W, Zn, Zr.

b) Silver wire: Specpure grade, supplied by Johnson, Matthey & Co. Ltd., Laboratory Report No. 24747. Spectrographic analysis revealed the presence of the following impurities

Element	Estimate of quantity present (Parts per million)
Bismuth, Cadmium, Copper, Iron, Magnesium, Sodium	each less than 1

The following elements were specifically sought but not detected.

Aℓ, As, Au, B, Ba, Be, Ca, Co, Cr, Cs, Ga, Ge, Hf, Hg, In, Ir, K, L, Mn, Mo, Nb, Ni, Os, P, Pb, Pd, Pt, Rb, Re, Rh, Ru, Sb, Se, Si, Sn, Sr, Ta, Te, Ti, Tℓ, V, W, Zn, Zr.

c) Antimony grain: Specpure grade, supplied by Johnson Matthey & Co. Ltd., Laboratory Report No. 10716. Spectrographic analysis revealed the presence of the following impurities.

Element	Estimate of quantity present (Parts per million)
Iron	5
Copper	3
Calcium, Magnesium, Silicon, Silver, Sodium	each element less than 1

The following elements were specifically sought but not detected.

Aℓ, As, B, Ba, Be, Bi, Cd, Co, Cr, Ga, Ge, Hg, In, Ir, K, Li, Mn, Mo, Nb, Ni, Os, P, Pb, Pd, Pt, Rb, Re, Rh, Ru, Sn, Sr, Ta, Te, Ti, Tℓ, V, W, Zn, Zr.

Nickel-63 was supplied in a nickel chloride solution (15 mg. of nickel in 7.5 ml. solution). No analysis of the solution was obtained.

APPENDIX 2

Radioactive Isotope Data

a) Characteristics of the radioactive isotopes

Silver-110m

Half-life	253 days
Production Process	$Ag^{109}(n,\gamma)\ Ag^{110m}$
Activation cross-section	1.56 barns

β-activity

Mev	%
0.087	55
0.530	43
2.87 (via silver-110)	2

γ-activity

Mev	%
0.66	94
0.68	12
0.71	17
0.74	5
0.76	21
0.81	8
0.88	69
0.94	29
1.38	26
1.48	5
1.51	14

Antimony-124

Half-life	60 days
Production Process	$Sb^{123}(n,\gamma)Sb^{124}$
Activation cross-section	1.07 barns

β-activity

Mev	%
0.22	11
0.61	51
0.95	6
1.59	7
1.66	2
2.31	23

γ-activity

Mev	%
0.60	99
0.65	8
0.72	14
0.97	3
1.37	5
1.45	2
1.70	50
2.09	6

Nickel-63

Half-life	125 years
Production Process	$Ni^{62}(n,\gamma)Ni^{63}$
Activation cross-section	0.77 barns

β-activity		γ-activity
Mev	%	Nil
0.067	100	

(b) Activity of Isotopes

The isotopes were produced by neutron bombardment in the Harwell experimental reactors. Large neutron flux intensities ($\sim 1.3.10^{12}$ Neutrons/cm^2/sec.) were necessary to produce the high specific activities requested.

	Irradiation time	Specific activity (millicuries/gm.)
Silver-110	2 days	75
Antimony-124	2 weeks	150
Nickel-63	not given	660

All the work using Ni-63 in solution was performed in the grade B laboratory of the Department of Medical Physics in liaison with the University Radiation Protection Officer. The Code of Practice recommended by the Ministry of Labour was observed at all stages of the work, special shielding precautions were necessary when working with silver-110 on account of the high γ-ray intensities.

(c) Penetration of the Radiations

The range R of β-particles can be calculated using the following equations given by Katz and Penfold[267] for mono-energetic electrons of energy E

$$R = 412\, E^{1.265-0.0954\, \ell nE} \text{ mg/cm}^2 \text{ for } 0.01 \leq E \leq 2.5 \text{ Mev.}$$

and $R = 530\, E - 106 \text{ mg/cm}^2$ for $E \geq 2.5$ Mev.

The average value of the energies of a β-particle spectrum is given by $\frac{1}{3}E_{max}$ where E_{max} is the maximum or end-point energy of the spectrum, and so the range of the β particles with average energy is $\frac{1}{3}R_{max}$. The thickness of the absorber which reduces the particle flux to one-half is given by $\frac{1}{8}R_{max}$.

The maximum ranges in copper of the particles from the principal β-spectra of the isotopes are given in Table 1A.

Table 1A

Isotope	Ni^{63}	Ag^{110}	Sb^{124}	Ag^{110}	Sb^{124}	Sb^{124}	Ag^{110}
E_{max} (Mev)	0.067	0.087	0.22	0.53	0.61	2.31	2.87
R_{max} (microns)	8	11	100	190	240	1100	1600

(The ranges in nuclear emulsions are approximately 4 times greater)

For γ-rays of initial intensity I_o, the decrease in intensity after penetrating a distance x is given by $I/I_o = \exp(-\mu x)$ where μ is the total absorption coefficient. In copper the half thickness values for γ-rays of 0.5 Mev, 1 Mev and 1.5 Mev are approximately 0.7 cm, 1 cm. and 1.5 cm. An indication of the extent to which the γ-rays affect the film can be obtained by comparing the values of Table 1A with the maximum extent of the spread function in Table 1.

APPENDIX 3

Summary of Computer Programs and Routines

(1) Voldif: numerical evaluation of equation (4.3) using routine (10).

(2) Incrementmufn: calculation of the $\mu(\gamma)$ values at chosen μ intervals.

(3) Funcform: calculation of the $\mu'(\xi)$ distribution from the $\mu(\gamma)$ distribution using equation (4.7) and a routine matrix inversion program, which is one of the computers library of standard programs.

(4) Condis: calculation of the concentration distribution for a given β value using routine (5).

(5) Condisautoint: check of condis using a routine (10) evaluation of equation (4.4).

(6) Laguerre: calculation of the concentration at a (ξ, η) point using a Laguerre quadrature[268] evaluation of C_2 in equation (4.4).

(7) Laguerre test: check of routine (5) with a routine (10) evaluation of equation (4.4) to determine the normalizing factor and the order of quadrature.

(8) Dendis: calculation of the density distribution using routine (8).

(9) Convolution: calculation of the density at a (ξ, η) point using a two dimensional numerical integration[268] of equation (4.6).

(10) Aubint: a fast version of the Simpson's Rule which reduces the number of steps of integration to suit the form of the integrand.

(11) Concontour: numerical display of lines of equiconcentration.

The programming language used on the KDF9 computer was Atlas Autocode.

APPENDIX 4

Published Work

1) The Measurement of Volume Diffusion by the Method of Autoradiography, by T.J. Renouf, 1964.
Phil. Mag. 9, 781.

2) The Measurement of Grain Boundary Diffusion by the Method of Autoradiography, by T.J. Renouf, 1970.
Phil. Mag., in press.

Reprinted from
PHILOSOPHICAL MAGAZINE, Vol. 9, No. 101, p. 781, May 1964

The Measurement of Volume Diffusion by the Method of Autoradiography

By T. J. RENOUF
Solid State Physics Laboratory, Department of Natural Philosophy,
University of Edinburgh

[Received 30 December 1963]

ABSTRACT

The application of autoradiography to the measurement of volume diffusion is limited because of the difficulty in interpreting the effects of the energy of the radiations, the scattering and absorption properties of the specimen and other complicating factors. A general method of interpretation is described in which the effects of these factors are suitably combined into a single function that is determined by one experiment. The method is applied by matching the experimental density trace of the diffusion zone, with a density curve which is computed from a derived expression.

As a trial of this treatment, the diffusion of ^{124}Sb into single crystals of copper has been studied over the penetration range $10\ \mu < (Dt)^{1/2} < 150\ \mu$ and in the temperature range 560°C to 896°C with specimens mounted singly and in a double sandwich-type arrangement. The results that have been produced show good agreement with the results obtained from mechanical sectioning and the accuracies of the two methods are comparable. In the case of small penetrations at low temperatures, anomalously low values of the diffusion coefficient are noted. The additional studies that have been made with ^{110}Ag as the tracer element, are also used to discuss the application and the limitation of the method.

§ 1. INTRODUCTION

ALTHOUGH a great variety of methods have been used to measure diffusion in solids, the most accurate is the direct observation of mass flow using radioactive tracers and the mechanical sectioning technique. When the penetration is small, or when the specimen material is not suitable for lathe sectioning, it may be possible to use precision grinding, although the accuracy of this technique is less. Other methods, such as measuring the decrease of activity at the initial surface and autoradiography, are taken to be less acceptable, because of the discrepancies found in results (see for instance, Tomizuka 1959). The purpose of the present work was to obtain a more exact and general treatment of the method of autoradiography.

Autoradiography has been applied to a wide range of problems, but the results that have been furnished are mainly qualitative. The application of the technique to quantitative studies on a microscopic scale has been restricted to cases where the active isotope was considered to be suitable by virtue of the low energy of its radiations. It is then possible to assume that the variation in the density of the autoradiograph is directly proportional to the variation in concentration of the isotope. Some results of

volume diffusion studies obtained in this way have been compared with those produced by the mechanical sectioning method, and the agreement was stated to be satisfactory (see, for instance, Mortlock and Tomlin 1956, Forestieri and Girifalco 1959 and Revo 1961). In cases where the range of the particles is not negligible in comparison with the dimension of the region that is being examined, simplifying assumptions of this sort cannot be made, and a quantitative interpretation of the autoradiograph may be difficult. The resolution attainable in autoradiography is related to this problem, and has been considered by Doniach and Pelc (1950) and Gross *et al.* (1951); Norris and Woodruff (1955) have reviewed other contributions. An absolute method of quantitative β-particle autoradiography has been described by Odeblad (1956), in which the effect of radiation from each part of the specimen was taken into account. This was used to determine the radioactive content of the several structures or entities of uniform concentration that compose a tissue sample. Marshall *et al.* (1959) analysed the calibration technique of Dudley and Dobyns (1949) and extended it to determine the total activity in uniform and non-uniform distributions in bone. In their work the method of analysis was obtained by a consideration of the line and the plane source of uniform activity commonly used in dosimetry (see Loevinger *et al.* 1956). In the present work similar considerations were made to derive a method of interpretation that gives the distribution of the active isotope for the case of volume diffusion in single crystals.

§ 2. Method of Interpretation

For volume diffusion in single crystals, with diffusion having taken place from a thin layer on a face into the body of a rectangular specimen, c the concentration per unit volume of the tracer element in a parallel plane at a distance y from the surface is given by:

$$c = \frac{c_0}{(\pi Dt)^{1/2}} \exp\left(-\frac{y^2}{4Dt}\right), \qquad \ldots\ldots\ldots \quad (1)$$

where D is the diffusion coefficient and t the time of anneal at the given temperature and c_0 is the initial total amount per unit area of the tracer element. If a surface perpendicular to the active face is prepared for autoradiography the density distribution of the resulting autoradiograph in the direction of diffusion is a measure of the concentration distribution. If the effective radiation is of a very short range, it may be possible to assume that the density variation is directly proportional to the concentration variation, so that eqn. (1) can be written as:

$$d = \frac{d_0}{(\pi Dt)^{1/2}} \exp\left(-\frac{y^2}{4Dt}\right), \qquad \ldots\ldots\ldots \quad (2)$$

where d is the density of the film in contact with a point at a distance y from the surface and d_0 some constant. In the general case such a dependence cannot be assumed, for if the range of the particles is comparable

with the penetration depth, then the diffusion zone will produce an image on the film showing considerable spread, and showing a density variation influenced by the range. Brown and Blackburn (1963) discussing this in terms of resolution of the method, have illustrated the magnitude of systematic error that can arise from an uncritical application of eqn. (2).

A treatment of the problem using fundamental principles presents difficulties. For example, the particles reaching the surface at P in fig. 1, might originate from any point within the diffusion zone nearer than some maximum distance. This distance is determined by the maximum energy associated with the disintegration schemes of the tracer element, and the stopping power of the specimen material. The contribution of the element of volume δv_1 to the number of emulsion grains developed at P, depends upon the number of particles reaching this point with an energy that can sensitize the film. This number is difficult to determine, depending upon such factors as concentration of the tracer in δv_1, the energies of the emitted particles, the distance r_1 to P, the absorption and scattering properties of the specimen material, the emulsion thickness, characteristics and exposure time. A summation to account for all contributing elements of volume would be required to obtain the total density at P, and the effect of each element would be different. Lengthy and difficult computations involving factors not readily determined would be necessary to obtain the density distribution of the film due to some known concentration distribution. In the following treatment the use of factors of this sort is avoided, by introducing a function that combines the effect of each of these, and which is determined by one experiment.

Consider the prepared specimen to be made up of a series of elementary slices each with the same area as the active face, parallel to it and of a thickness $d\zeta$. If $d\zeta \to 0$ then the concentration of isotope in each slice can be taken as constant and is given by eqn. (1). The radiations from a given element on reaching the surface will affect not only the film in contact with that element, but also the film in contact with adjoining elements. The density distribution or profile produced on the film by such an element would show a finite spread, and the complete density trace would be made up of the overlapping profiles of all elements of the diffusion zone. If this overlapping is considerable, then a relative reduction of the blackening of areas of high concentration and an increase of blackening of areas of low concentration would be expected to result.

Suppose the elementary slice at Q in fig. 1 to be the only element containing the active isotope, and let c be the concentration per unit volume. If a film is laid in contact with the polished surface Oy, then upon developing, the distribution of the density about the source would be:

$$\mu(\zeta)cd\zeta,$$

where ζ is measured from Q, $cd\zeta$ is a measure of the strength of the source and $\mu(\zeta)$ is a measure of the density distribution produced by an infinitely thin plane source of unit strength.

Now take the element at Q to be an element of the diffusion zone. The contribution of the source at Q to the resulting density of the film in contact with the point at P, a distance ζ from Q and a distance y from the origin is:

$$\mu(\zeta)cd\zeta.$$

Now the concentration at Q is given by eqn. (1), so that the contribution of Q to the density at P can be written as:

$$\mu(\zeta)\frac{c_0}{(\pi Dt)^{1/2}}\exp\left[-\frac{(y+\zeta)^2}{4Dt}\right]d\zeta.$$

The total resulting density d at P is found by summing the contribution of all such elements from $-y$ to $+\infty$:

$$d=\int_{-y}^{\infty}\frac{c_0}{(\pi Dt)^{1/2}}\mu(\zeta)\exp\left[-\frac{(y+\zeta)^2}{4Dt}\right]d\zeta. \quad . \quad . \quad . \quad (3)$$

Fig. 1

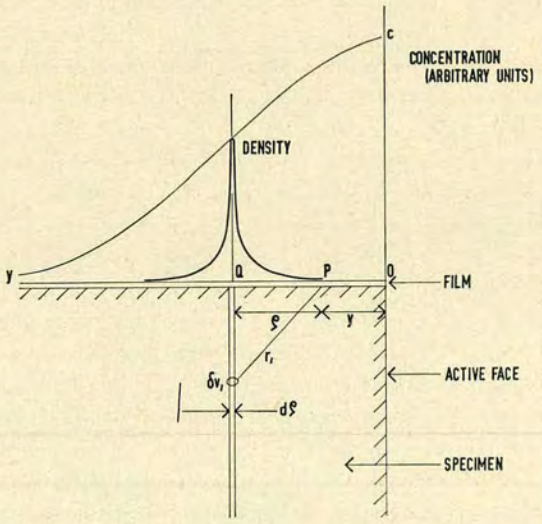

Cross section of the specimen normal to the active face and to the surface prepared for autoradiography showing the concentration distribution of the tracer element after diffusion. The density distribution of the film that would be due to a single activity containing elementary slice $d\zeta$ at Q is also shown.

Since it is sufficient to know the distribution of relative density due to the diffusion zone, $c_0/\pi^{1/2}$ can be taken as unity and the function $\mu(\zeta)$ can be taken as a measure of the density distribution from an infinitely thin plane source of any uniform concentration contained within the body of the specimen material. To simulate this arrangement, undiffused sandwich-type specimens are used and average values of the function $\mu(\zeta)$ are obtained experimentally.

The most expedient means of applying this treatment is to perform numerical evaluations of this integral so as to furnish a set of curves for assumed values of $(Dt)^{1/2}$. The computed density curves with the scale appropriately adjusted are compared with the experimental density trace of the diffusion zone, to obtain a degree of matching considered to be acceptable, and in this way the diffusion coefficient is found.

The diffusion of radioactive antimony–124 (^{124}Sb) into copper was considered suitable as a trial of this treatment, since results obtained by the method of mechanical sectioning were available for comparison, and since the radiations from this isotope contain a large number of high energy β-particles. Some additional measurements were made using radioactive silver–110 (^{110}Ag) as the diffusing element.

§ 3. Experimental Method

Single crystals of copper were grown in a graphite crucible by the Bridgman technique from pure (99·999%) copper supplied by Johnson Matthey. These were mounted in wax in thin-walled brass tubing and cut by a high speed carborundum wheel. The specimens so obtained were approximately 1·5 cm square and 3 mm thick. Mechanical polishing of the faces, using three grades of emery paper and four grades of diamond paste, was followed by a heat treatment of the specimens to remove lattice strains. A layer of the active element about 200 Å thick was deposited on one or on both of the larger faces by vacuum evaporation. The active layer was coated with a similar thickness of pure copper to reduce the possibility of evaporation.

The diffusion annealing was carried out in an evacuated ceramic sheath with two specimens, active faces touching, contained in a graphite crucible and in close contact with a platinum–13% rhodium–platinum, thermocouple. The temperature was found to remain constant to ± 1°C. A recorded trace of the temperature was made during the heating and cooling periods for the purpose of correction.

The diffused specimens were mated, secured in steel grips designed to obtain good contact and then mounted in Araldite using a $1\frac{1}{2}$ in. casting die. The mating was made so that the following specimen arrangements could be studied: (i) one active face in contact with Araldite or (ii) one active face in contact with a non-active face or (iii) two active faces in contact.

The autoradiographic exposure was carried out under dry conditions in a vacuum casette similar to that of Sherwood (1947), using Kodak A.R. 50 stripping film to produce a peak density of approximately 0·5 above background. The film was processed in a perspex frame which secured it along its edges and then mounted on a glass slide.

The density measurements were made on a Joyce–Loebl automatic recording micro-densitometer using an accurately calibrated 200 : 1 record to sample linkage. With suitable instrumental settings and accurate alignment of the film, tracking in the direction of diffusion will provide a

density trace of the diffusion zone suitable for analysis. Some specimens were autoradiographed several times and a number of traces taken from each. Film expansion was measured for each trace by comparing the distance between images on the autoradiograph with the distance between radioactive faces on the specimen. Expansion was of the order of 20% and was constant to within 1% on each autoradiograph.

The function $\mu(\zeta)$ was determined by using an undiffused sandwich-type specimen containing one active face. Several such specimens were prepared and examined under the microscope for good contact of the mating faces. A number of autoradiographs were made of the specimens considered to be suitable and one or two traces taken from each. The density values were measured on each trace at 10 μ intervals from the peak and these were taken as the values of $\mu(\zeta)$ from $\zeta = 0$ to $\zeta = 1000\,\mu$. Average values of the function were calculated from ten traces and an estimate of the accuracy was made. An example of such a trace is shown in fig. 2.

Fig. 2

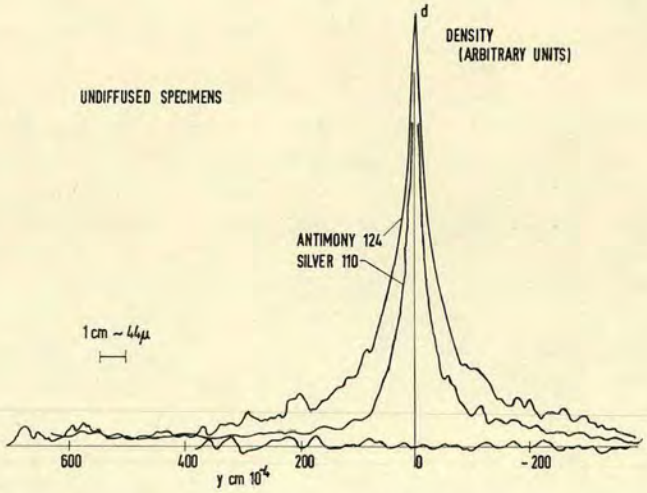

Density traces obtained from undiffused sandwich-type specimens containing ^{124}Sb and ^{110}Ag. The peak density of both curves is the same.

In the case of each required $(Dt)^{1/2}$ value, a numerical evaluation of eqn. (3) was carried out for chosen values of y and a computed density curve was drawn. The evaluation was performed on a Sirius computer by the application of Simpson's Rule with ζ intervals of 10 μ. The y intervals of 20 μ, 40 μ and 80 μ were chosen to suit the form of the curve, and the interval between the $(Dt)^{1/2}$ values was normally 10 μ. To obtain a density curve for comparison with specimens mounted in arrangement (iii), it was necessary to change the lower limit of integration to $-\infty$. The computer time taken to perform the calculations for one $(Dt)^{1/2}$ value was approximately 20 min.

§ 4. Results

To determine the diffusion coefficient for a given temperature, the computed density curves with the scale appropriately adjusted, were compared in turn with the experimental density trace obtained from the specimen. The adjustment of the density scale was made by a normalizing process on or in the region of the peak density. An illustration of some of the comparisons made are shown in fig. 3 (*a*)–(*d*). Matching was considered

Fig. 3

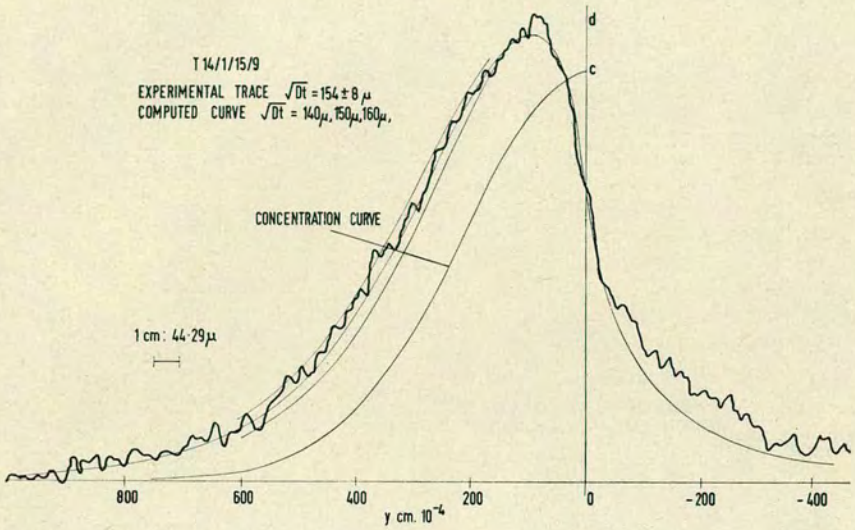

(*a*)

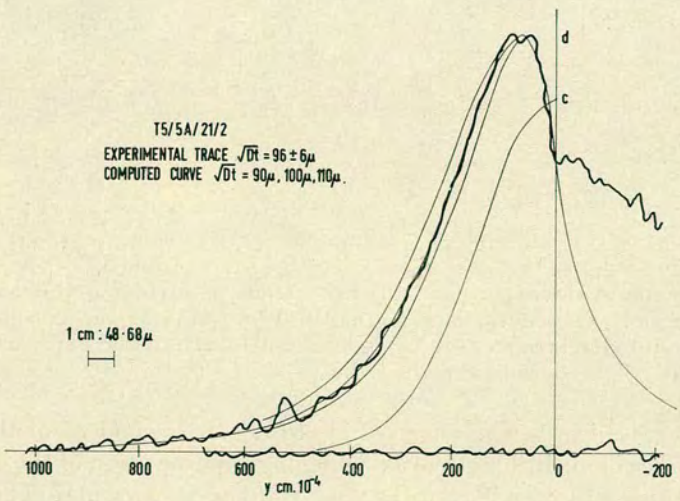

(*b*)

Fig. 3 (*continued*)

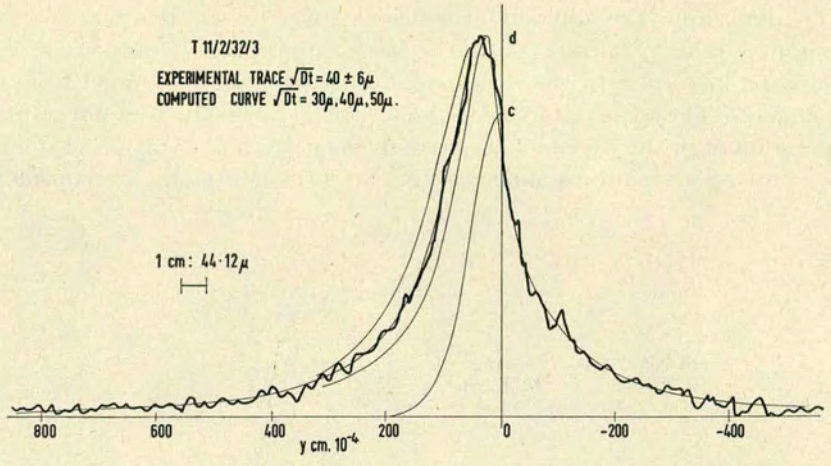

(*c*)

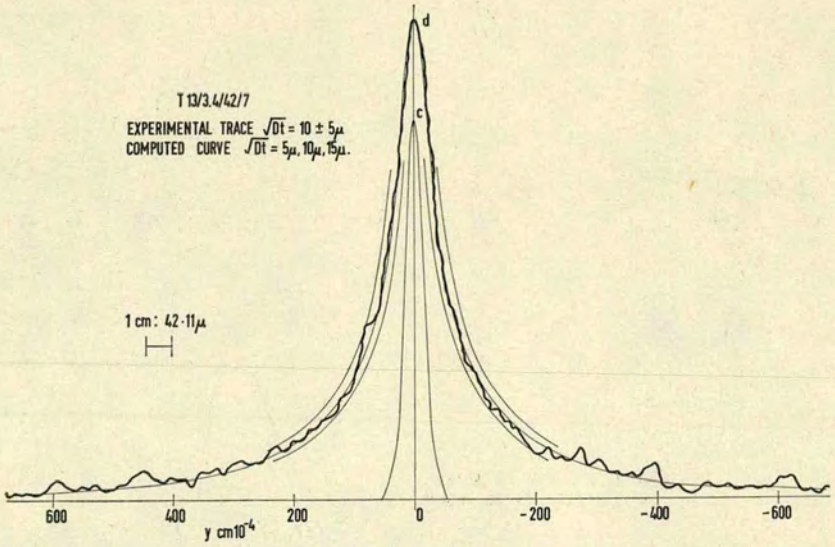

(*d*)

A comparison of the experimental density trace with computed density curves for several penetration depths. In (*a*) and (*c*) the specimens were mounted in arrangement (ii) in (*b*) arrangement (i) and in (*d*) arrangement (iii). The concentration distribution of the tracer element is also shown.

to be acceptable when it was possible to obtain a good fit of the experimental trace along its length after achieving superposition of the characteristic features—the origin and the peak and the background densities. It was then possible to assign a value of $(Dt)^{1/2}$ to the experimental trace and to

Table 1

Specimen number	14/1		12/1		11/1		11/2		13/1		13/3	
Specimen arrangement	(ii)		(ii)		(iii)		(ii)		(iii)		(iii)	
Uncertainty in matching	Autoradiograph plate/trace number and observed $(Dt)^{1/2}$ value in cm 10^{-4}											
	±8		±6		±6		±6		±5		±5	
	14/4	152	5/4	80	18/4	60	32/1	38	40/1	15	44/1	10
	14/5	150	5/5	82	18/5	56	32/2	38	40/2	16	44/2	8
	14/6	150	5/6	76	21/4	60	32/3	40	40/3	15	44/3	8
	15/7	150	8/10	80	21/5	58	29/4	40	41/4	19	42/7	8
	15/8	152	8/11	82	21/6	58	29/5	42	41/5	18	42/8	6
	15/9	154	8/12	84	23/2	53			41/6	19	42/9	10
			8/13	82	23/3	55			38/7	16	45/4	7
									38/8	15	45/5	7
									38/9	17	45/6	8
Average $(Dt)^{1/2}$ value	151 ± 3		81 ± 2		57 ± 2		40 ± 2		17 ± 2		8 ± 1	
$(Dt)^{1/2}$ value calculated from sectioning results.	150 ± 5		78 ± 3		59 ± 2		39 ± 2		20 ± 1		10 ± 1	

Table 2

Specimen number	Specimen arrangement	Annealing temperature (°C)	Annealing time (sec 10^4)	Observed $(Dt)^{1/2}$ value (cm 10^{-4})	Calculated $(Dt)^{1/2}$ value (cm 10^{-4})	Observed diffusion coefficient ($cm^2\ sec^{-1}$)	Calculated diffusion coefficient ($cm^2\ sec^{-1}$)
14/1	(i)	795	26·214	147 ± 4	150 ± 5	$8{\cdot}25 \pm 0{\cdot}45 \times 10^{-10}$	$8{\cdot}60 \pm 0{\cdot}45 \times 10^{-10}$
14/1	(ii)	795	26·214	151 ± 3	150 ± 5	$8{\cdot}70 \pm 0{\cdot}40 \times 10^{-10}$	$8{\cdot}60 \pm 0{\cdot}45 \times 10^{-10}$
4/4	(i)	700	110·880	121 ± 3	119 ± 4	$1{\cdot}32 \pm 0{\cdot}10 \times 10^{-10}$	$1{\cdot}27 \pm 0{\cdot}15 \times 10^{-10}$
5/5	(i)	651	222·840	98 ± 3	96 ± 4	$4{\cdot}30 \pm 0{\cdot}25 \times 10^{-11}$	$4{\cdot}00 \pm 0{\cdot}25 \times 10^{-11}$
12/1	(i)	856	2·406	79 ± 2	78 ± 3	$2{\cdot}60 \pm 0{\cdot}15 \times 10^{-9}$	$2{\cdot}50 \pm 0{\cdot}15 \times 10^{-9}$
12/1	(ii)	856	2·406	81 ± 2	78 ± 3	$2{\cdot}73 \pm 0{\cdot}15 \times 10^{-9}$	$2{\cdot}50 \pm 0{\cdot}15 \times 10^{-9}$
11/3	(iii)	896	1·542	80 ± 1	84 ± 3	$4{\cdot}15 \pm 0{\cdot}10 \times 10^{-9}$	$4{\cdot}60 \pm 0{\cdot}25 \times 10^{-9}$
11/1	(ii)	743	11·028	57 ± 2	59 ± 2	$2{\cdot}95 \pm 0{\cdot}20 \times 10^{-10}$	$3{\cdot}12 \pm 0{\cdot}20 \times 10^{-10}$
11/1	(iii)	743	11·028	57 ± 2	59 ± 2	$2{\cdot}95 \pm 0{\cdot}20 \times 10^{-10}$	$3{\cdot}12 \pm 0{\cdot}20 \times 10^{-10}$
11/2	(ii)	743	4·920	40 ± 2	39 ± 2	$3{\cdot}25 \pm 0{\cdot}20 \times 10^{-10}$	$3{\cdot}12 \pm 0{\cdot}20 \times 10^{-10}$
11/2	(iii)	743	4·920	37 ± 2	39 ± 2	$2{\cdot}80 \pm 0{\cdot}30 \times 10^{-10}$	$3{\cdot}12 \pm 0{\cdot}20 \times 10^{-10}$
13/1	(iii)	663	7·458	17 ± 2	20 ± 1	$3{\cdot}90 \pm 0{\cdot}40 \times 10^{-11}$	$5{\cdot}27 \pm 0{\cdot}25 \times 10^{-11}$
13/3	(iii)	560	31·266	8 ± 1	10 ± 1	$2{\cdot}10 \pm 0{\cdot}50 \times 10^{-12}$	$3{\cdot}23 \pm 0{\cdot}20 \times 10^{-12}$

estimate an error due to the uncertainty in matching. A matching process of this sort was carried out on a chosen number of traces from a given specimen. When a trace could not be fitted to a single computed curve, it was usually possible to interpolate between two curves. The characteristic random variation of the density which is present on all traces and which is associated with film fog, did not impair matching to any serious extent. In a very few cases the experimental trace could not be fitted satisfactorily by any computed curve and was discarded.

Table 1 shows the results that have been obtained from the matching of individual traces in the case of $(Dt)^{1/2}$ values of approximately 150 μ, 80 μ. 60 μ, 40 μ, 20 μ and 10 μ. This shows the error in the individual results as the uncertainty in matching. The average value has been calculated from each set of results, and the quoted errors correspond to the 95% reliability limit. Table 2 shows the average results for each of the penetrations used. The calculated values have been obtained by using the mechanical sectioning results of Inman and Barr (1960), and the errors quoted also refer to the 95% reliability limit. The low result obtained in the case of specimen 11/3 is believed to be due to the short annealing time. The results in the case of specimens 13/1 and 13/3 are discussed later.

§ 5. Discussion

An examination of fig. 3 (*a*)–(*d*) shows that there is good agreement between the experimental trace and the computed curve taken to match it. It is important to note the uncertainty in matching at each of the $(Dt)^{1/2}$ values. Table 2 shows that in general the results obtained by this method agree well with the results obtained by mechanical sectioning. A number of points require discussion.

For specimens mounted in arrangement (iii) it was possible to fix the peak of the curve to within two or three microns. This peak was taken to represent the active surfaces of the two specimens, and the origin of the computed curve. In the subsequent matching process, no significant adjustment of this point was normally necessary. In the case of the specimens mounted in arrangement (i) (fig. 3 (*b*)), it was possible to identify the origin with a point on the trace where the characteristic change in density was taken to result from the copper–Araldite interface. An adjustment of as much as 10 μ was found to be necessary on a few occasions in subsequent matching. In the case of specimens mounted in arrangement (ii), it was not possible to identify the origin with any point on the trace, but by superposing the curves in the region of the origin the subsequent matching process was found to be acceptable (fig. 3 (*c*)). In the range $-400\,\mu < y < -100\,\mu$, outside the diffusion zone, the matching of these curves is not good, and becomes progressively worse at high $(Dt)^{1/2}$ values. For example no matching at all was possible at a $(Dt)^{1/2}$ value of 150 μ, if this region was taken into consideration (fig. 3 (*a*)). No satisfactory explanation of this misfit can be offered, although it might be expected that

the effect of errors would first become apparent in this region as a result of the concentration discontinuity and sudden fall to low density values.

In the derivation of eqn. (3) it was assumed that the scattering of the particles is the same at all points. This requires that the diffusion zone is situated within an extended solvent material, and this condition cannot be fully satisfied. With unmated specimens mounted in arrangement (i) the scattering within the Araldite is different from the scattering within the copper and so the two density curves are very different in the region which corresponds to the Araldite. The change in scattering that occurs within the copper in a region near the copper–Araldite interface is taken to account for the difference observed between the two curves in this region (fig. 3 (*b*)), and although it has no significant effect on the matching process at large penetrations, it becomes increasingly serious for $(Dt)^{1/2}$ values lower than $30\,\mu$. At a copper–copper interface, any gap between the mating faces would produce a similar effect, but if the separation of these faces is only a few microns then the effect that is produced on a density pattern several hundred microns in extent will be very small. In the case of specimens mounted with active faces touching, no evidence of systematic variation between the two density curves is detectable (fig. 3 (*d*)). In the case of specimens mounted in arrangement (ii) the systematic variation between the curves previously noted, cannot be accounted for by bad contact. Good mating is particularly important in the case of undiffused specimens, because errors of any sort in the values of the function $\mu(\zeta)$ affect in turn the entire application of the method. If the variation in the values of $\mu(\zeta)$ is assumed to be random, then it is found that the errors in the computed density values are small in comparison with the error involved in matching.

Although the procedure of normalization and subsequent visual matching has been found adequate for the purpose of a preliminary trial, other methods of analysing the trace might require to be considered. In matching the traces individually the error in assigning a $(Dt)^{1/2}$ value is influenced by the interval between the computed density curves. For specimens mounted singly in arrangements (i) and (ii), the interval of $10\,\mu$ was found to be sensibly correct for a penetration of $60\,\mu < (Dt)^{1/2} < 120\,\mu$. For doubly mounted specimens, where the accuracy is correspondingly greater, this interval was found to be correct in the range $80\,\mu < (Dt)^{1/2} < 150\,\mu$. Outside these limits it is desirable to adjust the interval, and for $(Dt)^{1/2} < 20\,\mu$, steps of $5\,\mu$ have been used. The interval, which is also chosen from a consideration of the quality of the autoradiographs, must not be inconsistent with the errors in the calculated density values, or with the magnitude of the error produced by a set of individual results. Considerations of this sort suggest that a further attempt to refine or to revise the method of analysis might prove to be justified. A fuller and more comprehensive analysis however, would require to examine the trace over its entire length, and the necessary condition for this is that the trace should not deviate in any systematic manner from the ideal form. This condition is not satisfied in the case of unmated specimens, and at present appears to be completely satisfied only for specimens mounted in arrangement (iii). The magnitude

and extent of this deviation from the ideal form is the factor that determines not only the refinement that can be achieved, but ultimately the limitation of the method.

The work of Doniach and Pelc (1950) and of Stevens (1950) has illustrated how the resolution of the autoradiograph is affected by film thickness, specimen contact and film and radiation characteristics in the case of a line source of uniform activity. It follows from considerations of this sort, that in the present application these factors must remain the same for each exposure, the quality of the trace being a main consideration. If in this case the ability of the method to distinguish between two experimental traces for which the penetrations are approaching the same value is to be considered, then an indication of this is given by the uncertainty in matching and by the separation of the computed density curves. Of

Fig. 4

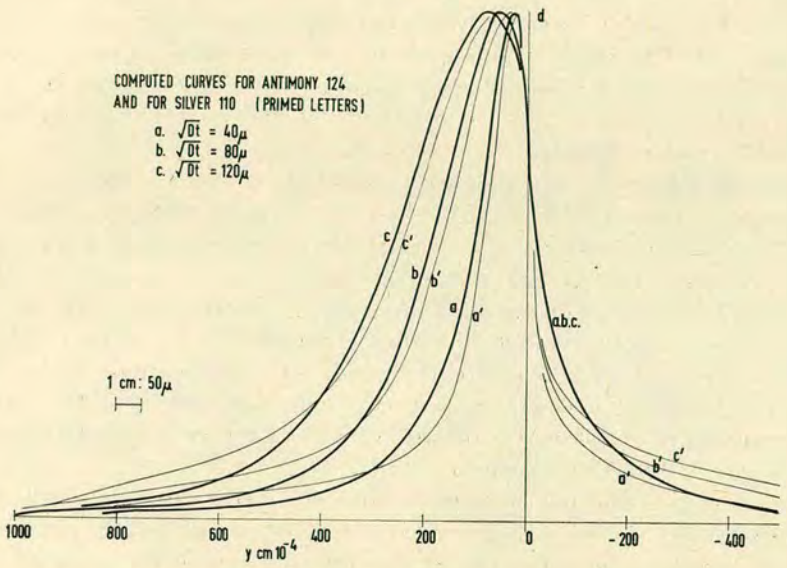

A comparison of the computed density curves for radioactive ^{124}Sb with those for radioactive ^{110}Ag, with assumed $(Dt)^{1/2}$ values of 40 μ, 80 μ and 120 μ.

particular interest in this respect is the effect of penetration depth and of radiation characteristics. Higher energy β-particles would in general give a greater separation of the computed curves, but for isotope emission the influence of penetration depth is important. As an illustration of this the case of ^{124}Sb is compared with ^{110}Ag, which emits much lower energy β-particles, apart from 3% which decay with a very high end point energy. The traces obtained from undiffused specimens (fig. 2) show that of ^{110}Ag to be sharp by comparison, although the effect of high energy particles is observed in the long tail. A comparison of the computed density curves for $(Dt)^{1/2}$ values of 40 μ, 80 μ and 120 μ (fig. 4) shows that ^{124}Sb would give

greater dispersion over the larger portion of the curves, but at the extremities, and particularly for the larger penetrations, ^{110}Ag would give the greater dispersion, assuming that the quality of the experimental traces are comparable. In each matching process therefore, more weight would be given to the fit in the region where the dispersion is greatest. Figure 4 also shows that the difference in the form of the curves is less than might be expected from a comparison of the energy spectra, except at the extremities where it is more than might be expected.

A qualitative examination of the properties of the curves reveals some interesting features. The form of the density distribution and the concentration distribution are quite different. The concentration falls to near zero at $5(Dt)^{1/2}$, but the tail of the density curve extends well outside this region. For specimens mounted singly, the maximum density occurs at some distance from the surface. In the case of ^{124}Sb this distance is 100 μ and 35 μ for $(Dt)^{1/2}$ values of 150 μ and 40 μ respectively. At some point on the trace, the value of the density is the same as that occurring at the origin. The distance between these points is 170 μ and 80 μ measured in the y direction for the penetrations quoted. By comparing adjacent curves it is evident that the largest difference between the computed density values occurs in the region $2(Dt)^{1/2}$ to $5(Dt)^{1/2}$. At the peak the difference is detectable, and at other points it is small.

Although the form of the density distribution and the concentration distribution are quite different, in the case of singly mounted specimens there is a similarity between a portion of the density curve and a portion of the concentration curve. This can best be seen by superposition, after suitable adjustment as in fig. 3 (*a*), (*b*) and (*c*), allowing one curve a two-degree freedom of movement with respect to the other. If the peaks of the two curves were taken to correspond, an identification of this sort might lead to the incorrect application of eqn. (2), and for $(Dt)^{1/2}$ values less than 60 μ, the systematic variation between the two curves identified in this way is found to be considerable.

An assumption that has been made throughout this work is that the film expansion does not vary with density at low densities and that the expansion over the small region activated by the diffusion zone is the same as that over the large region between the images used to determine its value. It is therefore necessary to observe adequate precautions during the processing and the mounting of the film.

It is found that there is no significant difference between the results from specimens mounted in arrangement (i) and those mounted in arrangement (ii). The advantage of arrangement (i) is that the origin can be fixed more accurately, but arrangement (ii) allows the whole length of the curve to be examined, and it can be applied at low penetration depths. It is in arrangement (iii) where each of these advantages are combined and where the spread of the trace is greater, that the highest accuracy is to be found. This is especially true at lowest penetrations, where the maximum accuracy that can be obtained is approximately the same as that obtained in determining the value of the function $\mu(\zeta)$.

A preliminary examination of the averaged values of the results showed no evidence of large systematic variation, although there is an indication of a small difference between the results of different autoradiographs, and on this basis the theory of random errors was applied. Table 2 reveals that the accuracy obtained in this work is comparable with the accuracy of mechanical sectioning. The results obtained in the case of $(Dt)^{1/2}$ values calculated as 20 μ and 10 μ are low when compared with the results of mechanical sectioning extrapolated to these lower temperatures, but this is in agreement with Barr *et al.* (1962) who, using a method of chemical sectioning reported low values of the diffusion coefficient for small penetrations in the temperature range 540°C to 600°C.

§ 6. Conclusion

The measure of agreement that is found when the results produced by this trial investigation are compared with the results obtained from mechanical sectioning, and the fact that the accuracies in the two cases are comparable, indicate that the method which is described is suitable for the accurate measurement of volume diffusion. The application of the method to the measurement of small penetration depths might prove particularly useful.

Acknowledgments

The financial support provided for this work by U.K.A.E.A., Harwell, is gratefully acknowledged. The author also thanks Professor N. Feather and Dr. A. F. Brown for the facilities which were made available and for their interest in this work.

References

Barr, L. W., Blackburn, D. A., and Brown, A. F., 1962, *Copenhagen Conference on Radioisotopes in the Physical Sciences and Industry*, Vol. 1 (Vienna : International Atomic Energy Agency), p. 137.

Brown, A. F., and Blackburn, D. A., 1963, *Acta Met.*, **11,** 1017.

Doniach, I., and Pelc, S. R., 1950, *Brit. J. Radiol.*, **23,** 184.

Dudley, R. A., and Dobyns, B. M., 1949, *Science*, **109,** 327.

Forestieri, A. F., and Girifalco, L. A., 1959, *J. phys. Chem. Solids*, **10,** 99.

Gross, J., Bogoroch, R., Nadler, N. J., and Leblond, C. P., 1951, *Amer. J. Roentgenol*, **65,** 420.

Inman, M. C., and Barr, L. W., 1960, *Acta Met.*, **8,** 110.

Loevinger, R., Japha, E. M., and Brownell, G. L., 1956, *Radiation Dosimetry*, edited by G. J. Hine and G. L. Brownell (New York : Academic Press Inc.), Chap. 16.

Marshall, J. H., Rowland, R. E., and Jowsey, J., 1959, *Radiat. Res.*, **10,** 213.

Mortlock, A. J., and Tomlin, D. H., 1956, *Proc. phys. Soc., Lond.* B, **69,** 250.

Norris, W. P., and Woodruff, L. A., 1955, *Annu. Rev. nucl. Sci.*, **5,** 297.

Odeblad, E., 1956, *Acta radiol., Stockh.*, **45,** 323.

Revo, A. L., 1961, *Phys. Metal. Metallog.*, **11,** 5, 77.

Sherwood, H. F., 1947, *Rev. sci. Instrum.*, **18,** 80.

Stevens, G. W. W., 1950, *Brit. J. Radiol.*, **23,** 723.

Tomizuka, C. T., 1959, *Methods of Experimental Physics*, Vol. 6A (London and New York : Academic Press), p. 364.